Design Optimization of Pressure Vessel with Particular Design Considerations

by

ARTIK PATEL

Presented to the
Faculty of the Graduate School of
The University of Texas at Arlington
in Partial Fulfillment of the Requirements
for the Degree of

MASTER OF SCIENCE IN MECHANICAL ENGINEERING

The University of Texas at Arlington
November 2016

Copyright © by Artik Patel 2016

All Rights Reserved

ACKNOWLEDGEMENTS

First of all, I would like to express my deep gratitude and admiration to my advisor and mentor Dr.Bo.P.Wang, who is a constant source of guidance and inspiration to me. I am very grateful to you for the encouragement and support which you have provided throughout my time as your student. I have been extremely lucky to have a supervisor who cared so much about my work, and who responded to my questions and queries so promptly.

I want to extend my sincere appreciation and thanks to my committee members, Dr. Kent Lawrence and Dr. Wen S. Chan, who have been extremely helpful during the whole process of thesis review and have helped enrich my thesis with their valuable suggestions. I would like to mention a special thanks to Professor Weiya Jin and Professor Mingjne Zhou from the Design Institute of Chemical Machinery, Zhejiang University for providing me the pressure vessel model. Their insight and expertise has greatly assisted this research. I would also like to thank my friends for the encouragement they made in support of my research.

Most importantly I would like to dedicate this work to my parents who have been there for me always and are responsible for what I am today and without whom, the joy of completing the educational phase of my life would be incomplete. This accomplishment would not have been possible without them. Finally, I would like to express my gratitude to one and all, who directly or indirectly, have lent their hand in the support of my thesis work. Thank you.

November 21, 2016

Design Optimization of Pressure Vessel with Particular Design Considerations

By

Artik Patel

Mechanical Engineering

M.S – The University of Texas at Arlington

B.E – PES Institute of Technology, Bangalore, India

Advisor: Dr. Bo. P. Wang

ABSTRACT

The pressure vessels in industries are generally designed with a high safety factor because the rupture of a pressure vessel can be extremely dangerous. A vessel that is poorly designed or ineffectively designed to handle high pressure pose a very significant threat to life and property. Because of this, the design and verification of pressure vessels is governed by design codes specified by the ASME (American Society of Mechanical Engineers) Boiler and Pressure Vessel Code. The objective of this thesis work is to minimize the total weight of a real-world pressure vessel structure subjected to stress constraints specified by the ASME section VIII division-2 code. Optimization is the process of finding the best feasible solution amongst the conventional designs which accepts almost all designs which merely satisfies the problem requirements. The main purpose of performing design optimization in pressure vessels is to reduce cost, by reducing the weight with sufficient strength to avoid any modes of failure in the design. This work discusses size optimization of axisymmetric pressure vessel considering an integrated approach in which the optimization procedure is implemented by interfacing the commercial finite element analysis software ANSYS with MATLAB optimization algorithm. A half model is used in conjunction with a single-objective function that aims to minimize the total weight of the pressure vessel equipment. Design parameters such as shell thickness and flange thickness are optimized while limiting the maximum linearized membrane and membrane plus bending stresses below the ASME code limits.

Table of Contents

LIST OF FIGURES

LIST OF TABLES

CHAPTER 1: INTRODUCTION

1.1 Introduction to Optimization

Optimization in general can be defined as the act of finding the best feasible solution with the most cost effective or highest achievable performance under the given constraints, by maximizing desired factors and minimizing undesired ones. The increased demand to cut down the production and manufacturing costs in the industries have encouraged engineers to use more robust decision making technique such as optimization. In any optimization problem, we seek values of the design parameters that minimize or maximize the objective while satisfying constraints.

Over a past few decades, the optimization techniques have found its applications in a wide variety of industries such as automotive, aerospace, chemical, electrical and manufacturing industries. Because of the advancement in computer technology, the complexity of a problem being solved by optimization methods is no longer a concerned issue. Although this process can sometimes be very time consuming, depending on the size and nature of problem in hand. With the advent of computers, engineers can exploit and implement this procedure in practice. To fully realize the power of computational Design Optimization, it is important to implement optimization methods through pertinent computer-based mathematical tools.

1.2 MATLAB Optimization Tool

To conduct optimization for the pressure vessel model, we use MATLAB software. MATLAB is a computational modeling and coding tool that is powerful, easy to use, and one that is widely applied in engineering and other fields. MATLAB is used worldwide to optimize both simple and complex systems or designs with effectiveness and efficiency. It provides a variety of inbuilt optimization functions like fmincon, fminsearch, genetic algorithm, etc which uses search algorithms that are executed iteratively by comparing various solutions till an optimum or a satisfactory solution is found. It is entirely dependent on the analyst to choose an appropriate optimization function which is computationally efficient and accurate for the design problem in hand. In this thesis work, we will restrict the analysis to fmincon function only. FMINCON is a MatLab inbuilt nonlinear solver for optimization. It has proved to be a suitable tool to solve many optimization problems in the mechanical engineering field.

1.3 Finite Element Analysis using ANSYS

A completely accurate representation of the physical model may lead to an extremely complex mathematical model that may be hard to solve with the available hardware and software resources. For this reason, we use a finite element model which is a mathematical representation of a real-life component or system that is being analyzed. FEA consists of three main steps: Pre-processing, solution and post-processing. Often in the engineering world, the structural analysis

is carried out using the Finite Elements Method. In this method, the physical model is discretized into several small and simple parts called ‘finite elements’. The simple equations that model these finite elements are then assembled into a larger system of equations that models the entire problem. Finite elements are employed to determine the deformation and stresses in a structure subjected to loads and boundary conditions. Mathematically it may be considered as a numerical tool to analyze problems governed by partial differential equations that describe the behavior of the system being studied.

There are a lot of commercial finite element analysis software available in the market such as ANSYS, ABAQUS, ALTAIR HYPERWORK, NASTRAN, etc. In the present work, ‘ANSYS v17.0’ was used for finite element analysis of the pressure vessel model. ANSYS is one of the most powerful engineering analysis software. It is widely used in the engineering industries to perform finite element analysis, structural analysis, computational fluid dynamics, and heat transfer. This computer simulation product provides finite elements to model behavior, and supports material models and equation solvers for a wide range of mechanical design problems.

The finite element model of the pressure vessel was created using three dimensional solid elements. An APDL (ANSYS Parametric Design Language) script file was written to automate the pre-processing, solution and post-processing phase in ANSYS. The obtained stress intensity results were linearized along 20 different stress classification lines(SCL/paths) to extract the membrane and membrane plus bending stress generated in the different components of the pressure vessel like nozzles, flanges cylindrical vessel body and the vessel head. These stresses are then classified as primary or secondary, depending on the influence from stress singularity region. Finally, both primary and secondary membrane and membrane plus bending stresses are compared against their respective ASME code limits.

1.4 Objective and Approach

The main objective of this thesis work is to minimize the total weight of a Pressure vessel subjected to stress constraints specified by the ASME ‘Design by Analysis of Boiler and Pressure Vessel’ code limits. This is achieved by using FEA results obtained from ANSYS in conjunction with MATLAB fmincon optimization solver for the sole purpose of minimizing the objective. Solving complex design problems by integrating robust optimization tools like MATLAB with powerful FEA softwares such as ANSYS has opened a new door in the field of design optimization. Optimization methods, combined with more detailed and accurate simulation methods can improve the experimental process of conceptual and detailed design of engineering systems.

Finite Element Analysis of the pressure vessel model is executed through MATLAB by running ANSYS script file in Batch mode. The post-processing results such as total volume of the equipment, deformation, von-mises stress and linearized membrane and membrane plus bending stresses are stored in a text file. Objective function and constraints are defined in MATLAB by extracting appropriate data from this result file generated by ANSYS. The volume data gives the value of the objective function, whereas the linearized stress results which are verified against their ASME allowable values, forms the constraint. Finally, the MATLAB optimization algorithm evaluates the objective function iteratively by comparing various solutions till an optimum design is found. The proposed methodology is completely automated and does not require any kind of user intervention until the optimal solution is found.

CHAPTER 2: LITERATURE SURVEY

2.1 History

In the industrial sector, the pressure vessels are used as storage tanks, diving cylinder, recompression chamber, distillation towers, autoclaves and many other vessels in mining or oil refineries and petrochemical plants, nuclear reactor vessel, habitat of a space ship, habitat of a submarine, pneumatic reservoir, hydraulic reservoir under pressure, rail vehicle airbrake reservoir, road vehicle airbrake reservoir and storage vessels for liquefied gases. The design analysis of pressure vessels is an important and practical topic which has been investigated for decades. Even though optimization techniques have been extensively applied to design structures in general, very few pieces of work can be found which are directly related to optimization of pressure vessels by interfacing different software packages like MATLAB and ANSYS. These few references include the design optimization of homogeneous as well as composite pressure vessels with different optimization methods.

2.2 Literature Review

In the paper 'Integration of MATLAB and ANSYS for Advanced Analysis of Vehicle Structures', A.Gauchia and B.L.Boada has explained the optimization of a complex bus structure in weight and stiffness by means of coupling MATLAB and ANSYS. For the optimization loop analyzed in this study the genetic algorithm toolbox has been employed, having shown to be a very useful tool. A reduction of 4% of the weight was achieved while improving the torsion stiffness in 0,23%. Prior to this optimization, a sensitivity analysis was carried out in order to apply the optimization loop on certain beams more sensitive to variations in weight and torsion stiffness. [1]

In the work by Levi B. de Albuquerque and Miguel Mattar Neto, design criteria were developed to preclude the various pressure vessel failure modes through the so-called "Design by Analysis" method. In the "Design by Analysis" approach, also used in Section VIII, Division 2 of the Code, the design limits were established in correspondence to each failure mode. A typical Pressurized Water Reactor (PWR) nozzle to pressure vessel connection subjected to internal pressure and concentrated loads was modeled with 3D solid finite elements in linear elastic and limit load analyses. Using some stress categorization approaches, the results from linear elastic and limit load analyses were compared to each other and also with results obtained by formulae for simple shell geometries. Based on the result comparison, some conclusions and recommendations on the type of finite element analysis (linear elastic or limit load) and on the stress categorization were addressed for the studied cases. [2]

The research conducted by Carlos A. de J. Miranda, Altair A. Faloppa, Miguel Mattar Neto and Gerson Fainer shows a discussion on how to perform the stress verifications based on a generic geometry found in many plants, from petrochemical to nuclear. In this study, the author discusses the nuclear piping analysis with a non-standard item when the item should be modeled as a 3D solid with its verification done per the Sub-section NB 3300 of the ASME Code. Only the primary stresses due to the internal pressure were considered since the scope of the work was to emphasize some of the issues that arise from the stress classification and linearization in discontinuities, which are common in the nuclear area. Along with the modeling, analysis and verification a discussion on how to perform the Code verifications was presented, pointing some differences between the present(simplified) analysis, just one load – pressure, and an actual one, with several applied loads. [3]

The research paper by R. Carbonari, P Munoz-Rojas discuses shape optimization of axisymmetric pressure vessels considering an integrated approach in which the entire pressure vessel model is used in conjunction with a multi-objective function that aims to minimize the von-Mises mechanical stress from nozzle to head. Representative examples are examined and solutions obtained for the entire vessel considering temperature and pressure loading [4].

The paper submitted on 'Design & Weight Optimization of Pressure Vessel Due to Thickness Using Finite Element Analysis' by Vishal V.Saidpatil and Arun S.Thakare explains the detailed design & analysis of Pressure vessel used in boiler for optimum thickness, temperature distribution and dynamic behavior using ANSYS. Their work involves design of a cylindrical

pressure vessel to sustain 5 bar pressure and determine the wall thickness required for the vessel to limit the maximum shear stress [5].

Sulaiman Hassan and Kavi Kumar considered a metaheuristic approach to optimize the pressure vessel design. The work parameters such as thickness of the shell, and dish end, length and radius of the pressure vessel were optimized by making use of Ant colony optimization (ACO) Algorithm. They found that the results obtained from ACO are better as its search is for global optimum as against the local optimum in traditional search methods [6].

K. Sahitya Raju and Dr. S. Srinivas Rao conducted Design optimization of a composite cylindrical pressure vessel using FEA. In this work, design analysis of fiber reinforced multi layered composite shell, with optimum fiber orientations; minimum mass under strength constraints for a cylinder under axial loading for static and buckling analysis on the pressure vessel has been studied. It involves the comparison of conventional steel and Composite material cylindrical pressure vessel under static loading conditions. [7].

A very few research is found that directly relates to the optimization of pressure vessel by interfacing FEA software with an optimization tool. Many other researches found including analytical, experimental and numerical investigations have been devoted to the design optimization of head and nozzle connections in pressure vessels subjected to different external loadings.

CHAPTER 3: Finite Element Analysis of the pressure vessel

3.1 Modelling of cylindrical pressure vessel

An ANSYS command file was written based on the design data of a real-world pressure vessel equipment provided by the ‘Design Institute of Chemical Machinery’, Zhejiang University. This script file is executed in ANSYS APDL v17.0 to generate the geometrical entities such as keypoints, lines, areas and volumes. The ANSYS model as shown in figure-1 below, represents an axisymmetric cylindrical pressure vessel used in chemical industries, that is approximately 6 meter-long and 2 meter-wide, with elliptical heads and four rectangular nozzles supported by the flange. Due to symmetry of the vessel along the z-plane, we consider only half model for our analysis. This saves a lot of computational time during the FEA as well as during the optimization process. A full model displayed in figure-2 can be used for FEA, in case, when large amount of memory(RAM) along with sufficient hardware and software resources are available, or when the computational time is not an issue.

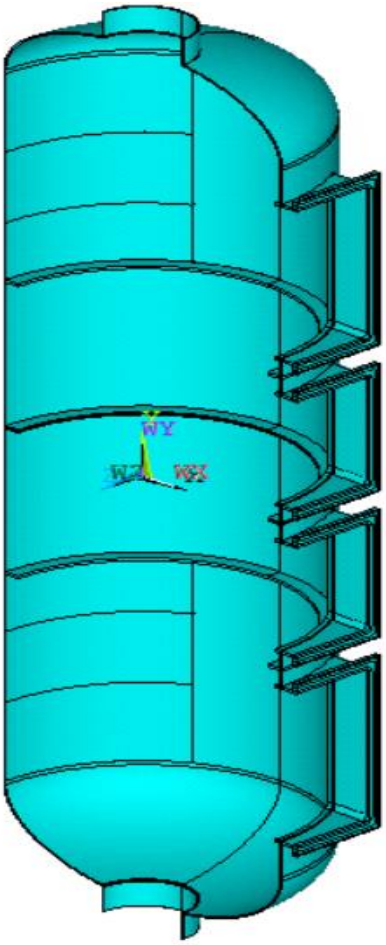

Figure 1: Pressure Vessel half-model

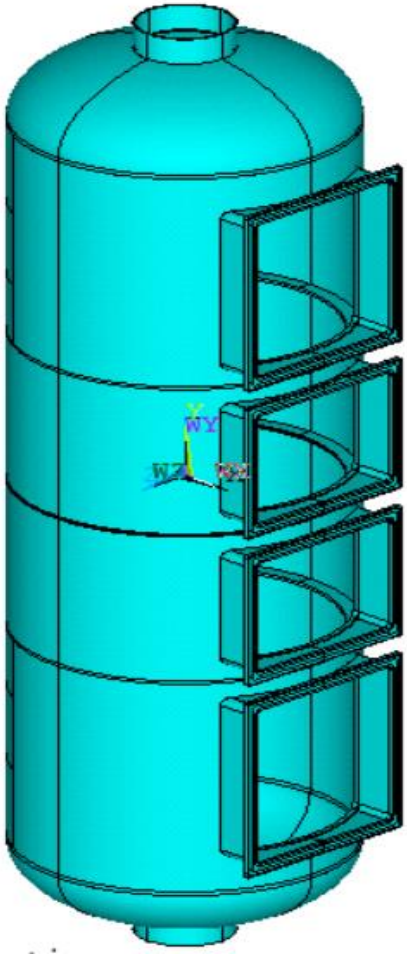

Figure 2: Pressure Vessel full-model

As shown in figure-4, the geometry of the pressure vessel is defined based on the parameters such as shell radius, shell height, shell thickness, head height etc. A quarter model is created by rotating the cross-sectional area of the pressure vessel by 180 degrees about the y-axis. Symmetricity of the structure was fully exploited by mirroring the volumes created in the quarter model about the x-z plane to generate half model (figure-1). Nozzle and flange supports were created with the help of ANSYS pre-processing functions like extrude and volume delete. The sharp corners on nozzle edges and on flange edges have been filleted to reduce the stress concentration around these corners. Note that, the lateral nozzle openings are longer than the medial nozzle openings. The complete structure was subdivided into volume blocks to satisfy the conditions of hexa-meshing to generate brick elements throughout the model. One more reason to divide the volume blocks is to apply constraints in some specified location of the geometry.

The main Pressure bearing components of this pressure vessel equipment are shown in figure-3 below.

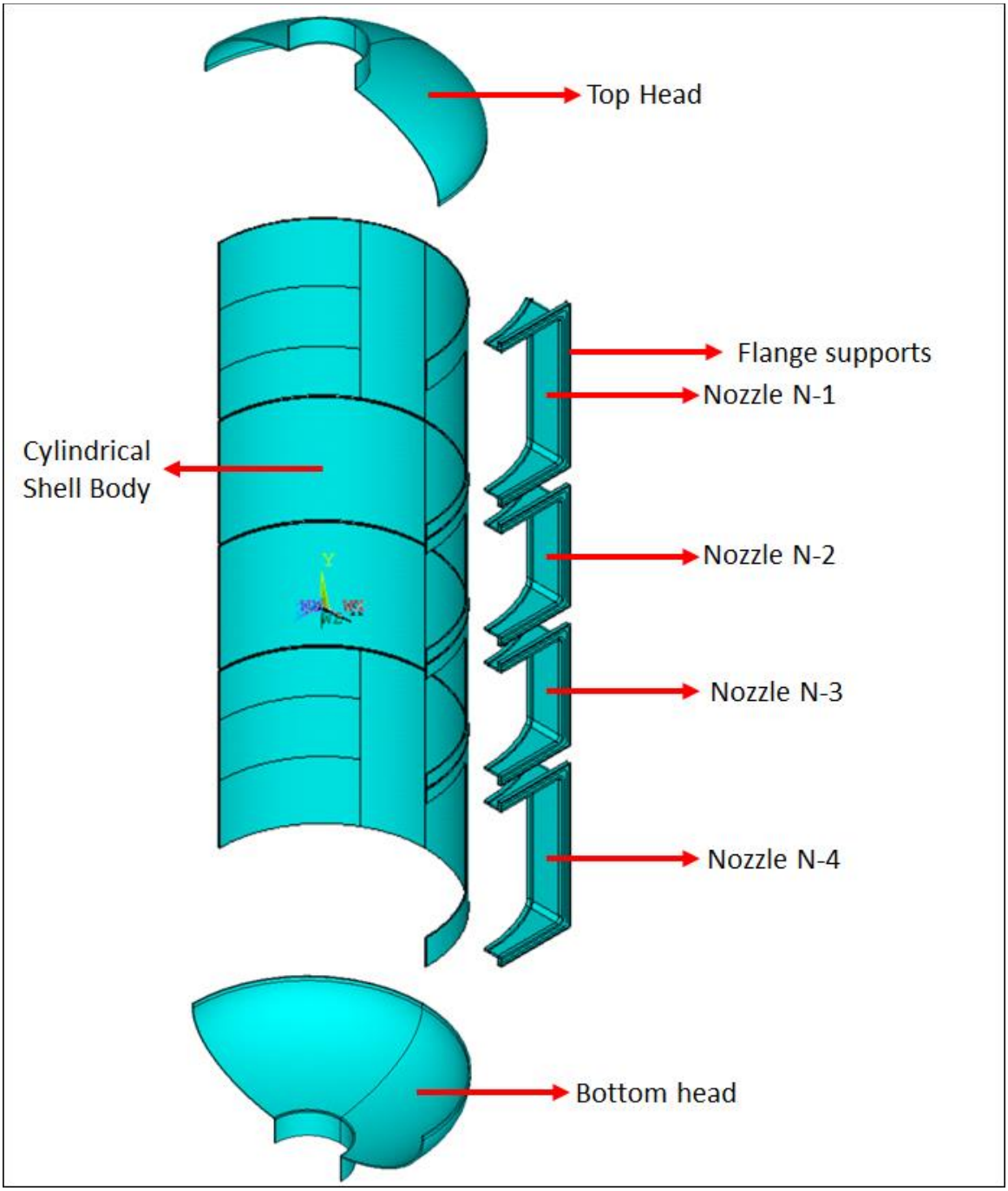

Figure 3:Main Components of the Pressure Vessel Equipment

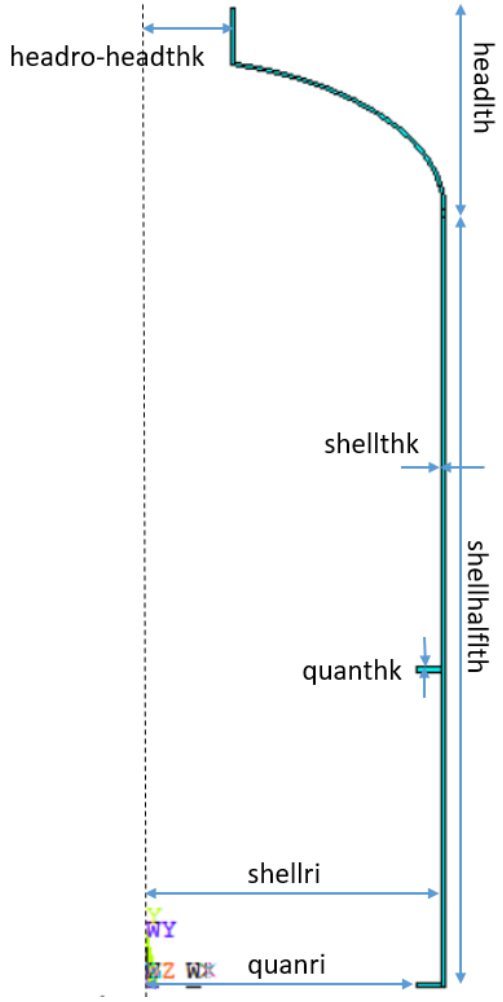

Figure 4: Cross-sectional area of the vessel

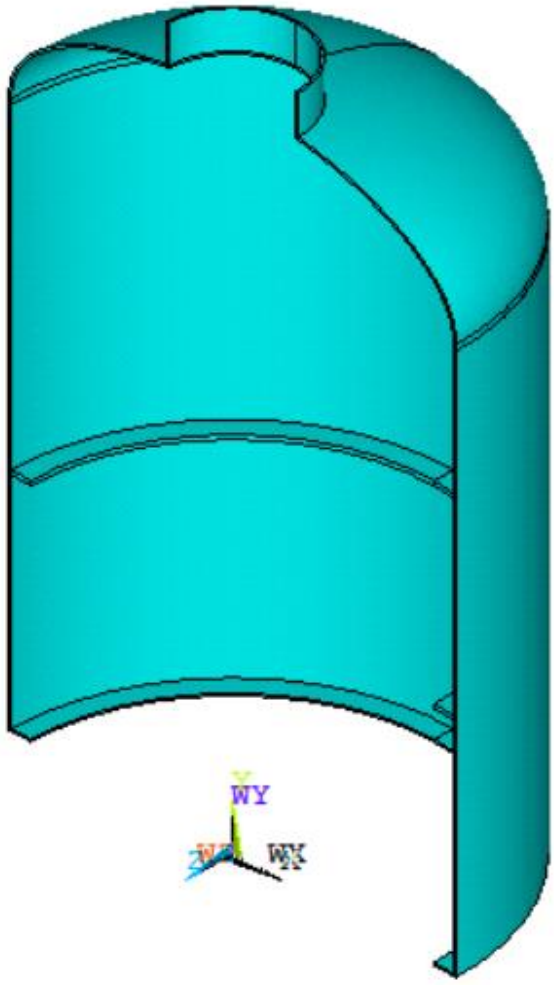

Figure 5: Rotating cross-sectional area to generate the vessel volume

3.2 Material Properties and Element Type

Steel alloy 'S30408' standard 'GB24511' is the material used to create the pressure vessel equipment. In general, this material is extensively used in Chinese steel industries to produce products such as steel oils, sheets, plates, round bars, steel wires, pipes, forgings etc. GB standards are the Chinese national standards issued by the Standardization Administration of China (SAC), the Chinese National Committee of the ISO and the IEC. This Chinese standard specifies classification and designation, dimensions, shapes and tolerances, technical requirements, test methods, inspection rules, package, marks and product quality certificates of Stainless steel plate, sheet and strip for pressure equipments. This standard applies to width of not less than 600mm of pressure equipment with hot-rolled, cold-rolled stainless steel sheet and

strip. The chemical composition of this steel alloy is displayed below in table 1. The design stress intensity of the materials at different temperatures is shown in Table 2. The material of the main pressure-bearing components of this equipment is shown in Table 3 and the mechanical properties are presented in Table 4.

Table 1: Chemical composition % of steel grade S30408

C(%)	Si(%)	Mn(%)	P(%)	S(%)	Cr(%)	Ni(%)
Max 0.08	Max 1.0	Max 2.0	0.045	0.03	18.0-20.0	8.0-11.0

Table 2: Design Stress Intensity of Material at different Temperatures

Steel	Type	Standard	Thickness (mm)	Normal Temperature Strength (MPa)		Design Stress(MPa) at different Temperatures (℃)					
				R_m	R_{el}	<20	100	150	200	250	300
S30408	Steel Plate	GB 24511	1.5~80	520	205	137	137	137	130	122	114
				520	205	137	114	103	96	90	85
S3408	Steel Pipe	GB 13296	≤13	520	205	137	137	137	130	122	114

Table 3: Material of the main pressure-bearing components of the pressure vessel

S.No	Pressure Vessel Component	Material	Standard
1	Case	S30408	GB 24511
2	Forming Head	S30408	GB 24511
3	Support	Q235A/S3408	GB/T3274{GB150.2} / GB 24511
4	Flange	S30408	GB 24511

Table 4: Mechanical Properties of the Material

PROPERTY	VALUE
Young's Modulus	200 *GPa*
Poisson's Ratio	0.3
Density	7.9e-6 Kg/mm^3
Yield Strength	345 *MPa*

In ANSYS software, the user can select from over 100 different element types to construct their model. Solid95 20-nodes hexahedral/brick element was used for finite element analysis of the pressure vessel model. As shown in figure-6 below, Solid95 is a 3-dimensional solid element. It can tolerate irregular shapes without as much loss of accuracy. Solid95 elements have compatible displacement shapes and are well suited to model curved boundaries. The hexahedral/Brick element is defined by 20 nodes (including mid-nodes) whereas the tetrahedral element consists of 10 nodes (including mid-node). Each node has three degrees of freedom: translations in the nodal x, y, and z directions. Therefore, each brick element consists of 60 DOF. The element may have any spatial orientation. The element has plasticity, creep, stress stiffening, large deflection, and large strain capabilities.

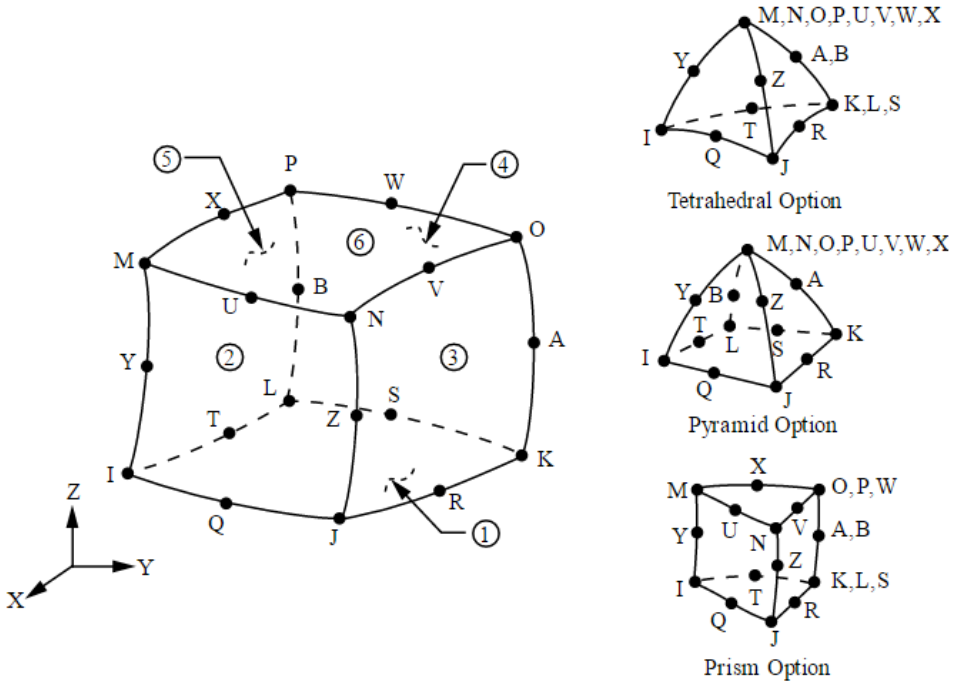

Figure 6: SOLID95 3-D 20-Node Structural Solid

3.2.1 SOLID95 Assumptions and Restrictions:

- The element must not have a zero volume.
- The element may not be twisted such that the element has two separate volumes. This occurs most frequently when the element is not numbered properly.
- Elements may be numbered either as shown in figure above: SOLID95 Geometry or may have the planes IJKL and MNOP interchanged.

- An edge with a removed midside node implies that the displacement varies linearly, rather than parabolically, along that edge.
- Degeneration to the form of pyramid should be used with caution. The element sizes, when degenerated, should be small to minimize the stress gradients.

3.3 Boundary Conditions

Three different boundary conditions are imposed on the design model:

1) Symmetry boundary condition is applied to the structural symmetry plane (all area at Z=0).

2) Fixed support in X-axis and Y-axis on the position of one bearing. (fig-8)

3) Fixed support in X-axis on the position of another bearing. (fig-9)

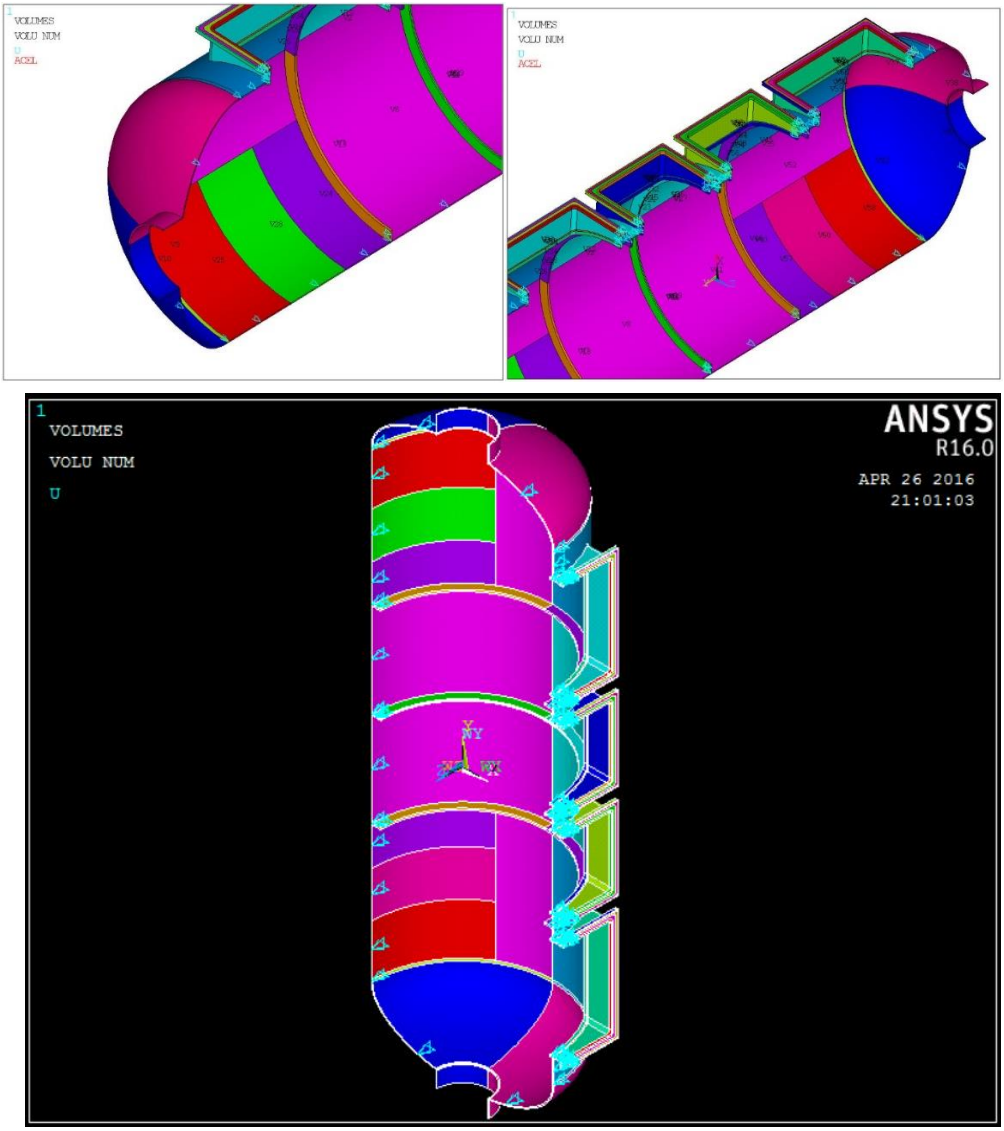

Figure 7: Symmetry constraint on the z-plane

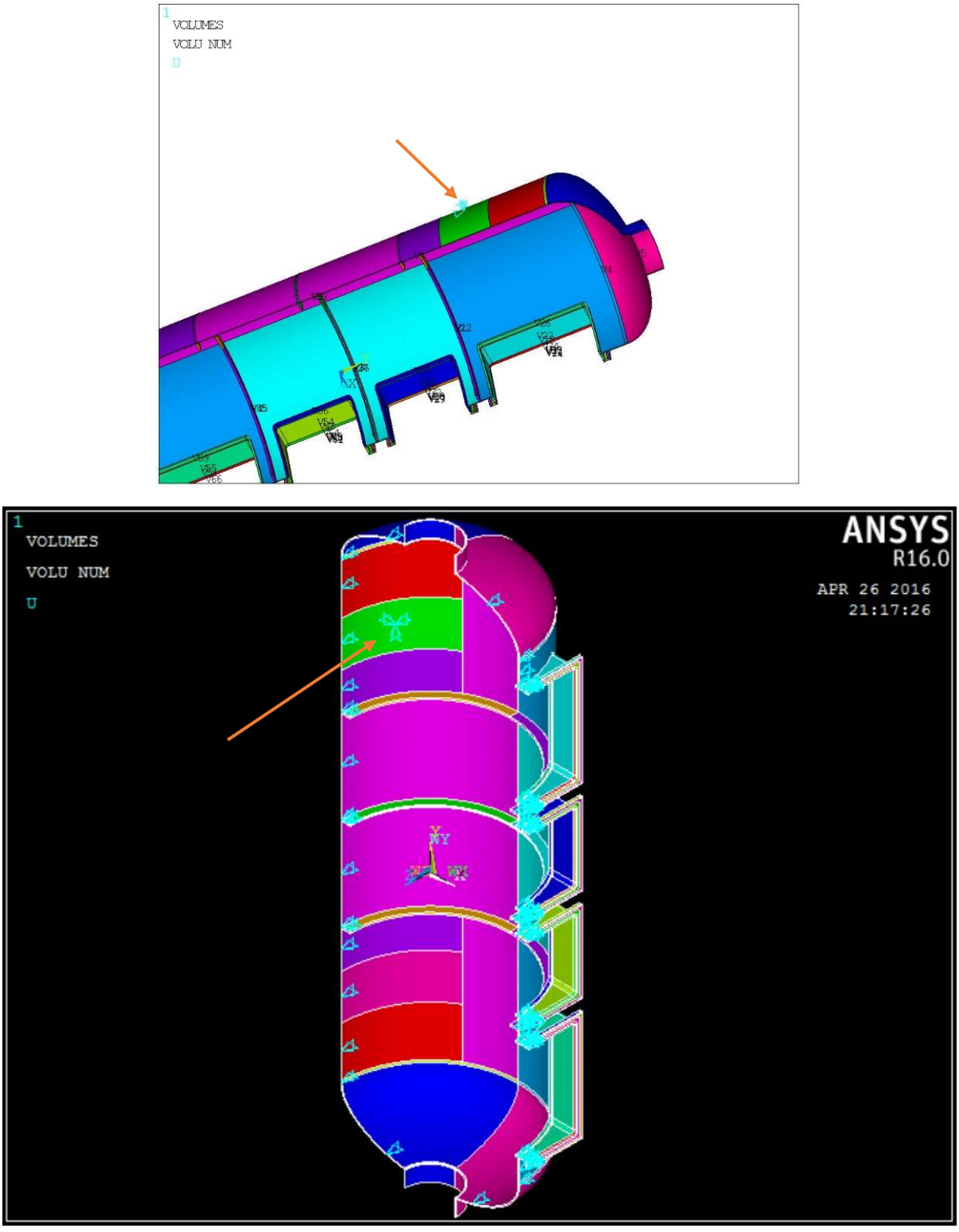

Figure 8: Fixed support on the position of 1st bearing

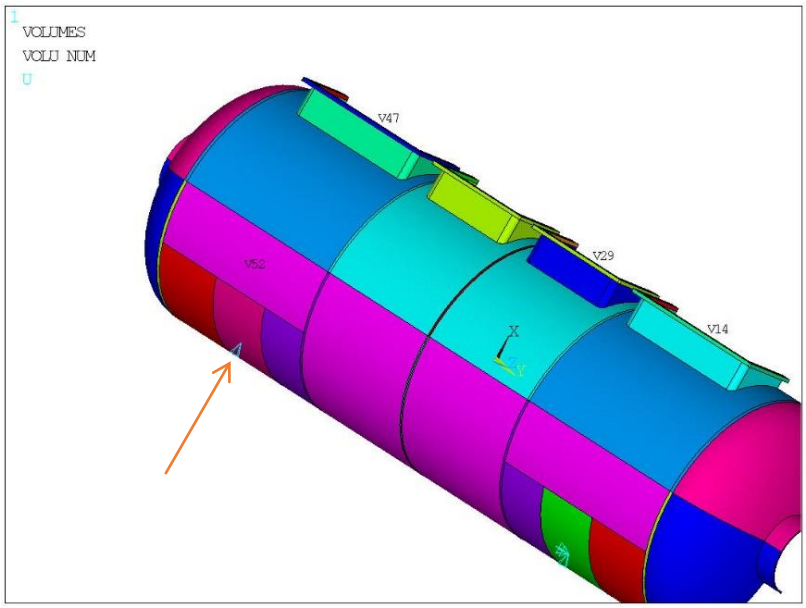

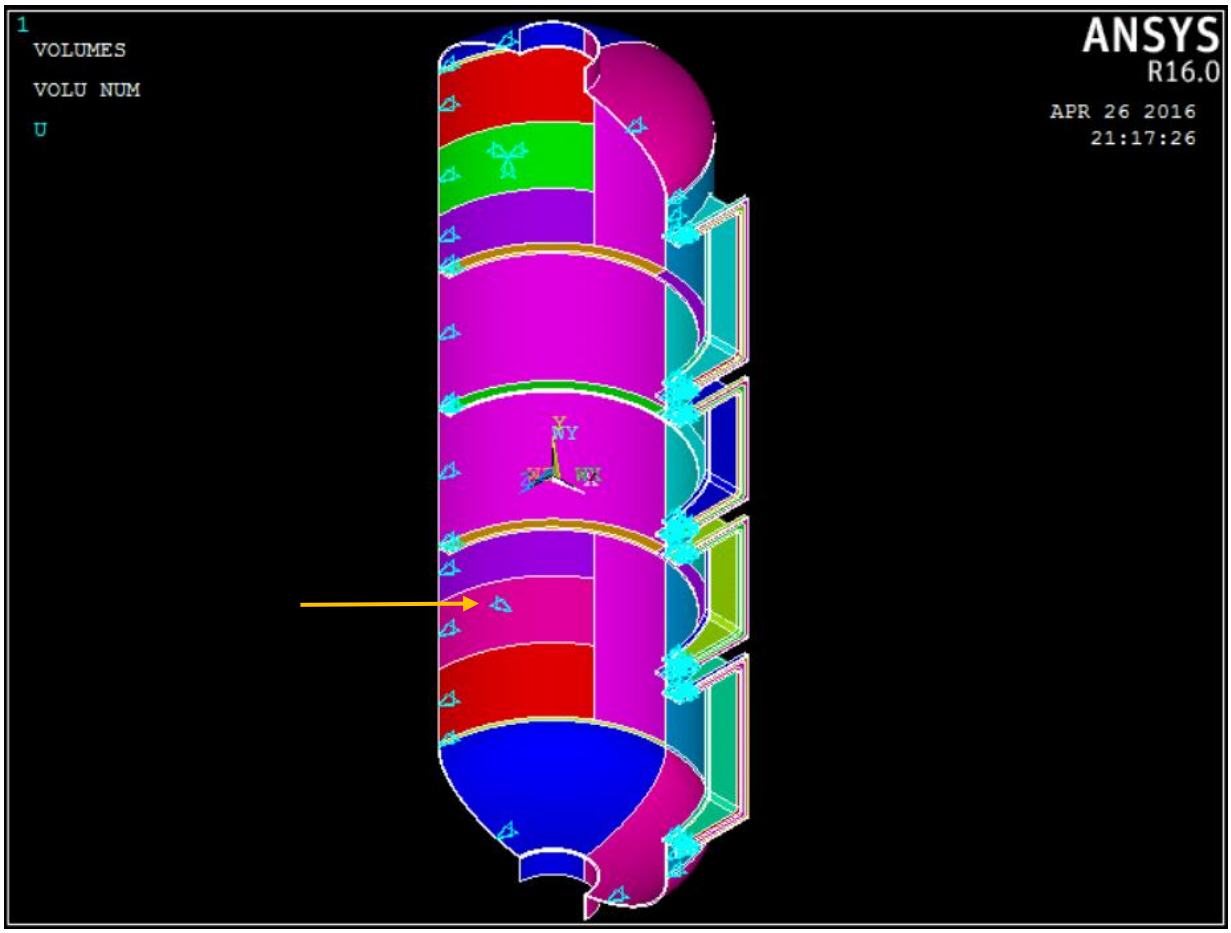

Figure 9: Constraint along X-axis on the position of 2nd bearing

3.4 Loadings

Seven different loadings conditions are applied on the pressure vessel model:

1) Acceleration due to gravity along X-axis. (figure-10)
2) Internal pressure of 0.2 MPa. (figure-11)
3) The average bolt pressure on the lower bolt surface (surface near the cylinder) of the two lateral flanges. (figure-12)
4) The average bolt pressure on the upper bolt surface (surface far away from the cylinder) of the two lateral flanges. (figure-13)
5) The average bolt pressure on the lower bolt surface (surface near the cylinder) of the two inner flanges. (figure-14)
6) The average bolt pressure on the upper bolt surface (surface far away from the cylinder) of the two inner flanges. (figure-15)
7) The pull on the cross section of the two end nozzles. (figure-16)

3.4.1 Gravity along X-axis

Gravity in negative X-axis, -9.8 m/s2 (So it is acceleration in forward of X-axis, 9.8)

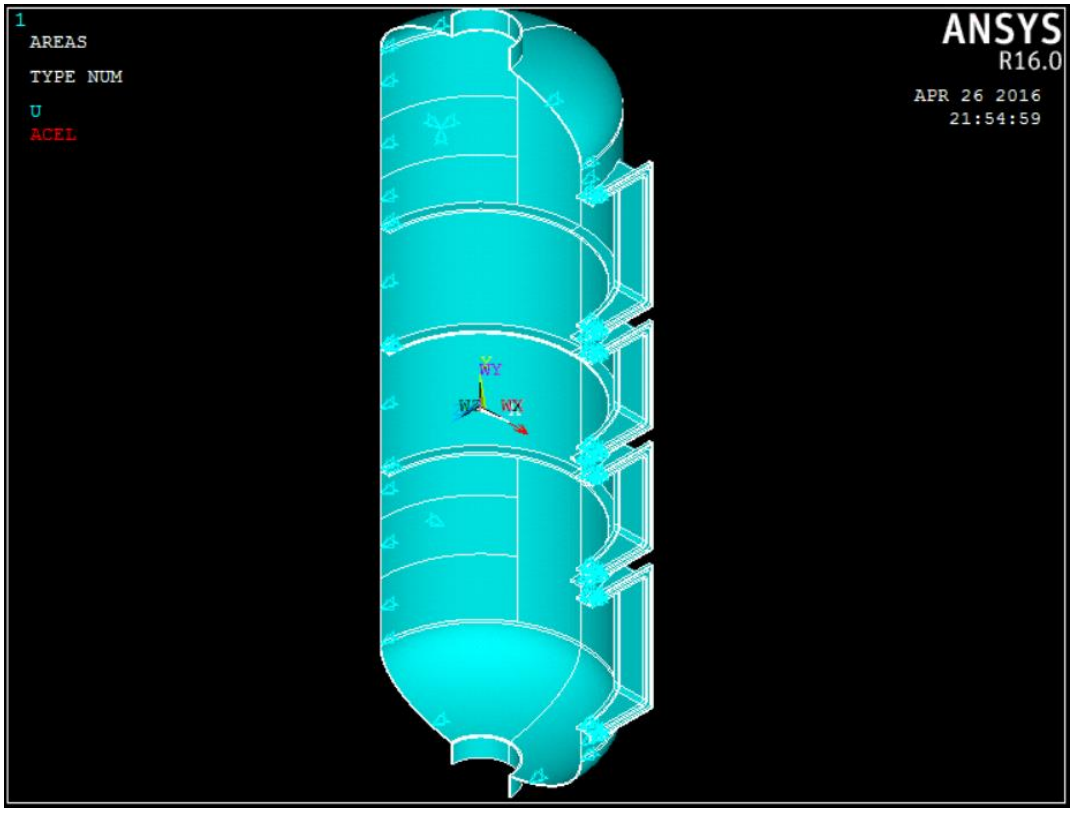

Figure 10: Acceleration due to gravity

3.4.2 Internal Pressure

The Pressure Vessel holds an internal pressure of 0.2 MPa.

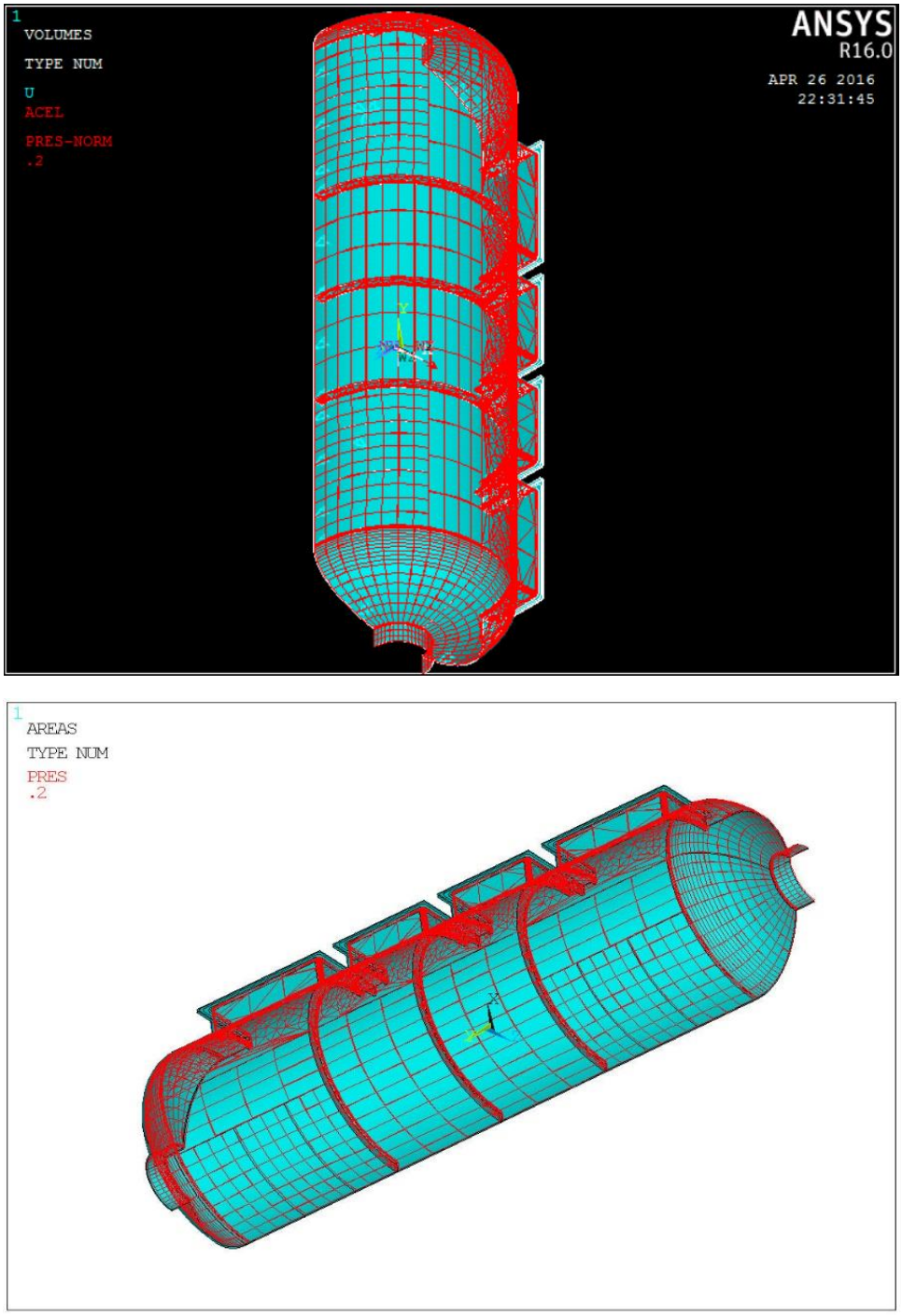

Figure 11: Internal Pressure of 0.2 MPa

3.4.3 The average bolt pressure on the lower bolt surface of the two lateral flanges

The average bolt pressure on the lower bolt surface (near the cylinder) of the two lateral flanges. On one flange, the total force is 193623 N, the area is 78100 mm^2, the pressure is 2.479162149 MPa.

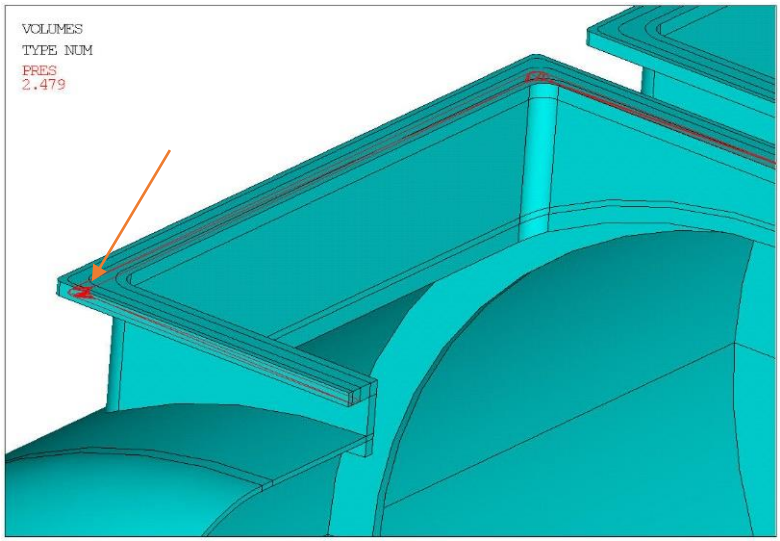

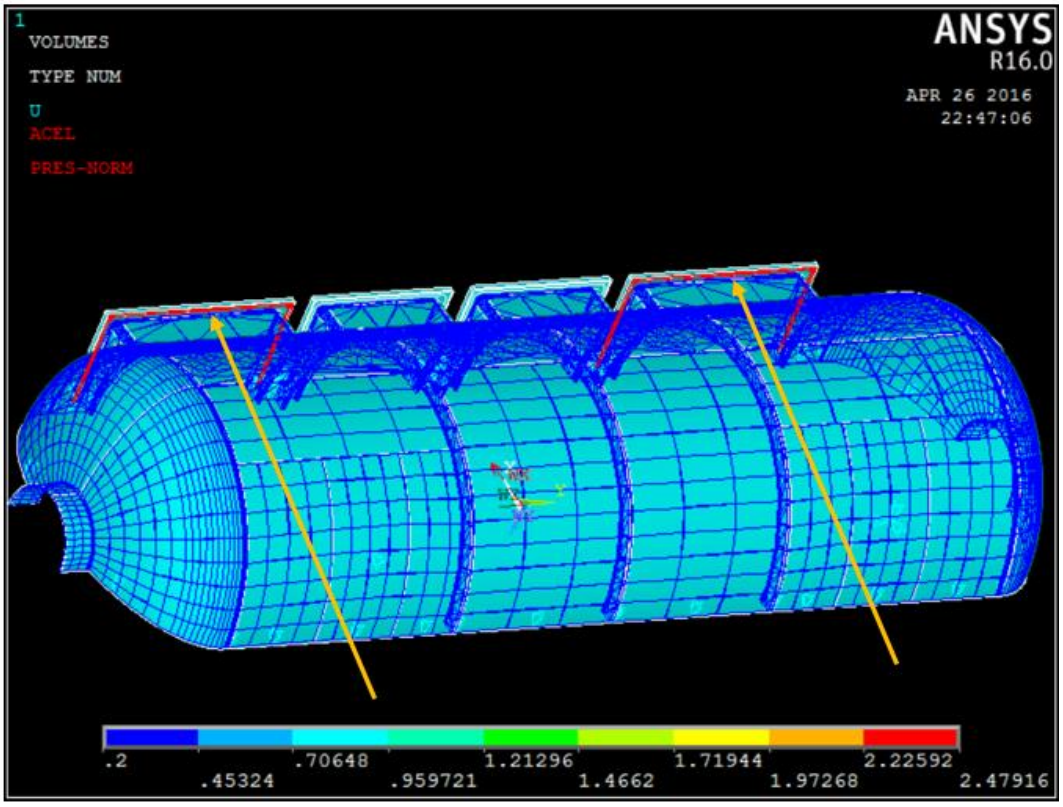

Figure 12: Bolt pressure on the lower bolt surface of the two lateral flanges

3.4.4 The average bolt pressure on the upper bolt surface of the two lateral flanges

The average bolt pressure on the upper bolt surface (far away from the cylinder) of the two lateral flanges. On one flange, the total force is 19397 N, the area is 78100 mm2, the pressure is 0.2483645393 MPa.

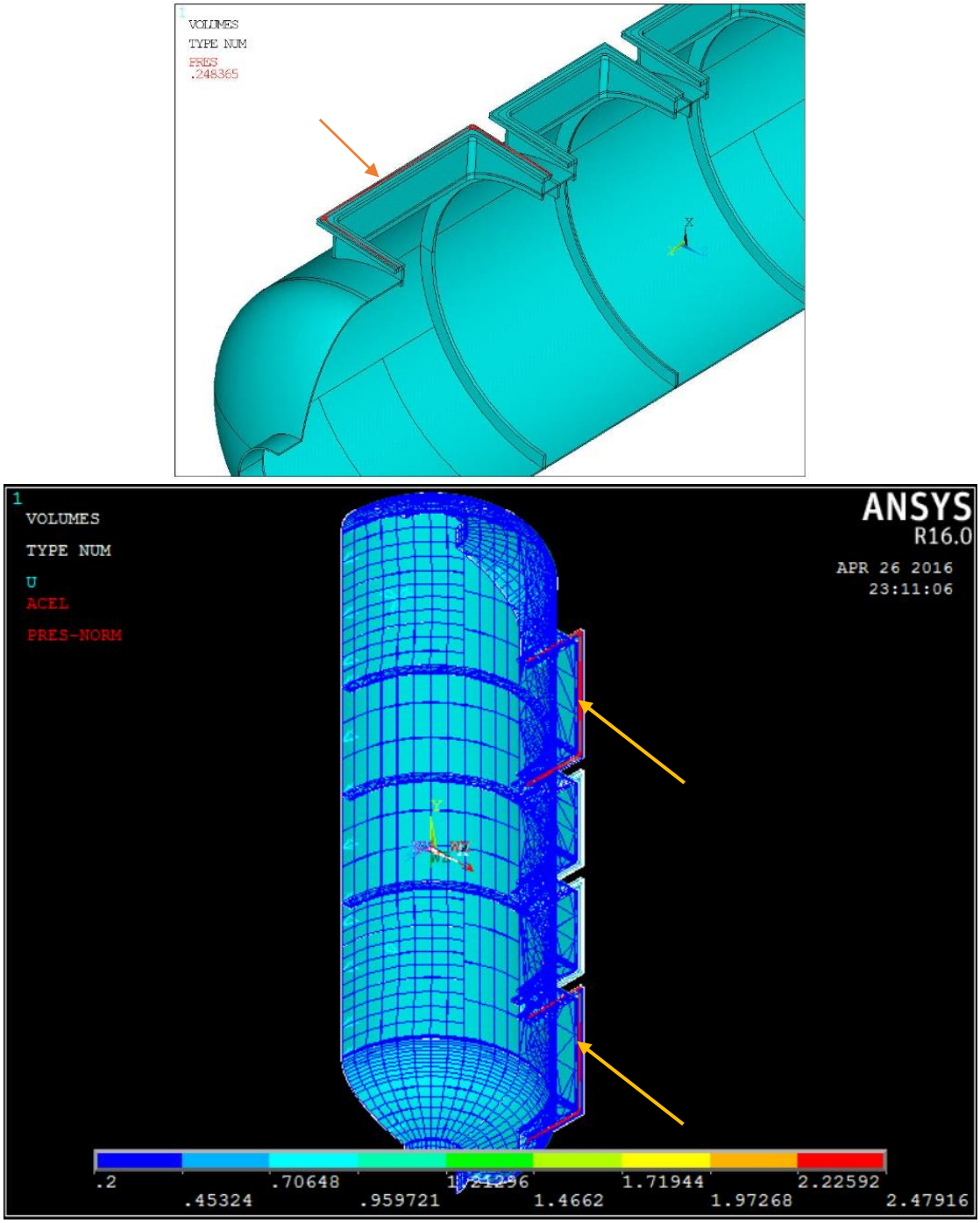

Figure 13: Bolt pressure on the upper bolt surface of the two lateral flanges

3.4.5 The average bolt pressure on the lower bolt surface of the two inner flanges

The average bolt pressure on the lower bolt surface (near the cylinder) of the two inner flanges. On one flange, the total force is 143408 N, the area is 67740 mm2, the pressure is 2.117037053 MPa.

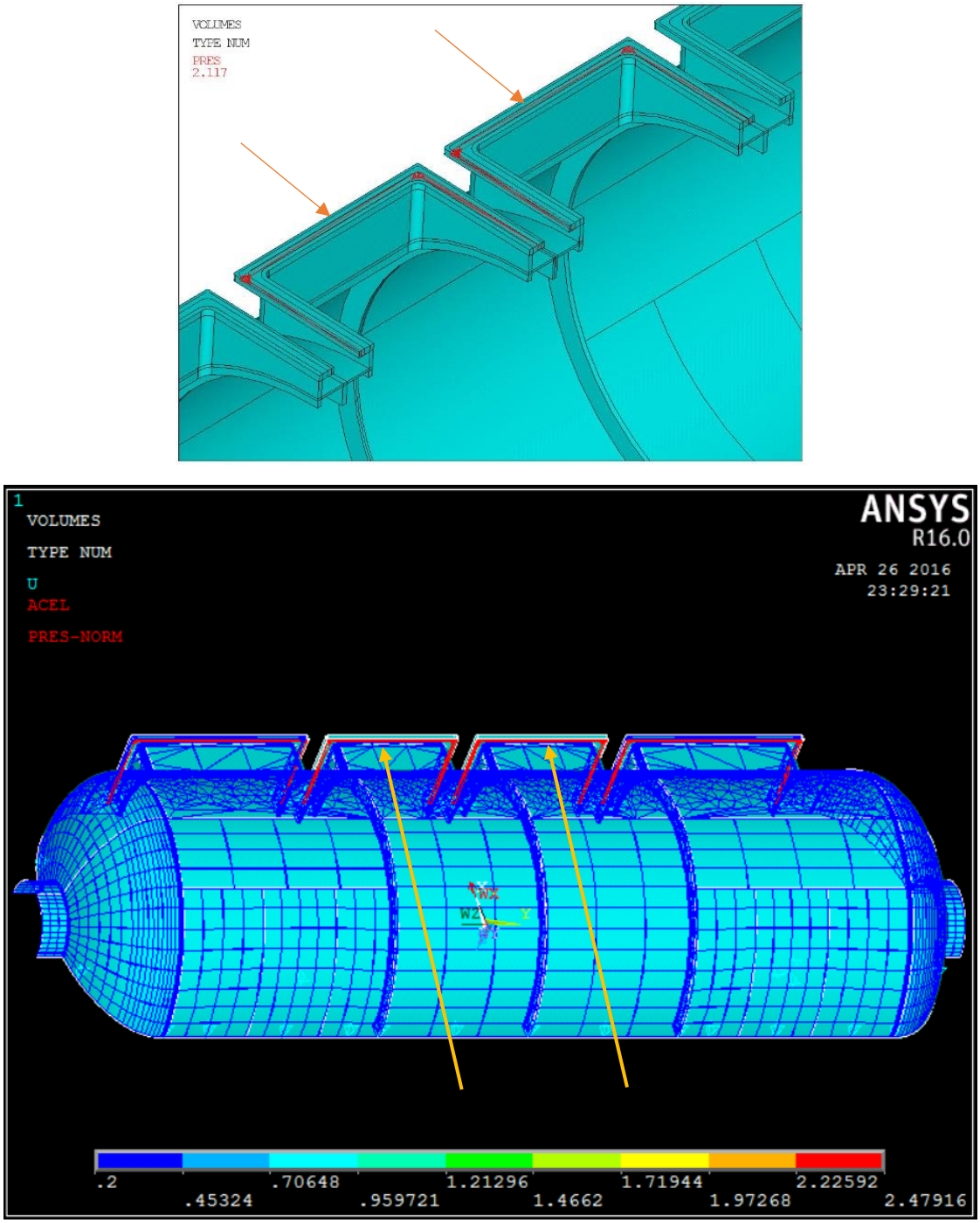

Figure 14: Bolt pressure on the lower bolt surface of the two inner flanges

3.4.6 The average bolt pressure on the upper bolt surface of the two inner flanges

The average bolt pressure on the upper bolt surface (far away from the cylinder) of the two inner flanges. On one flange, the total force is 19400 N, the area is 67740 mm2, the pressure is 0.2863877948 MPa.

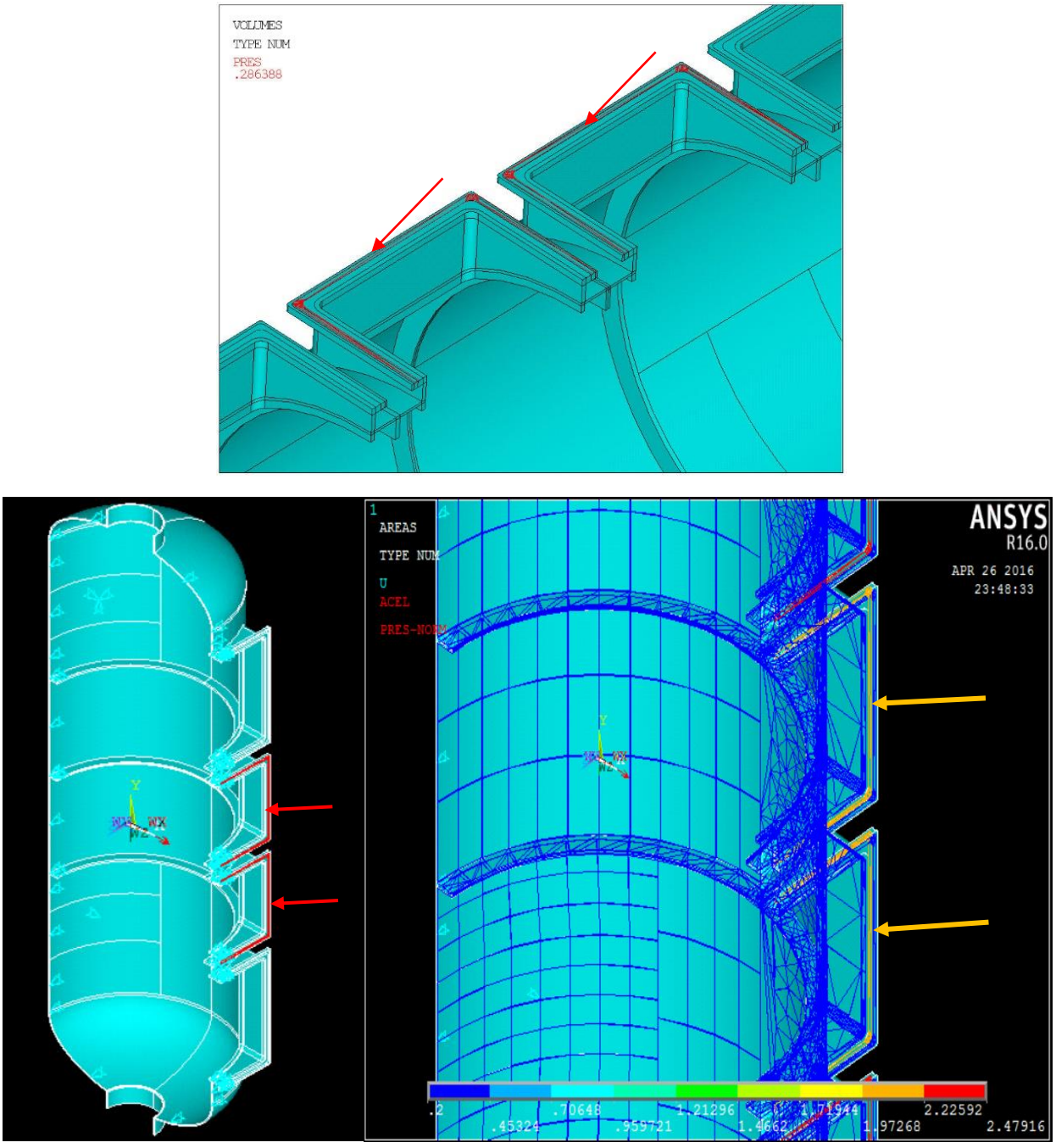

Figure 15: Bolt pressure on the upper bolt surface of the two inner flanges

3.4.7 The pull on the cross section of the two end nozzles

The pull on the cross section of the two end nozzles (Compensate for the gas pressure on the cross section). On one nozzle, the total force is -40856 N, the area is 16336 mm2, the pressure is -2.500961538 MPa.

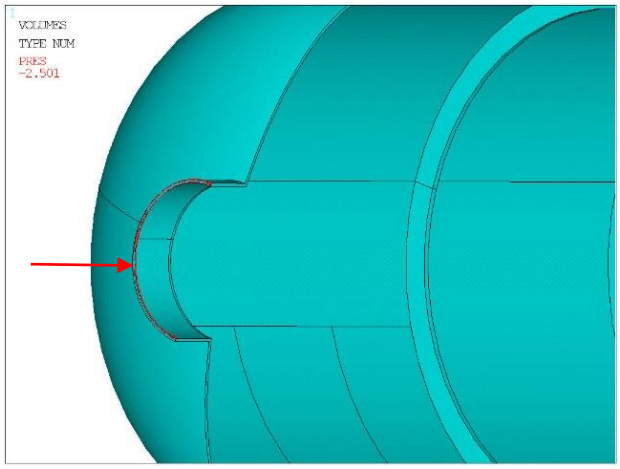

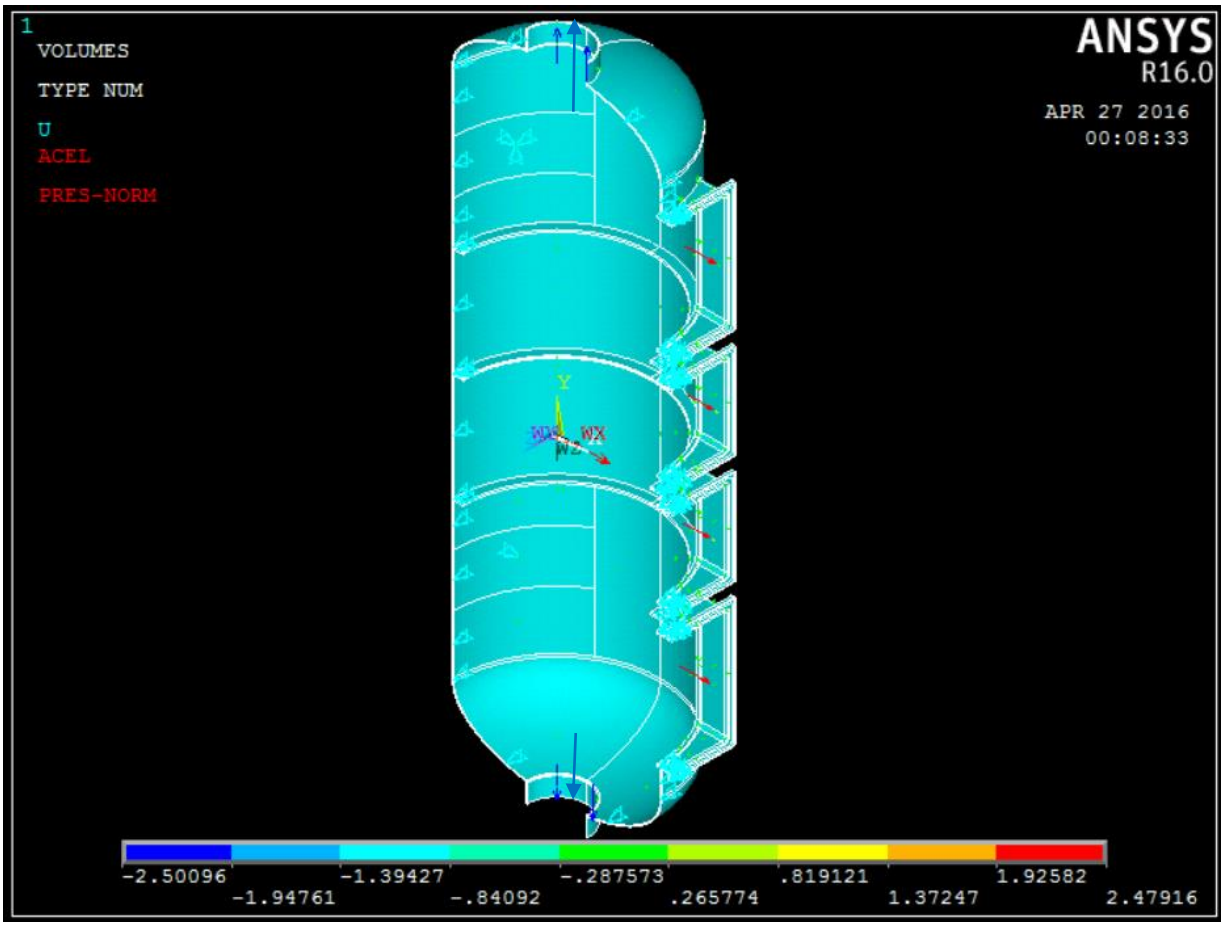

Figure 16: The pull on the cross section of the two end nozzles

3.5 Meshing

Meshing is one of the most important aspect of finite element analysis. The accuracy of the FEA results predominantly depends on the mesh size and element quality. The larger the density of meshing, the greater is the accuracy of the geometry and greater is the difficulty in solving the problems. Therefore, a preferred meshing approach is to employ fine meshes only in the area of focus whereas larger meshes should be used in the region where we expect relatively low activity. The pattern and relative positioning of the nodes also affect the solution, the computational efficiency & time. This is why good meshing is very essential for a sound computer simulation to give good results.

For the pressure vessel model, besides four volume block, the entire model was meshed with 20-node Brick elements. Since these four volumes does not meet the hexa-meshing criteria, they were meshed with 10-node tetrahedral elements. The ANSYS software automatically uses pyramid elements as filler elements in between the mesh transition zones. The Hexahedral meshed model of the pressure vessel used during optimization is shown below in figure-19.

3.5.1 Tetrahedral Mesh VS Hexahedral Mesh

Unlike tetrahedron meshing that can be performed on nearly any geometry, hex meshing (Brick elements) requires a certain amount of topology cleaning and decomposition to achieve an all or nearly all brick mesh. This type of meshing is generally preferred when less nodes and elements are required but need to achieve high solution accuracy. A brick meshed model can save orders of magnitudes of CPU time and require significantly less RAM and disk space over an all tetrahedron mesh with often better accuracy. But the downside of Brick meshing or a hexahedral mesh is that it is very difficult to generate for a complex geometry because it requires map meshable sides to sweep through the volume.

The figure-17 displayed below shows a tetra mesh of the pressure vessel model. Ten node tetrahedral elements were used to produce the tetra mesh model. For free meshing, a smart sizing level-2 was set to obtain a very fine mesh with better element quality. Whereas, a hexa-mesh model was produced by sweep meshing the volumes. The total vessel volume was split into different blocks for more control and to meet topology requirement of map meshable sides. The element sizes generated on swept volume were defined by assigning line divisions, taking into account curvature of the line, its proximity to holes, element order and other features. Below mentioned guideline was followed to achieve the volume sweep.

1. The source and target faces for all sweepable bodies are automatically detected by the ANSYS software. If desired, the user can specify the source/target faces manually.
2. All source/target face topology needs to be same for all sources/targets.
3. All side faces need to be able to be mapped meshed.

It is evident from the figures below, that the tetra meshed model contain eight times more elements compared to the number of elements in brick meshed model. The stress results obtained from both the meshes are more or less similar but the time taken to solve the tetra-meshed model is about five times more when compared to the computational time taken to solve the brick meshed model.

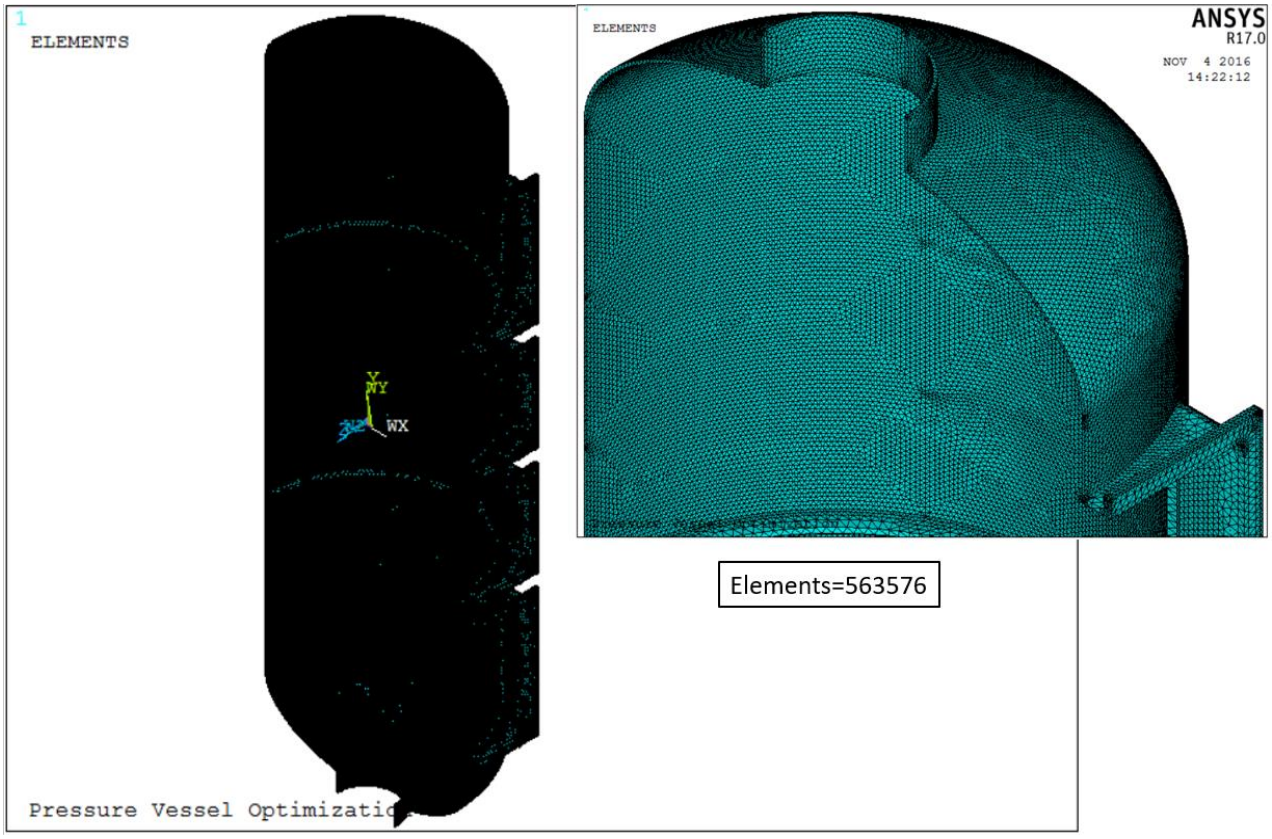

Figure 17: Tetra-meshed Model of the Pressure Vessel

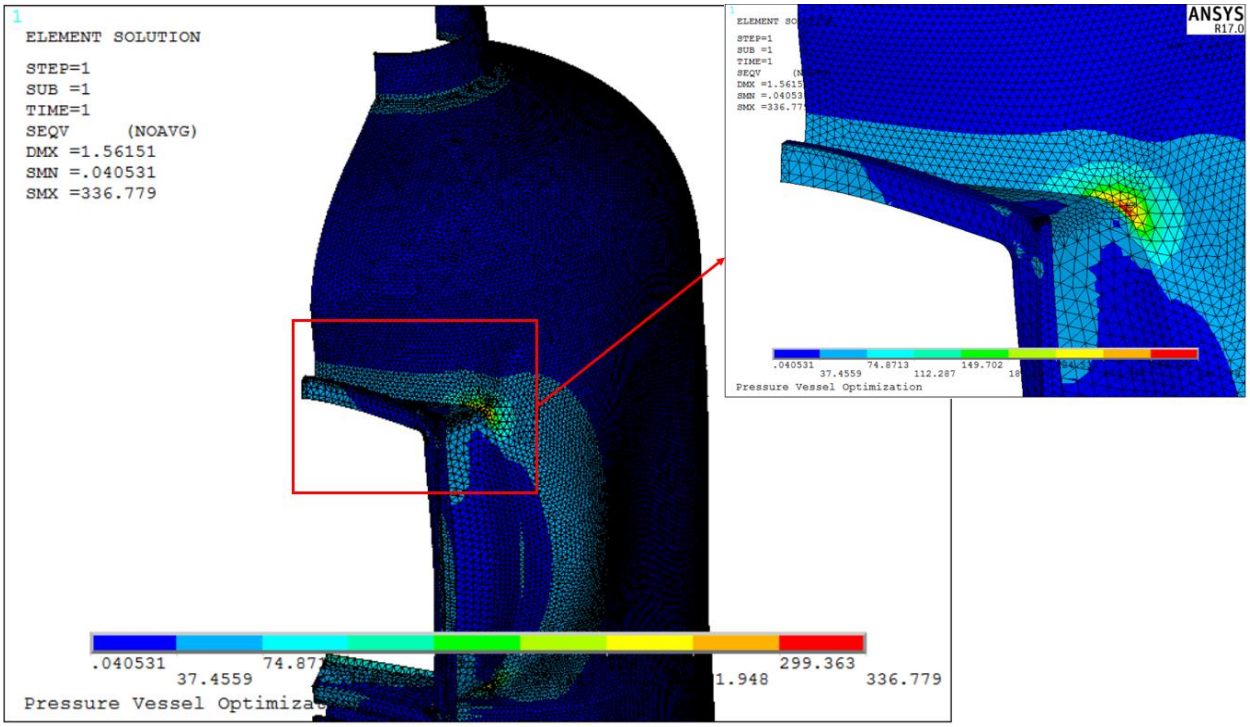

Figure 18: Unaveraged Von-Mises Stress Contour for Tetra-meshed Model

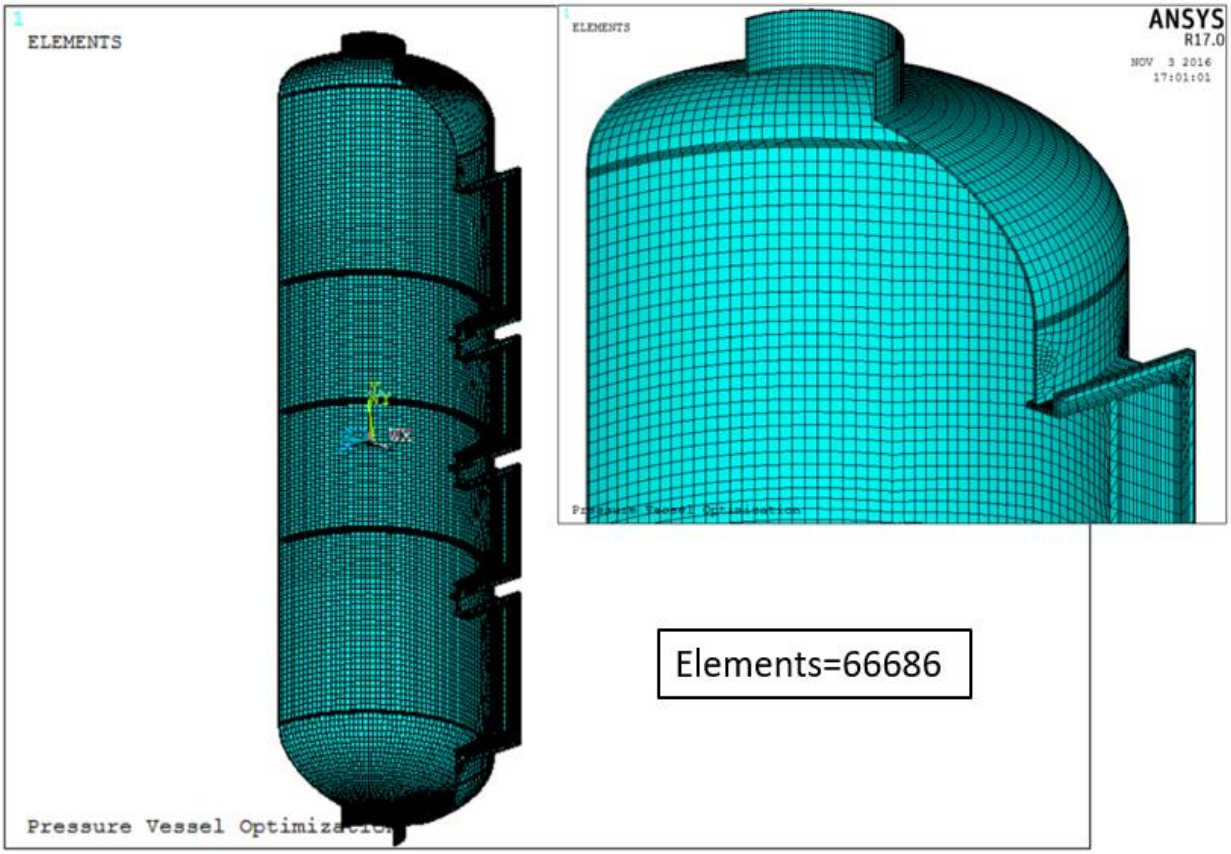

Figure 19: Brick-meshed Model of the Pressure Vessel

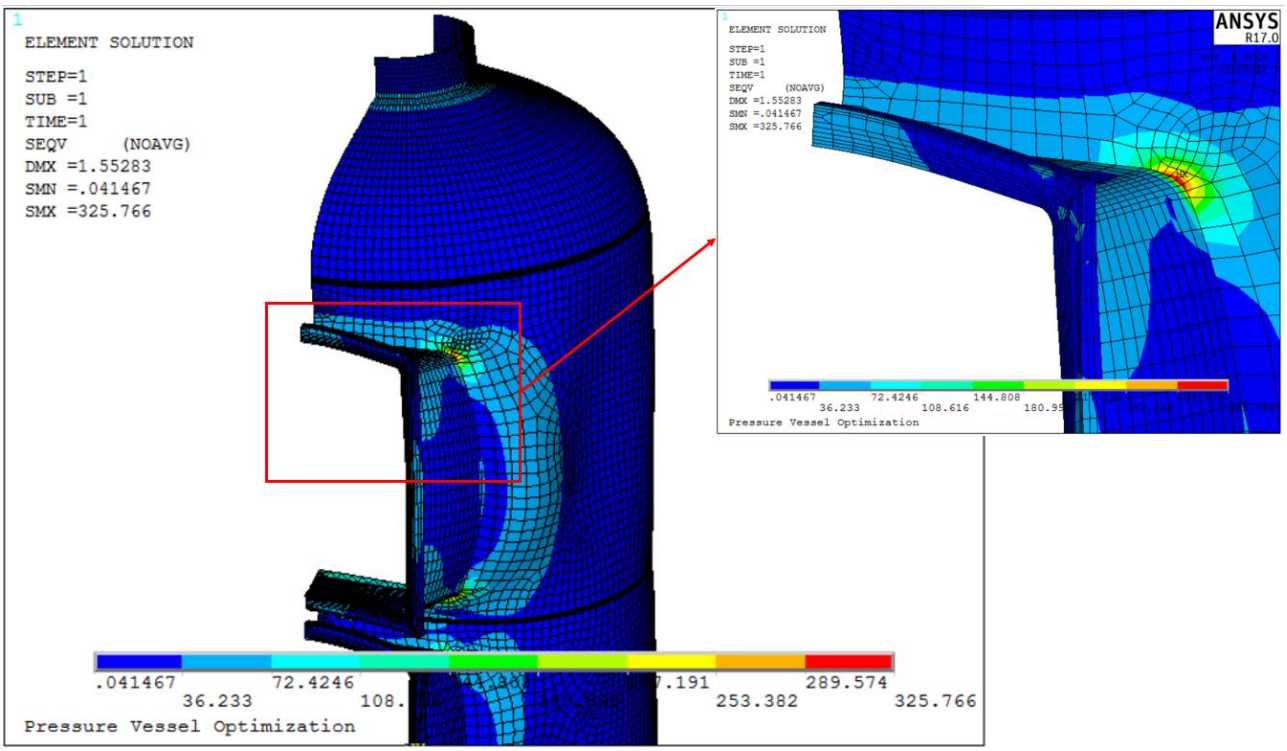

Figure 20: Unaveraged Von-Mises Stress Contour for Hexa-meshed Model

3.5.2 Comparison between free mesh and controlled mesh

The figure 21 to 24 below displays the comparison between a free and a controlled brick mesh of the pressure vessel model. During free mesh, line divisions are not considered and the software automatically determines the size and number of elements generated through the swept volumes. Whereas, the controlled mesh is created by specifying number of line divisions on the sweepable faces of the model geometry to produce different element sizes on different components of the pressure vessel. Latter is preferred as it gives more control over the mesh size and element quality. Note that, the free mesh generated by ANSYS, has less number of elements when compared to elements in controlled mesh model. Although controlled mesh increases the number of brick elements, the computational time taken to solve this model in a 16GB RAM system is approximately same when compared to the time taken to solve free mesh model. We also achieve a high solution accuracy due to the increased number of elements. Hence, controlled brick meshed model is preferred for the finite element analysis as well as during the optimization run.

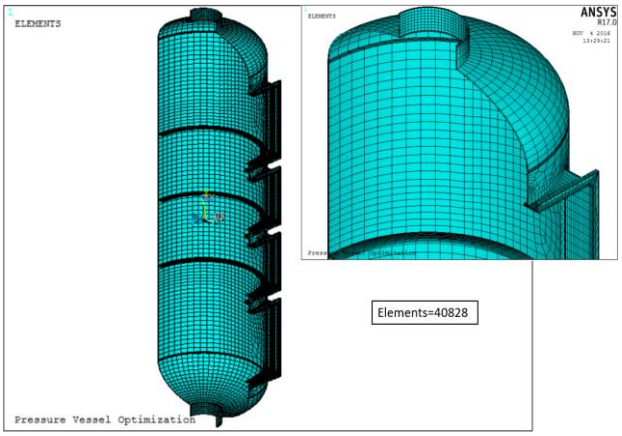

Figure 21: Free mesh with Brick elements

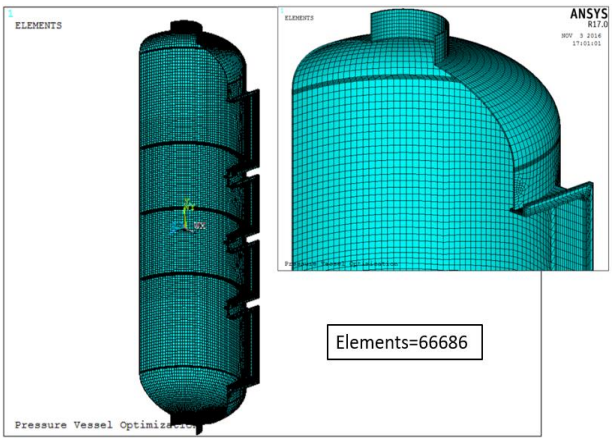

Figure 22: Controlled mesh with Brick elements

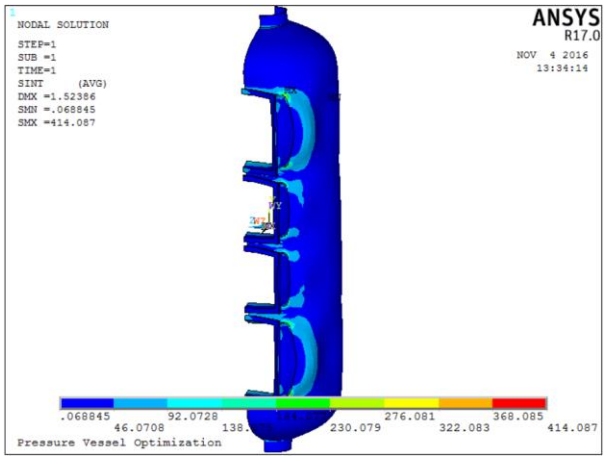

Figure 23: Stress Intensity for Free Hexahedral mesh

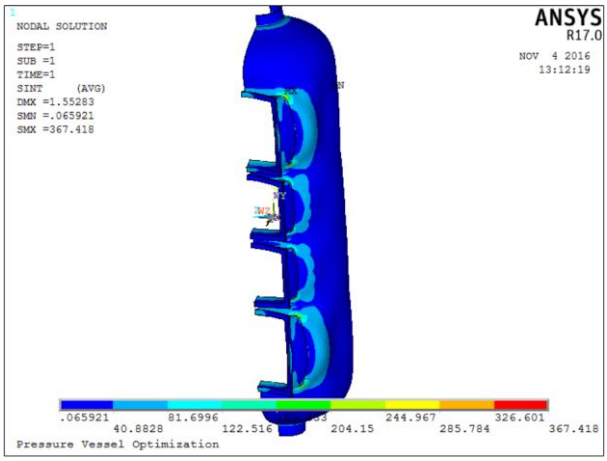

Figure 24: Stress Intensity for Controlled Hexahedral mesh

3.5.3 Mesh Convergence and Stress Singularity

A mesh convergence study when performing Stress Analysis is necessary to instill confidence in FEM results from the standpoint of mathematics. As we progressively refine the mesh, the size of the elements reduces, which theoretically increases the solution accuracy and given enough iterations it converges towards a specific result. If there is an analytical solution for the given problem, the mesh refinement procedure will converge towards the exact solution. As mesh elements decrease in size but increase in quantity, the computational requirements to solve a given model increase. As mesh elements decrease in size, they reach a point of diminishing returns on the level of accuracy compared to the computational overhead and time required to compute the result. This means that a simulation requires much more time to compute the results, but the result may change by an insignificant value. Hence, to overcome this problem, mesh

convergence study is performed to determine a mesh with minimum number of elements required to maintain a satisfactorily balance between accuracy and computing resources.

However, as shown in table-5 and figure-25 below, the mesh convergence study when applied to the 20-node brick meshed pressure vessel model resulted in non-convergence. The stress solution does not converge with mesh refinement because of the stress singularity present at the joint corner of cylindrical shell body and nozzle. A stress singularity is a point of the mesh where the stress does not convergence towards a specific value. As we keep refining the mesh, the stress at this point keeps on increasing. Theoretically, the stress at the singularity is infinite. Typical situations where stress singularities occur are the appliance of a point load, sharp re-entrant corners, corners of bodies in contact and point restraints. These singularities occurs often in pressure vessel and boiler designs is practically unavoidable.

Since the pressure vessel model is analyzed as whole structure, the stress singularity at the filleted corner is of importance. The mesh around this region is refined locally to capture the effects of high stress concentration. Despite of removing sharp re-entrant edges by filleting the corners, the stress concentration around these corners increases with increase in the elements. However, displacement solution does converge to a value of 1.56 mm. Through path operations for critical stress concentration lines at stress singularity region, we can predict probable value of true stress at the elements near this singularity. While running the optimization loop, mesh density of the pressure vessel model was kept fixed and the stresses evaluated near the singularity were verified against the allowable local stress limits. The path operations and stress limits are discussed in the next chapter. The figures 26-30 displayed below, shows the increase in maximum local unaveraged von-mises stress with the increase in number of elements at the corner of the nozzle and shell body joint.

Table 5: Mesh Convergence Results

No. of Elements	**Maximum unaveraged Von-Mises Stress** (MPa)
66686	325.76
95363	339.37
110604	381.94
143492	437.58
170770	449.09

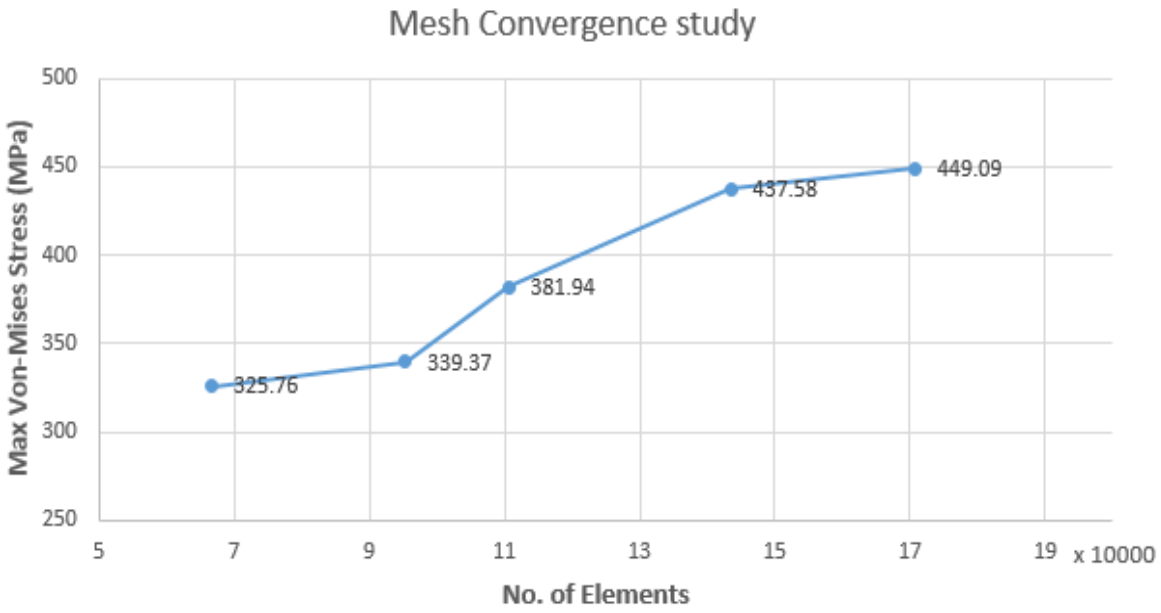

Figure 25: Mesh Convergence Plot

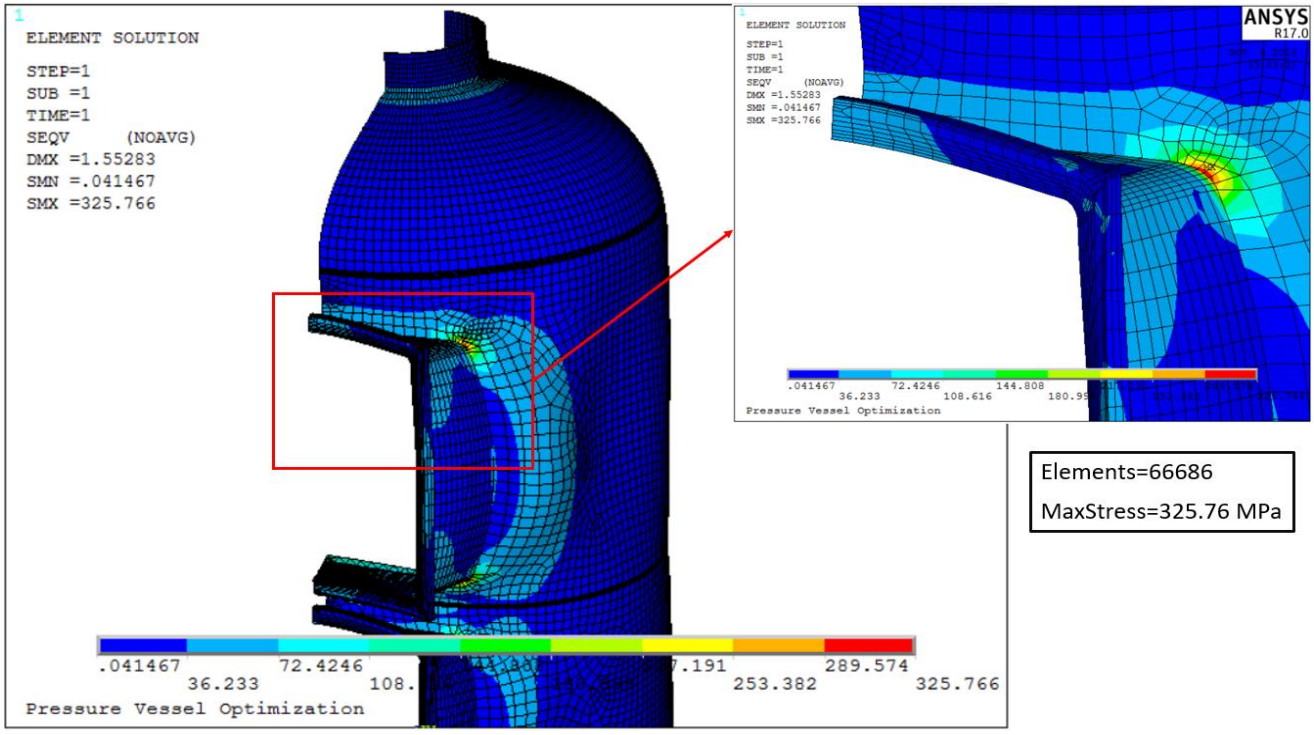

Figure 26: Maximum Local Unaveraged Von-Mises stress

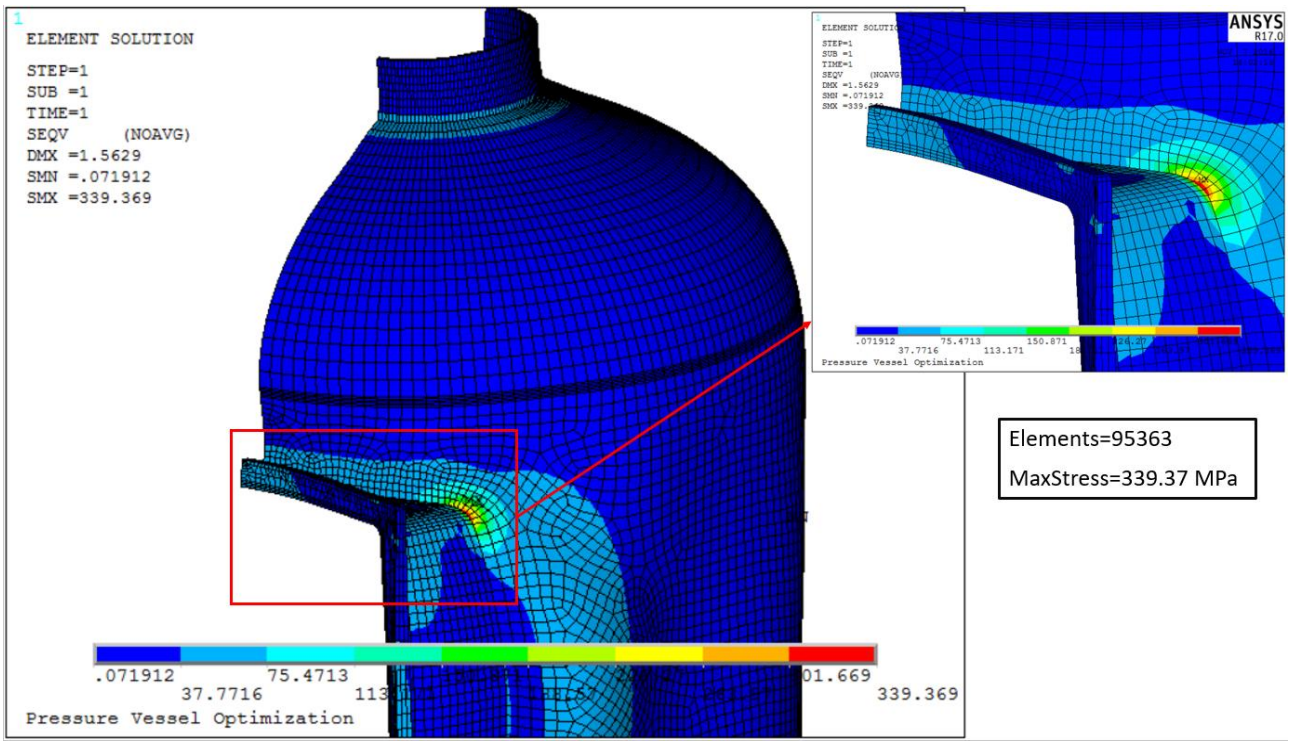

Figure 27: Increase in Maximum Local Unaveraged Von-Mises stress for mesh refinement-1

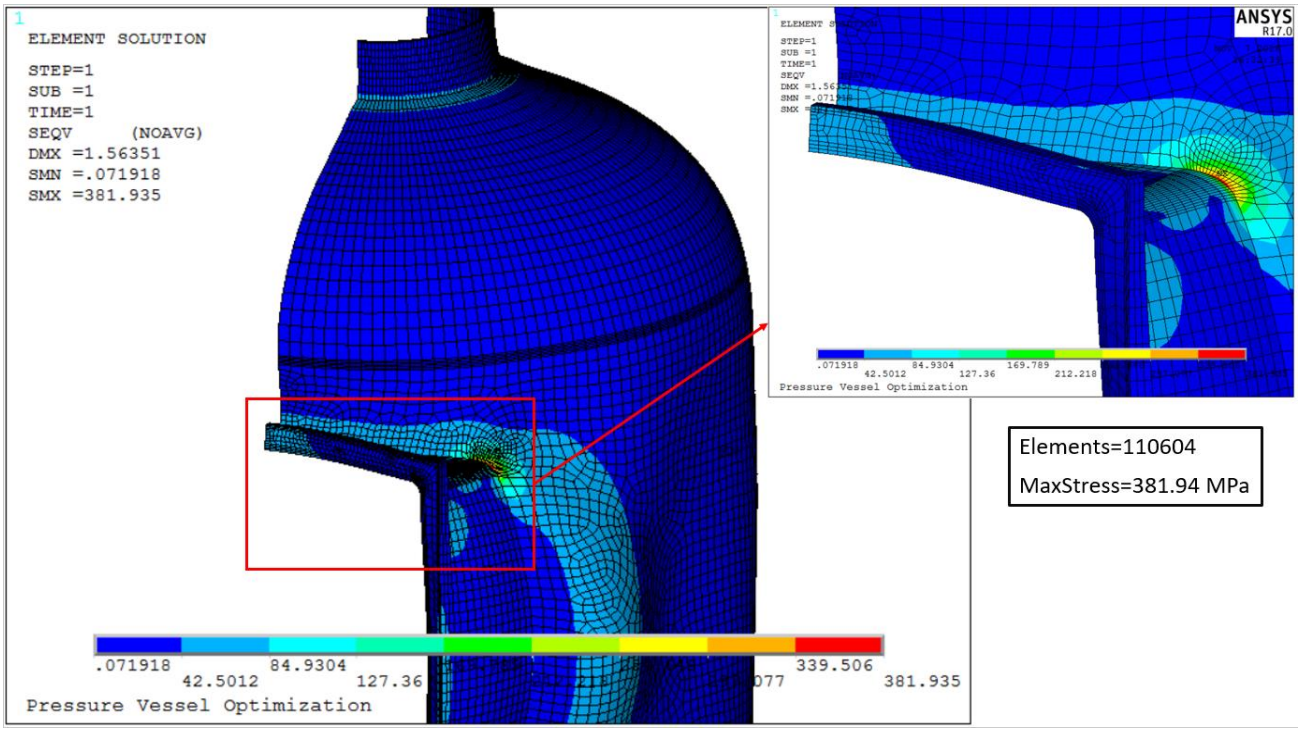

Figure 28: Increase in Maximum Local Unaveraged Von-Mises stress for mesh refinement-2

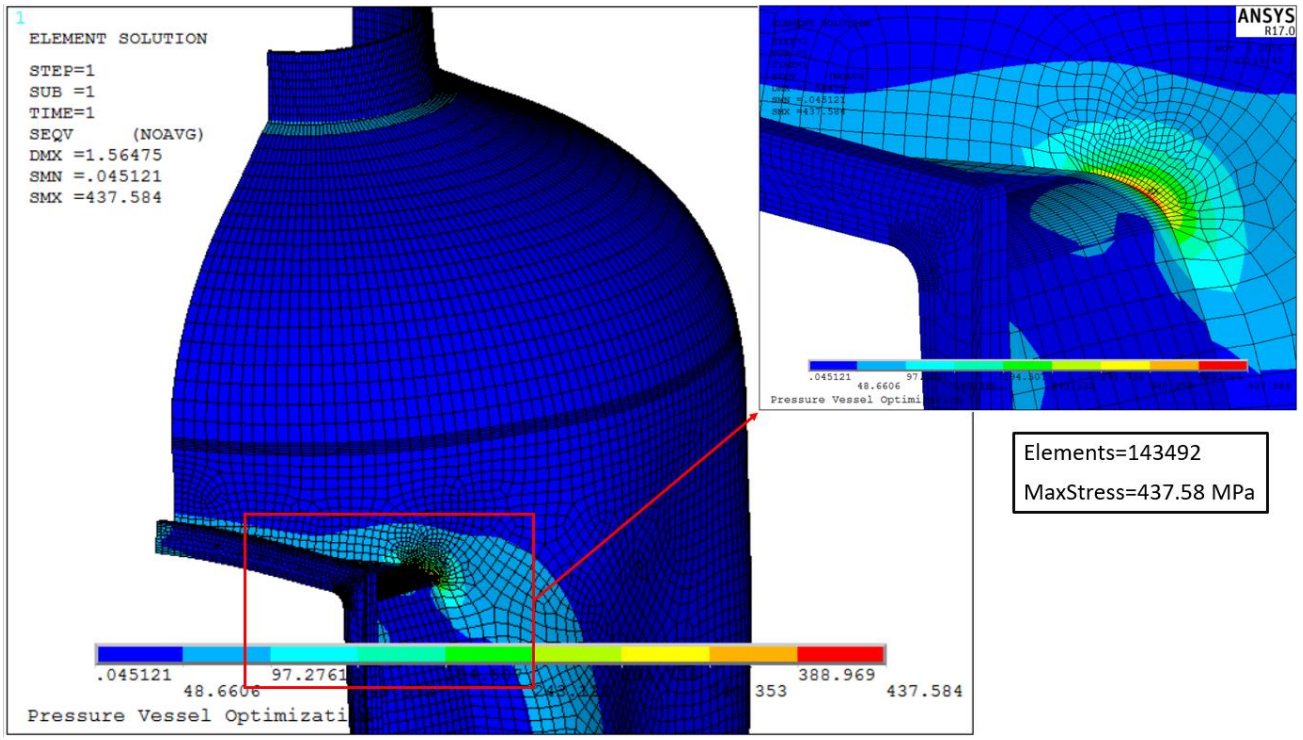

Figure 29: Increase in Maximum Local Unaveraged Von-Mises stress for mesh refinement-3

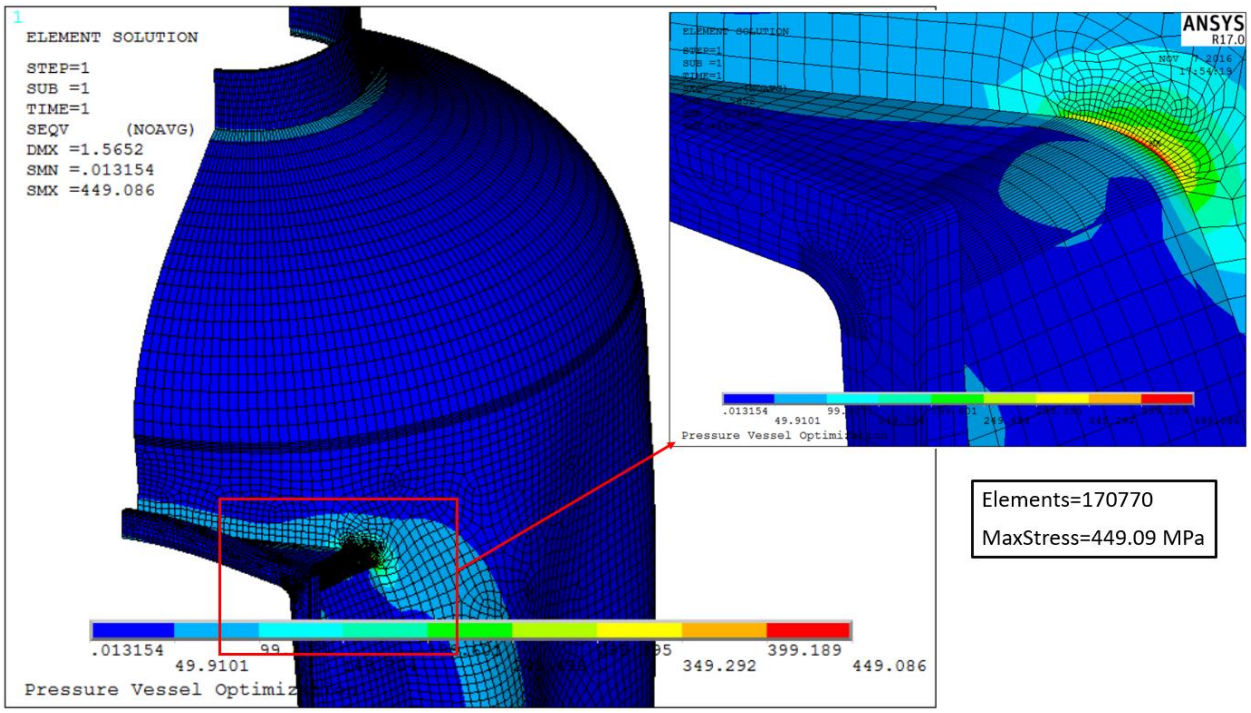

Figure 30: Increase in Maximum Local Unaveraged Von-Mises stress for mesh refinement-4

CHAPTER 4: Stress Analysis and Verification

4.1 Introduction to ASME Boiler and Pressure Vessel – Verification Code

Relevant Codes of Practice, Industry Standard and/or Statement of Assessment Criteria:
ASME Boiler and Pressure Vessel Code, Section VIII, Rules for Construction of Pressure Vessels, Division 2

Boilers and pressure vessels are used worldwide in various industries. They are naturally present in the power engineering and gas engineering sectors. In order to ensure the safety and operational efficiency of these vessels, necessary legal regulations have been developed by the American Society of Mechanical Engineers (ASME). These regulations constitute the basis for design and manufacture of these equipments.

One of the most important goal in a pressure vessel design is to assure safe and satisfactory performance of the vessel. The ASME pressure vessel code is based on the observed safety of vessels. The observations were turned into design rules and the vessels became safer through their efforts. It is a real world working standard – its roots were born of failed vessels and dead operators in an era long before concepts like stress concentrations were even known.

The ASME 'Design by analysis' code, particularly in its Section VIII division-2, has specific requirements on how to assess the results from the stress analyses to make the necessary verifications to avoid failure. They wrote the VIII-2 rules and developed the stress linearization method as a guideline to check for the safe design. This division covers the mandatory requirements, specific prohibitions and nonmandatory guidance for materials, design, fabrication, inspection and testing, markings and reports, overpressure protection and certification of pressure vessels having an internal or external pressure which exceeds 103 KPa. These requirements apply to those equipments which are part of the pressure boundary for example valves, pumps, pressure vessels, piping, etc. In this work, only the maximum allowable stress verifications were made as per the ASME code. Stress linearization method was implemented to verify the design of pressure vessel equipment under study. The details of the ASME codes are not included in this report. The reader is encouraged to the read the ASME related reference material mentioned at the end of this report.

4.2 Stress Linearization

Generally, the prototypes and models used in the analyses are developed with 2D plane or 3D solid finite elements, and membrane and bending stresses cannot be evaluated directly from the FEA results for these types of elements. Due to this fact, no direct comparison with the code limits

can be done and, besides that, the commercial finite element software's like ALTAIR, ANSYS, ABAQUAS, etc do not distinguish between primary and secondary stresses. Therefore, to implement the required ASME Pressure Vessel and Boiler Code stress verifications for our finite element model, we should perform stress linearization to extract the membrane and bending stresses from the 3D solid model and, also, should classify these stress components as primary and secondary for the purpose of stress verification against the ASME allowable limits.

Linearization is a decomposition of the stress distribution we see in FEA of pressure vessels. It decomposes a basically parabolic distribution into a uniform value (membrane stress), a linearly varying value (bending stress), and possibly an extra component (peak stress). The stress linearization is performed along a stress classification line. The stress classification line (SCL) are created to linearize the stresses along a line, usually cutting through the thickness of the component. A Stress Classification Line or SCL is a straight line defined by two nodes/points, usually more or less perpendicular to both the inside and outside surfaces. Stress components through the section/SCL are linearized by a line integral method and are separated into constant membrane stresses, bending stresses varying linearly between end points, and peak stresses (defined as the difference between the maximum and minimum principal stress). The stress linearization tool takes the nodal data for the complex stress pattern found along this line and breaks it down into membrane and bending stress components.

Stress Linearization is used to comply with design codes and requirements of the pressure vessel industry. However, applicability of the utility is not limited to pressure vessels. You can use this method to graph local stress tensors along a linear path and/or to determine the relative contributions of bending and membrane stress for any type of structure. Stress linearization is not required in the models with beam or shell elements because these elements naturally give the stresses separated in membrane and bending components.

Note:

- Stress linearization is available for brick, tetrahedral, plate, shell, and 2D elements, with or without mid-side nodes.
- Stress linearization is available for all linear and nonlinear analysis types that produce stress results.
- Stress Classification lines are created as paths in ANSYS.

4.3 Stress Classification

The purpose of stress classification is to identify the Primary(P) and the Secondary(Q) stresses. Primary stresses are defined as the stresses developed by an imposed loading that is necessary to satisfy the laws of equilibrium in terms of the external and internal forces and moments. Secondary stresses are the stresses that are developed by constraints due to geometrical discontinuities and self-constraint. The classification of stresses into primary and secondary categories separates the issues regarding overall strength, which is of primary importance and therefore referred to the realm of primary stresses, from the issues of local behavior, which is of secondary importance and therefore referred to the realm of secondary stresses.

It should be acknowledged that different kinds of stress have different degrees of significance and thus should have different safety implications. For example, the objective of primary stress limits is to prevent the loss of load-carrying capacity of the vessel, which is referred to as collapse whereas type of failure that a secondary stress may cause is ratcheting or incremental collapse. Hence, it is necessary to classify the stresses into different categories. The stress categories of interest for the design analysis of our pressure vessel model are the primary stress, and its subcategories of general and local primary membrane and bending stress, and the secondary stresses. The peak stress is related to the assessment of fatigue failure of the material and will not be used in our analysis.

For design purposes, the primary membrane stress is further divided into general primary membrane stress and local primary membrane stress subcategories. The average value acting on the whole section/line that is equivalent to the net force acting in the section due to the actual stress distribution will be classified as P_m or P_L depending on the distance of the section from the discontinuity: P_m for those far sections and P_L otherwise. This P_L classification is justified because there is a secondary ‘aspect’ in this stress near a discontinuity even if it comes from a mechanical load.

The maximum value of the linear stress distribution which produces a net bending moment equivalent to the moment produced by the actual stress distribution is called ‘bending stress’ P_b. For mechanical loads, if the section is near a discontinuity this stress component is classified as secondary, ‘Q’. The difference between the actual stress distribution and the sum of the average and linear (membrane + bending) stress distributions give an equilibrated stress distribution.

P_m – Generalized Primary Membrane Stress

P_L – Localized Primary Membrane Stress

P_b – Primary Bending Stress

F – Peak Stress

Q – Secondary Stresses

These steps, the stress classification and the stress linearization, are not straightforward ones and needs some 'engineering' judgment to choose the right section to evaluate the stresses in discontinuities. This task, most of the time is not a simple one due to the nature of the involved load and/or the complex geometry under analysis. In fact, there are several studies discussing on how to perform these stress classification and linearization.

4.4 Design Limits and Verifications

ASME Section VIII-2 provides a guide to what the maximum stresses are allowed for different locations of the pressure vessel. The combination of this ASME code and the output from the stress linearization and classification tool is used to produce pass fail judgments on the pressure vessel model. This will form the basis of constraint function in the optimization process.

As the ASME limits are developed aiming to prevent some typical failure modes besides the Primary and Secondary classification, the stresses should be linearized to obtain the generalized (P_m) or localized (P_L) membrane component, the bending (P_b) and the Peak (F) stress. Because different modes of failure are associated with primary membrane, primary bending and secondary stress, different allowable values are defined for each category. These are not given as absolute values in the pressure vessel codes, but as a proportion of the basic allowable stress intensity of the material (Sm) at design/working temperature. For the pressure vessel model in hand, standard steel S30408 was used, which has a basic allowable stress intensity value of 137 MPa at the working temperature of 20°C - 150°C.

Five Basic Stress Categories used for code verification are:

1) General Primary Membrane Stress Intensity (P_m)
2) Local Primary Membrane Stress Intensity (P_L)
3) Primary Membrane Plus Primary Bending Stress ($P_L + P_b$) – either General or Local Membrane Stress

4) Primary Plus Secondary Stress Intensity ($P_L + P_b + Q$)
5) Peak Stress Intensity ($P_L + P_b + Q + F$)

According to the ASME code, the maximum allowable stress limits for the pressure vessel model in consideration are shown below:

Table 6: Stress Limits as per the ASME code

Stress Category	Limits Based on Sm	Allowable Value (MPa) for current Pressure Vessel model
General Primary Membrane Stress Intensity (P_m)	S_m	137
Local Primary Membrane Stress Intensity (P_L)	$1.5*S_m$	205.5
Primary Membrane Plus Primary Bending Stress Intensity ($P_L + P_b$)	$1.5*S_m$	205.5
Primary Plus Secondary Stress Intensity ($P_L + P_b + Q$)	$3.0*S_m$	411

Design Stress Intensity (Sm): Basic allowable stress intensity of the material at design/working temperature. Typically, the lesser of 2/3 the Yield Stress (YS) or 1/3 of the Ultimate Tensile Stress (UTS).

$$P_m \leq Sm = 137 \text{ MPa}$$

$$P_L \leq 1.5 \times Sm = 205.5 \text{ MPa}$$

$$P_L + P_b \leq 1.5 \times Sm = 205.5 \text{ MPa}$$

$$P_L + P_b + Q \leq 3 \times Sm = 411 \text{ MPa}$$

The above indicated limits along with the equipment operating conditions shown in table-7 are the so-called Design Condition. When the Operational Conditions are verified the pressure and temperature are lower, but the earthquake should be considered, the limits are slightly different as well as the Sm value (which depends on the temperature).

Primary generalized membrane stresses are not allowed to exceed the basic allowable stress Sm, otherwise there is the possibility of a catastrophic plastic collapse e.g. a burst under pressure. For the primary localized membrane stress, a margin of safety is included by specifying an allowable membrane stress of $1.5\times Sm$. The total primary (membrane plus bending) allowable stress has an allowable limit of $1.5\times Sm$. Secondary stress can comfortably exceed the material allowable limit but must be limited to ensure shakedown under cyclic load. Hence the range of secondary stress is limited to $3\times Sm$. Local stresses around nozzles or transitions could be higher than global stresses – sometimes 2x as high, depending on the location and cause.

Table 7: Design Conditions for Pressure Vessel Equipment

medium	Wet air
Design pressure (MPa)	0.2
Design temperature (°C)	110
Working pressure (MPa)	≤ 0.2
Working temperature (°C)	95
Hydraulic test pressure (MPa)	0.25
Corrosion allowance (mm)	0
Seismic fortification intensity	8-level (0.3 g)
Main pressure bearing Material	S30408

4.5 ANSYS Stress Linearization Results

In its post-processor module, the ANSYS program can linearize the stresses along a given section defined by two nodes –the SCL(Path). It linearizes all six stress components (SX, SY, SZ, SXY, SYZ, SXZ). Also, the Tresca (SINT) and von Mises (SEQV) equivalent stresses are reported by ANSYS software. To perform the linearization, the program considers 47 internal points along the SCL. With this procedure, the Membrane (average), the Bending (linear), the Membrane ± Bending, the Peak stress, the total stress, are calculated.

The stress linearization was performed on the nominal design of the pressure vessel model with shell thickness of 10 mm and flange thickness of 16 mm. 20 sections or SCL were chosen to linearize and classify the stresses, to cover all critical parts and regions in the analyzed geometry of the pressure vessel, aiming to verify them against the Code limits. These sections are shown in figures below where they are named PATH-X where X is the stress classification line number. Using the ANSYS post processor, the linearized stresses along the defined classification lines are extracted. The Tresca equivalent stress or the averaged stress intensity is used for linearization. This is given directly by the software so it is not required to do the calculations manually. The software first linearizes the stresses at a component level and then calculates the equivalent stress on the results. The stresses are then classified as necessary and the linearized stresses are checked against the allowable stress limits. Two elements throughout the shell of the pressure vessel has been used during the linearization process.

It may be noted that the membrane plus bending plot is not linear across the section thickness for some of the evaluations, depending on the stress location. However, the graphs shown are for the equivalent stress intensity which due to the nature of its calculation will result in the contours shown. ANSYS lists both the component linearized stresses and the calculated Tresca's and von Mises' equivalent stress. The results are grouped by type, namely; membrane, bending, membrane plus bending, peak and total. The tables below, list the linearization results for all the 20 stress classification lines defined in ANSYS. The maximum membrane and membrane plus bending stress along all these paths are listed in the path evaluation table. For each path, the table also shows the assigned stress categories, allowable and calculated stresses.

4.5.1 Path-1

This path is created along the thickness of the cylindrical shell where the shell body of the pressure vessel connects to the Top-Head of the vessel. Since this path lies away from the discontinuity, the average membrane stress and membrane plus bending stress along this path are classified as primary and hence checked against the $1.5 \times Sm$ limit.

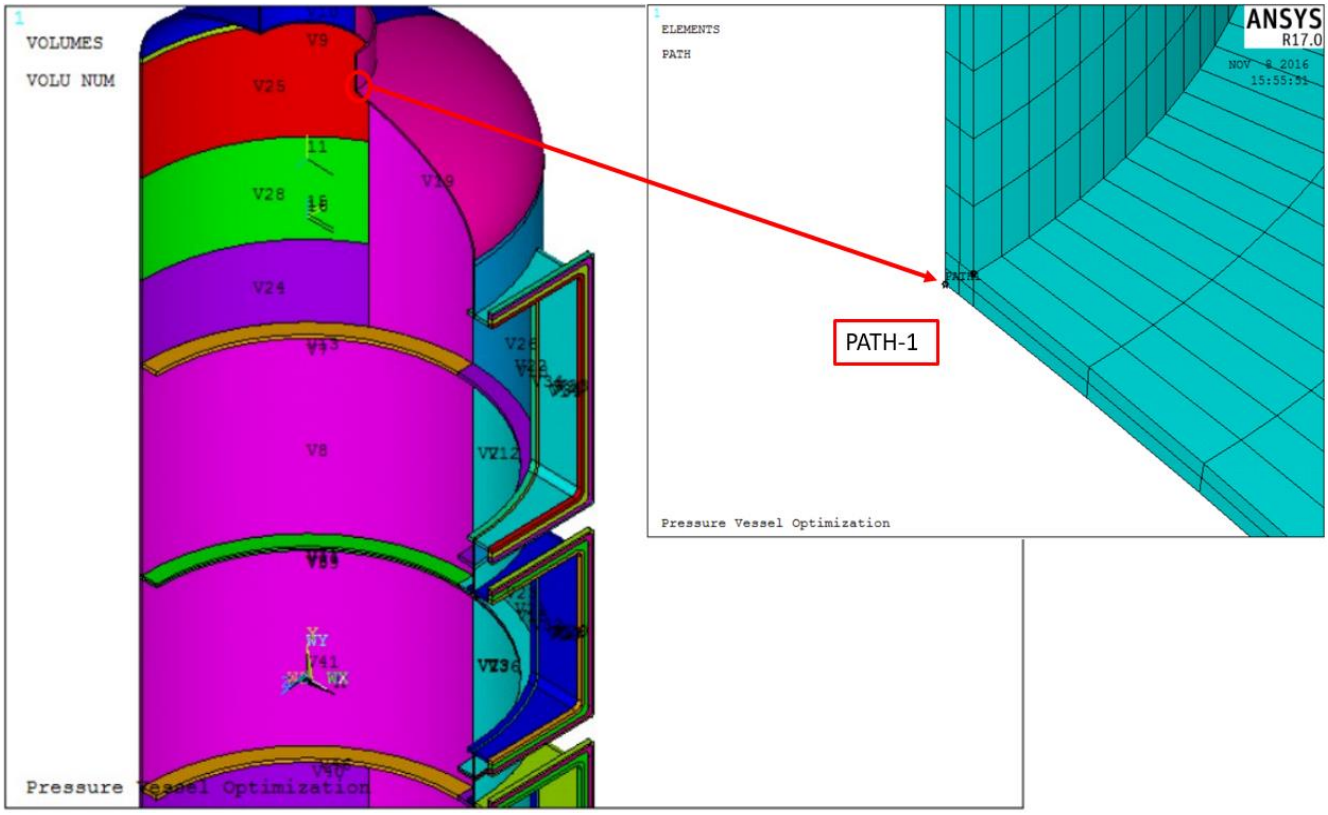

Figure 31: Path-1 plot on geometry

Table 8: Path-1 Evaluation

Load Condition	Allowable Stress S_m (MPa)	ANSYS linearization Type of stress	Stress Classification symbol	Equivalent Stress Intensity SINT (MPa)	Stress Control Value	Evaluation Result
Design Conditions A	137	MEMBRANE	$S_I\ (P_m)$	N/A	$1.0 \times S_m$=137	N/A
			$S_{II}\ (P_L)$	59.85	$1.5 \times S_m$=205.5	PASS
		MEMBRANE PLUS BENDING	$S_{III}\ (P_L + P_b)$	73.26	$1.5 \times S_m$=205.5	PASS

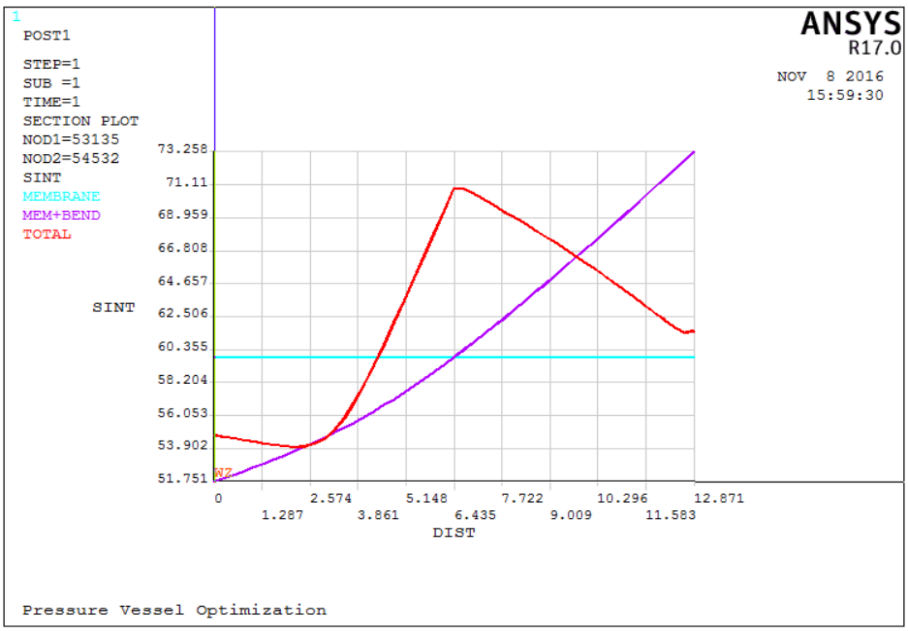

Figure 32: Stress variation through the thickness along Path-1

Table 9: ANSYS Path-1 Linearized Results

```
** MEMBRANE **
    SX        SY        SZ        SXY       SYZ       SXZ
  5.688     0.7020     59.05     3.127     0.8968E-03 0.1197E-02
    S1        S2        S3        SINT      SEQV
  59.05     7.194    -0.8039     59.85     56.28

        ** BENDING **  I=INSIDE C=CENTER O=OUTSIDE
    SX        SY        SZ        SXY       SYZ       SXZ
I  14.28     9.627     2.678    -4.999     0.6269E-02 0.2835E-02
C  0.000     0.000     0.000     0.000     0.000     0.000
O -14.28    -9.627    -2.678     4.999    -0.6269E-02 -0.2835E-02
    S1        S2        S3        SINT      SEQV
I  17.47     6.439     2.678     14.79     13.31
C  0.000     0.000     0.000     0.000     0.000
O -2.678    -6.439    -17.47     14.79     13.31

        ** MEMBRANE PLUS BENDING **  I=INSIDE C=CENTER O=OUTSIDE
    SX        SY        SZ        SXY       SYZ       SXZ
I  19.97     10.33     61.73    -1.872     0.7166E-02 0.4031E-02
C  5.688     0.7020    59.05     3.127     0.8968E-03 0.1197E-02
O -8.592    -8.925     56.37     8.126    -0.5372E-02 -0.1638E-02
    S1        S2        S3        SINT      SEQV
I  61.73     20.32     9.978     51.75     47.43
C  59.05     7.194    -0.8039    59.85     56.28
O  56.37    -0.6310   -16.89     73.26     66.63

        ** PEAK **  I=INSIDE C=CENTER O=OUTSIDE
    SX        SY        SZ        SXY       SYZ       SXZ
I  8.600     9.224     5.545    -8.759     0.5825E-02 0.3777E-02
C -4.566    -6.121    -3.289     9.437    -0.3068E-02 0.7286E-03
O  10.46     10.41     6.424    -8.530     0.1181E-02 0.1473E-02
    S1        S2        S3        SINT      SEQV
I  17.68     5.545     0.1478    17.53     15.55
C  4.125    -3.289    -14.81     18.94     16.53
O  18.97     6.424     1.908     17.06     15.31

        ** TOTAL **  I=INSIDE C=CENTER O=OUTSIDE
    SX        SY        SZ        SXY       SYZ       SXZ
I  28.57     19.55     67.27    -10.63     0.1299E-01 0.7809E-02
C  1.122    -5.419     55.76     12.56    -0.2172E-02 0.1925E-02
O  1.871     1.490     62.80    -0.4048   -0.4191E-02 -0.1648E-03
    S1        S2        S3        SINT      SEQV      TEMP
I  67.27     35.61     12.51     54.76     47.62     0.000
C  55.76     10.83    -15.13     70.89     62.12
O  62.80     2.128     1.233     61.56     61.12     0.000
```

4.5.2 Path-2

Path-2 is the path along cylindrical shell thickness at the corner where the shell body of the vessel connects rectangular Nozzle-1. Due to singularity around the corner, the stresses linearized along this path are influenced by the local stress concentration effect. As the result of this discontinuity, the total membrane plus bending stress near this region also comprises of some secondary stresses, which needs to be considered when comparing with the allowable limits. Thus, total membrane plus bending stress in this region is the sum of primary stress '$P_L + P_b$'and secondary stress 'Q'. Due to the presence of this secondary stress component, the allowable limit for total membrane plus bending stress along this path is set to three times the basic allowable limit 'Sm'.

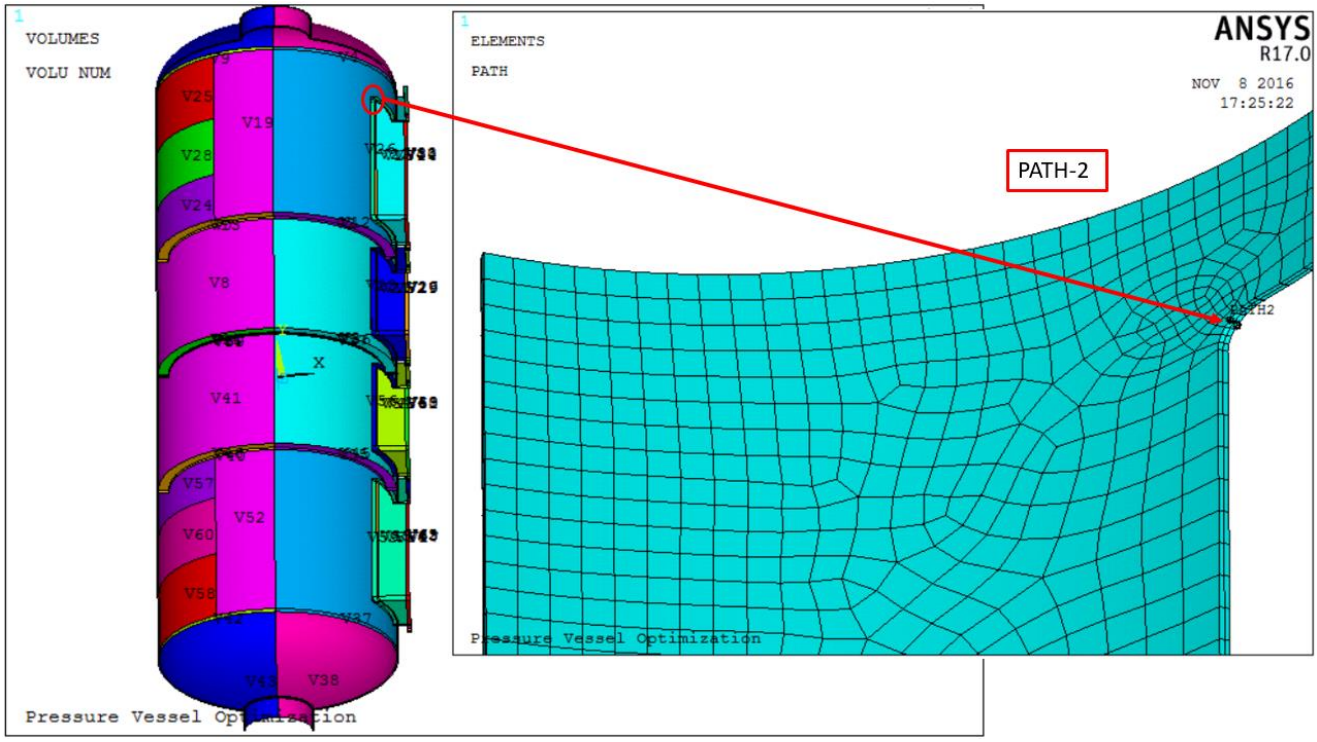

Figure 33: Path-2 plot on geometry

Table 10: Path-2 Evaluation

Load Condition	Allowable Stress S_m (MPa)	ANSYS linearization Type of stress	Stress Classification symbol	Equivalent Stress Intensity SINT (MPa)	Stress Control Value	Evaluation Result
Design Conditions A	137	MEMBRANE	S_I (P_m)	N/A	1.0×S_m=137	N/A
			S_{II} (P_L)	105.1	1.5×S_m=205.5	PASS
		MEMBRANE PLUS BENDING	S_{IV} $(P_L + P_b + Q)$	206.6	3×S_m=411	PASS

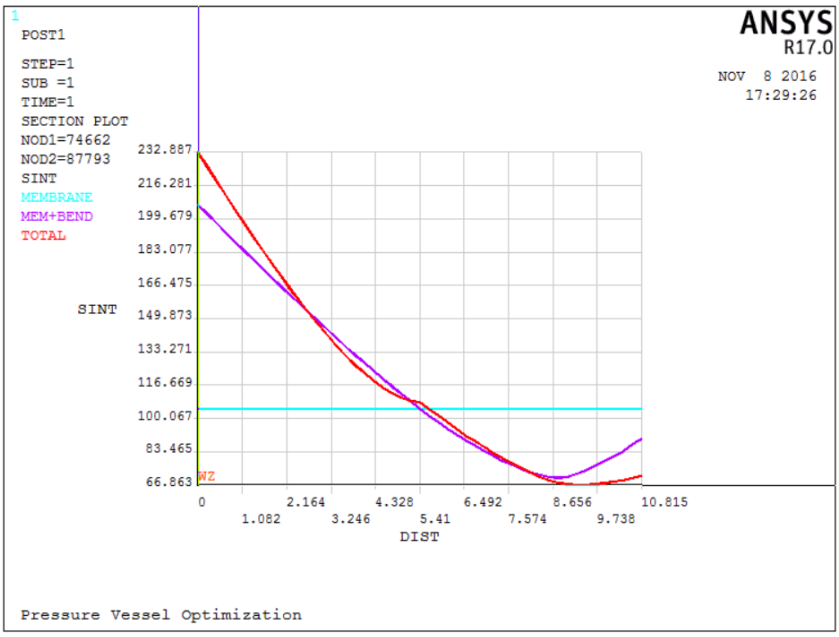

Figure 34: Stress variation through the thickness along Path-2

Table 11: ANSYS Path-2 Linearized Results

** MEMBRANE **

SX	SY	SZ	SXY	SYZ	SXZ
83.59	68.85	102.0	-11.66	-1.259	50.07

S1	S2	S3	SINT	SEQV
144.7	70.23	39.58	105.1	93.61

** BENDING ** I=INSIDE C=CENTER O=OUTSIDE

	SX	SY	SZ	SXY	SYZ	SXZ
I	105.7	84.83	54.25	-27.04	-20.30	43.92
C	0.000	0.000	0.000	0.000	0.000	0.000
O	-105.7	-84.83	-54.25	27.04	20.30	-43.92

	S1	S2	S3	SINT	SEQV
I	148.6	67.52	28.70	119.9	105.9
C	0.000	0.000	0.000	0.000	0.000
O	-28.70	-67.52	-148.6	119.9	105.9

** MEMBRANE PLUS BENDING ** I=INSIDE C=CENTER O=OUTSIDE

	SX	SY	SZ	SXY	SYZ	SXZ
I	189.3	153.7	156.3	-38.70	-21.55	93.98
C	83.59	68.85	102.0	-11.66	-1.259	50.07
O	-22.13	-15.98	47.79	15.38	19.04	6.153

	S1	S2	S3	SINT	SEQV
I	282.9	140.0	76.34	206.6	183.2
C	144.7	70.23	39.58	105.1	93.61
O	54.39	-9.239	-35.47	89.87	80.04

** PEAK ** I=INSIDE C=CENTER O=OUTSIDE

	SX	SY	SZ	SXY	SYZ	SXZ
I	15.92	-5.494	-23.60	-11.68	5.468	5.556
C	-14.52	5.189	23.97	12.89	-6.174	-4.784
O	15.11	-6.068	-23.04	-12.25	5.825	5.647

	S1	S2	S3	SINT	SEQV
I	21.25	-7.442	-26.98	48.23	42.02
C	27.66	7.924	-20.94	48.60	42.34
O	20.89	-7.882	-27.01	47.90	41.76

** TOTAL ** I=INSIDE C=CENTER O=OUTSIDE

	SX	SY	SZ	SXY	SYZ	SXZ
I	205.2	148.2	132.7	-50.38	-16.09	99.54
C	69.07	74.04	126.0	1.225	-7.433	45.28
O	-7.025	-22.04	24.75	3.123	24.86	11.80

	S1	S2	S3	SINT	SEQV	TEMP
I	292.7	133.6	59.80	232.9	206.1	0.000
C	151.5	74.31	43.34	108.1	96.47	
O	38.68	-10.08	-32.93	71.61	63.35	0.000

4.5.3 Path-3

Path-3 is the path along Rectangular Nozzle thickness at the corner where the pressure vessel shell body connects rectangular Nozzle N-1. Since this path lies very close to the singularity at corner, the secondary stresses need to be considered for this path. The total membrane plus bending stress in this region is the sum of primary stress '$P_L + P_b$'and secondary stress 'Q'. Therefore, the allowable limit for total membrane plus bending stress along this path is three times the basic allowable limit 'Sm'.

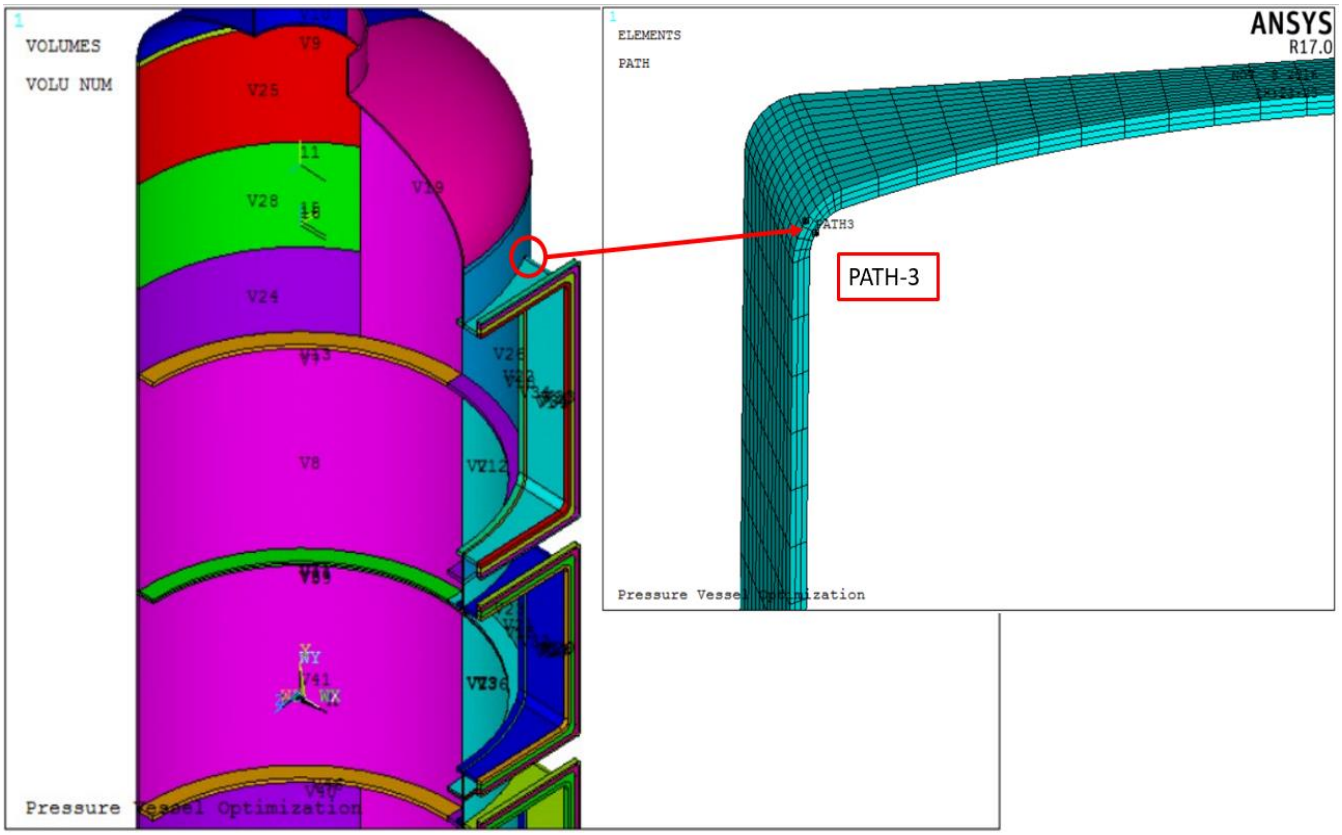

Figure 35: Path-3 plot on geometry

Table 12: Path-3 Evaluation

Load Condition	Allowable Stress S_m (MPa)	ANSYS linearization Type of stress	Stress Classification symbol	Equivalent Stress Intensity SINT (MPa)	Stress Control Value	Evaluation Result
Design Conditions A	137	MEMBRANE	S_I (P_m)	N/A	1.0×S_m=137	N/A
			S_{II} (P_L)	157.1	1.5×S_m=205.5	PASS
		MEMBRANE PLUS BENDING	S_{IV} $(P_L + P_b + Q)$	235.0	3×S_m=411	PASS

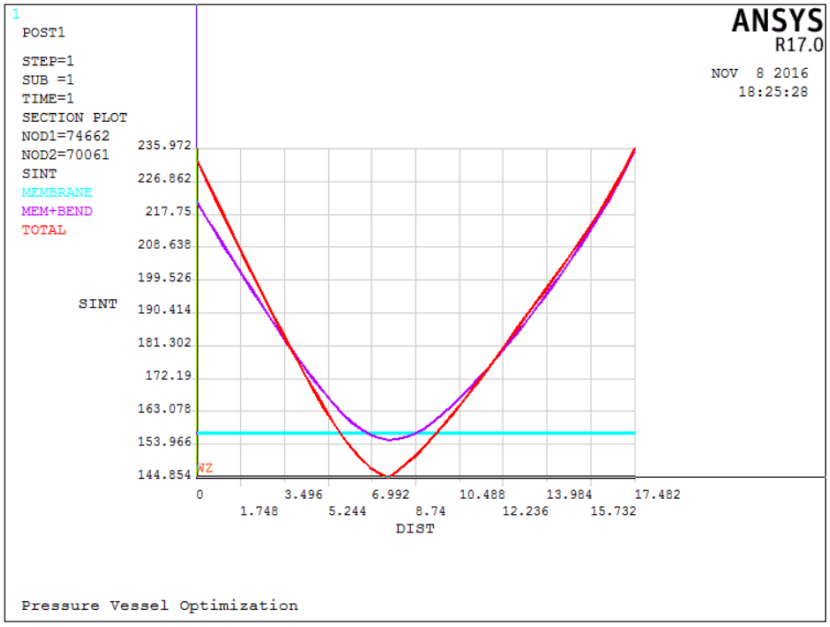

Figure 36: Stress variation through the thickness along Path-3

Table 13: ANSYS Path-3 Linearized Results

** MEMBRANE **						
	SX	SY	SZ	SXY	SYZ	SXZ
	65.96	108.3	76.24	-0.3819	31.33	70.10
	S1	S2	S3	SINT	SEQV	
	153.6	100.4	-3.504	157.1	138.4	
** BENDING ** I=INSIDE C=CENTER O=OUTSIDE						
	SX	SY	SZ	SXY	SYZ	SXZ
I	107.6	14.25	35.06	-46.25	-51.37	25.78
C	0.000	0.000	0.000	0.000	0.000	0.000
O	-107.6	-14.25	-35.06	46.25	51.37	-25.78
	S1	S2	S3	SINT	SEQV	
I	145.3	42.64	-31.03	176.4	153.4	
C	0.000	0.000	0.000	0.000	0.000	
O	31.03	-42.64	-145.3	176.4	153.4	
** MEMBRANE PLUS BENDING ** I=INSIDE C=CENTER O=OUTSIDE						
	SX	SY	SZ	SXY	SYZ	SXZ
I	173.6	122.6	111.3	-46.63	-20.04	95.88
C	65.96	108.3	76.24	-0.3819	31.33	70.10
O	-41.69	94.06	41.17	45.87	82.71	44.32
	S1	S2	S3	SINT	SEQV	
I	261.0	106.6	39.86	221.2	196.5	
C	153.6	100.4	-3.504	157.1	138.4	
O	173.1	-17.60	-61.93	235.0	216.3	
** PEAK ** I=INSIDE C=CENTER O=OUTSIDE						
	SX	SY	SZ	SXY	SYZ	SXZ
I	31.63	25.63	21.39	-3.745	3.953	3.657
C	-21.80	-17.04	-15.01	2.263	-2.782	-3.076
O	31.62	28.17	23.20	3.460	7.073	-3.438
	S1	S2	S3	SINT	SEQV	
I	33.69	27.74	17.23	16.46	14.44	
C	-11.63	-18.99	-23.23	11.60	10.17	
O	33.97	32.38	16.64	17.33	16.59	
** TOTAL ** I=INSIDE C=CENTER O=OUTSIDE						
	SX	SY	SZ	SXY	SYZ	SXZ
I	205.2	148.2	132.7	-50.38	-16.09	99.54
C	44.16	91.27	61.23	1.881	28.55	67.02
O	-10.07	122.2	64.37	49.33	89.78	40.88
	S1	S2	S3	SINT	SEQV	TEMP
I	292.7	133.6	59.80	232.9	206.1	0.000
C	133.2	81.26	-17.76	150.9	132.8	
O	206.5	-0.5129	-29.46	236.0	222.9	0.000

4.5.4 Path-4

Path-4 is the path along the thickness of the rectangular Nozzle at the middle section where cylindrical shell body of the vessel connects the Nozzle N-1. This path is far from the singularity. The average membrane stress and membrane plus bending stress along this path are classified as primary and therefore, are checked against the $1.5 \times Sm$ limit.

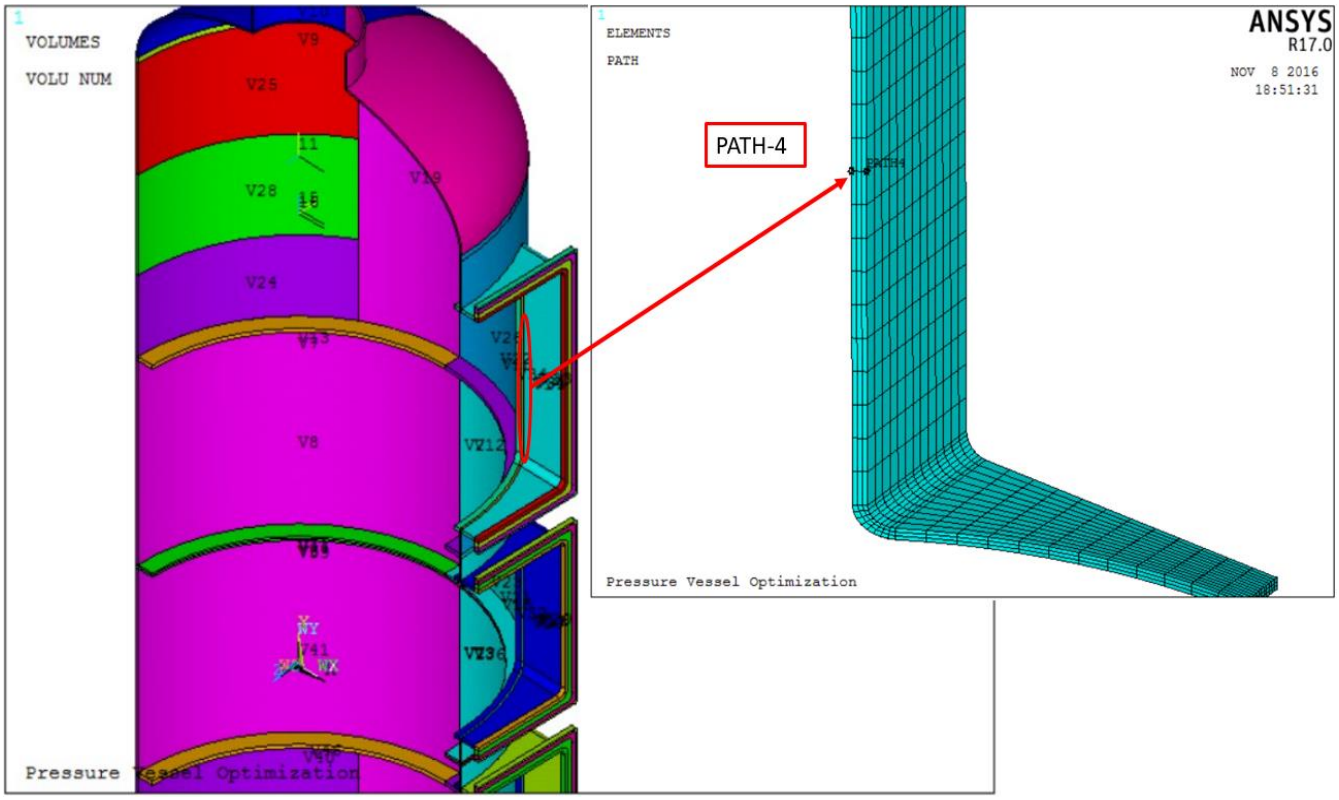

Figure 37: Path-4 plot on geometry

Table 14: Path-4 Evaluation

Load Condition	Allowable Stress S_m (MPa)	ANSYS linearization Type of stress	Stress Classification symbol	Equivalent Stress Intensity SINT (MPa)	Stress Control Value	Evaluation Result
Design Conditions A	137	MEMBRANE	S_I (P_m)	N/A	$1.0 \times S_m$=137	N/A
			S_{II} (P_L)	45.48	$1.5 \times S_m$=205.5	PASS
		MEMBRANE PLUS BENDING	S_{III} ($P_L + P_b$)	59.05	$1.5 \times S_m$=205.5	PASS

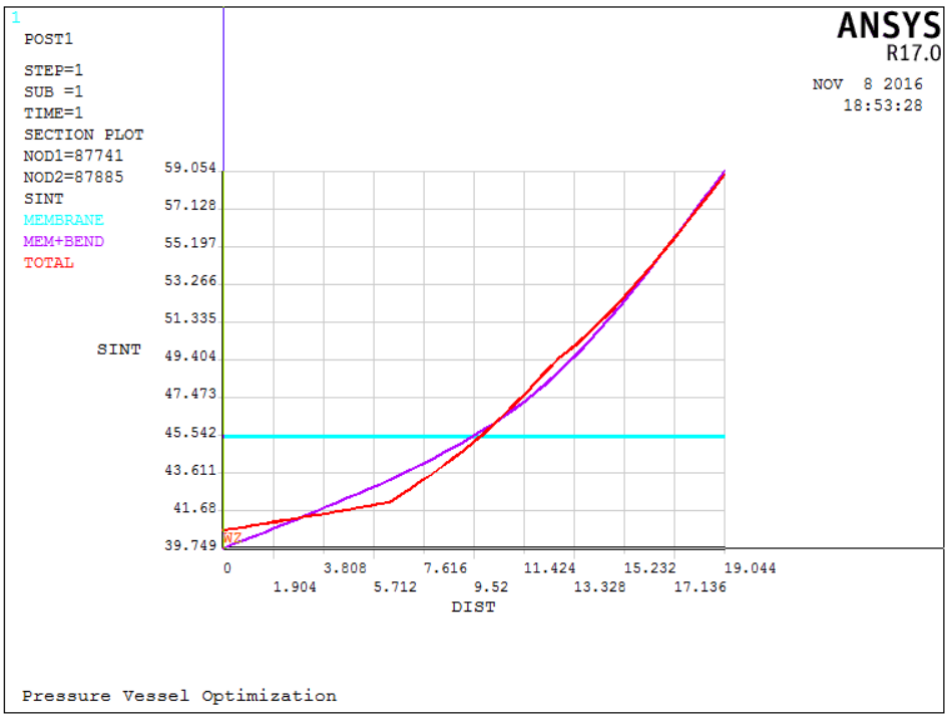

Figure 38: Stress variation through the thickness along Path-4

Table 15: ANSYS Path-4 Linearized Results

** MEMBRANE **						
	SX	SY	SZ	SXY	SYZ	SXZ
	-3.653	-45.35	-3.842	-0.1255	-0.7024E-01	-3.875
	S1	S2	S3	SINT	SEQV	
	0.1287	-7.622	-45.36	45.48	42.15	
** BENDING ** I=INSIDE C=CENTER O=OUTSIDE						
	SX	SY	SZ	SXY	SYZ	SXZ
I	-18.03	-0.6795	-6.520	-0.2210	-0.7751E-01	-4.039
C	0.000	0.000	0.000	0.000	0.000	0.000
O	18.03	0.6795	6.520	0.2210	0.7751E-01	4.039
	S1	S2	S3	SINT	SEQV	
I	-0.6766	-5.244	-19.31	18.63	16.82	
C	0.000	0.000	0.000	0.000	0.000	
O	19.31	5.244	0.6766	18.63	16.82	
** MEMBRANE PLUS BENDING ** I=INSIDE C=CENTER O=OUTSIDE						
	SX	SY	SZ	SXY	SYZ	SXZ
I	-21.68	-46.03	-10.36	-0.3464	-0.1477	-7.913
C	-3.653	-45.35	-3.842	-0.1255	-0.7024E-01	-3.875
O	14.38	-44.68	2.679	0.9551E-01	0.7274E-02	0.1642
	S1	S2	S3	SINT	SEQV	
I	-6.293	-25.74	-46.04	39.75	34.43	
C	0.1287	-7.622	-45.36	45.48	42.15	
O	14.38	2.676	-44.68	59.05	54.16	
** PEAK ** I=INSIDE C=CENTER O=OUTSIDE						
	SX	SY	SZ	SXY	SYZ	SXZ
I	-0.8169	-0.8586	-2.555	0.7577E-02	-0.4231E-01	-2.510
C	0.5149	0.4812	1.308	0.2712E-02	0.1348E-01	0.7247
O	-1.294	-1.095	-2.728	-0.1873E-01	-0.1286E-01	-0.4113
	S1	S2	S3	SINT	SEQV	
I	0.9706	-0.8589	-4.342	5.313	4.675	
C	1.738	0.4811	0.8550E-01	1.653	1.494	
O	-1.093	-1.187	-2.838	1.745	1.700	
** TOTAL ** I=INSIDE C=CENTER O=OUTSIDE						
	SX	SY	SZ	SXY	SYZ	SXZ
I	-22.50	-46.89	-12.92	-0.3388	-0.1901	-10.42
C	-3.138	-44.87	-2.533	-0.1227	-0.5676E-01	-3.150
O	13.08	-45.77	-0.4940E-01	0.7677E-01	-0.5591E-02	-0.2471
	S1	S2	S3	SINT	SEQV	TEMP
I	-6.236	-29.17	-46.90	40.67	35.31	0.000
C	0.3290	-6.000	-44.87	45.20	42.39	
O	13.09	-0.5405E-01	-45.77	58.86	53.51	0.000

4.5.5 Path-5

Path-5 is the path along the thickness of the rectangular Nozzle around the middle section where cylindrical shell body of the vessel connects the upper side of Nozzle N-1. Since this path is far from the singularity, the average membrane stress and membrane plus bending stress along this path are classified as primary and hence, checked against the $1.5\times Sm$ limit.

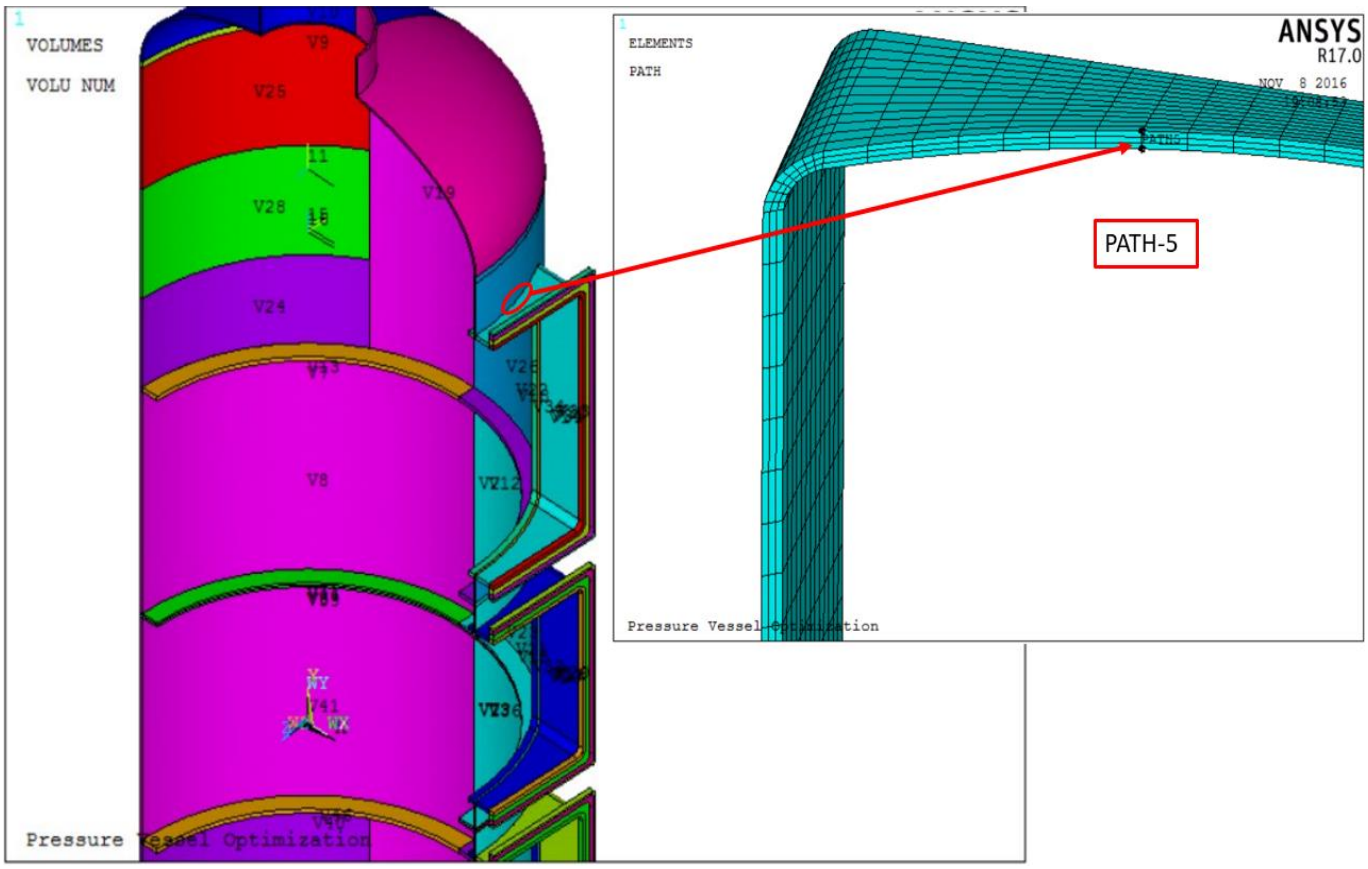

Figure 39: Path-5 plot on geometry

Table 16: Path-5 Evaluation

Load Condition	Allowable Stress S_m (MPa)	ANSYS linearization Type of stress	Stress Classification symbol	Equivalent Stress Intensity SINT (MPa)	Stress Control Value	Evaluation Result
Design Conditions A	137	MEMBRANE	$S_I\ (P_m)$	N/A	$1.0\times S_m$=137	N/A
			$S_{II}\ (P_L)$	73.18	$1.5\times S_m$=205.5	PASS
		MEMBRANE PLUS BENDING	$S_{III}\ (P_L + P_b)$	80.24	$1.5\times S_m$=205.5	PASS

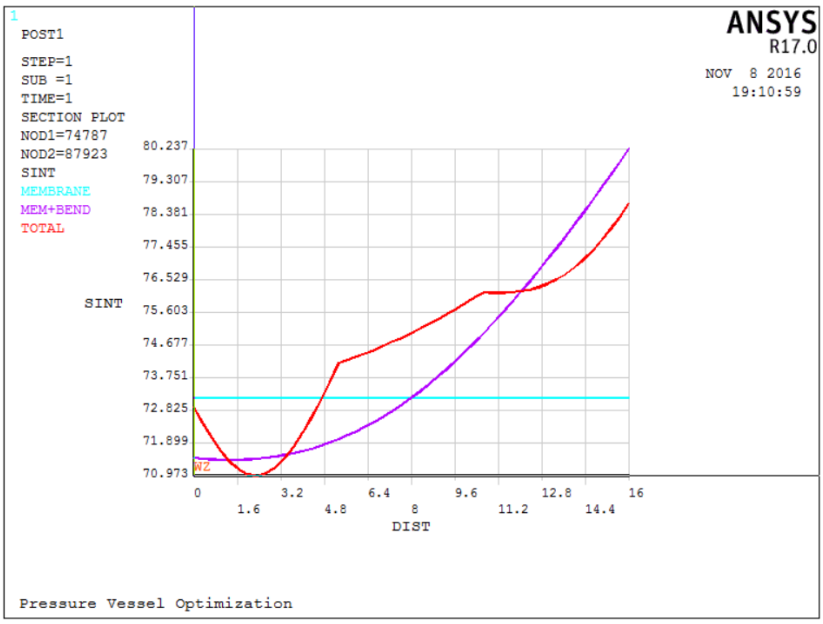

Figure 40: Stress variation through the thickness along Path-5

Table 17: ANSYS Path-5 Linearized Results

** MEMBRANE **						
	SX	SY	SZ	SXY	SYZ	SXZ
	3.226	1.848	72.03	2.603	2.607	7.413
	S1	S2	S3	SINT	SEQV	
	72.93	4.421	-0.2525	73.18	70.96	
** BENDING ** I=INSIDE C=CENTER O=OUTSIDE						
	SX	SY	SZ	SXY	SYZ	SXZ
I	6.374	3.337	2.147	-0.5371	5.414	-6.421
C	0.000	0.000	0.000	0.000	0.000	0.000
O	-6.374	-3.337	-2.147	0.5371	-5.414	6.421
	S1	S2	S3	SINT	SEQV	
I	12.61	4.020	-4.774	17.39	15.06	
C	0.000	0.000	0.000	0.000	0.000	
O	4.774	-4.020	-12.61	17.39	15.06	
** MEMBRANE PLUS BENDING ** I=INSIDE C=CENTER O=OUTSIDE						
	SX	SY	SZ	SXY	SYZ	SXZ
I	9.600	5.186	74.17	2.066	8.021	0.9929
C	3.226	1.848	72.03	2.603	2.607	7.413
O	-3.148	-1.489	69.88	3.140	-2.806	13.83
	S1	S2	S3	SINT	SEQV	
I	75.12	10.21	3.633	71.48	68.43	
C	72.93	4.421	-0.2525	73.18	70.96	
O	72.48	0.5252	-7.761	80.24	76.43	
** PEAK ** I=INSIDE C=CENTER O=OUTSIDE						
	SX	SY	SZ	SXY	SYZ	SXZ
I	0.1005	0.9221	-0.3797E-01	-3.672	4.338	0.3388
C	0.8079E-01	-0.5089	-0.1062E-01	1.604	-1.753	-0.1174
O	-0.4237	1.113	0.8043E-01	-2.744	2.676	0.1309
	S1	S2	S3	SINT	SEQV	
I	6.021	0.3768	-5.413	11.43	9.902	
C	2.219	-0.7805E-01	-2.580	4.799	4.158	
O	4.306	-0.2965E-01	-3.506	7.813	6.780	
** TOTAL ** I=INSIDE C=CENTER O=OUTSIDE						
	SX	SY	SZ	SXY	SYZ	SXZ
I	9.701	6.108	74.13	-1.606	12.36	1.332
C	3.307	1.339	72.01	4.207	0.8542	7.296
O	-3.572	-0.3758	69.96	0.3957	-0.1308	13.96
	S1	S2	S3	SINT	SEQV	TEMP
I	76.33	10.21	3.408	72.92	69.77	0.000
C	72.80	6.068	-2.211	75.02	71.24	
O	72.52	-0.3464	-6.164	78.69	75.94	0.000

Now we repeat the above stated paths for smaller rectangular Nozzle N-2

4.5.6 Path-6

Path-6 is the path along cylindrical shell thickness at the corner where the shell body of the vessel connects rectangular nozzle-2. Since this path is near the singularity at the corner, the membrane plus bending stress consists of primary as well as secondary stress components. Due to presence of this secondary stress component, the allowable limit for total membrane plus bending stress along this path is $3\times Sm$.

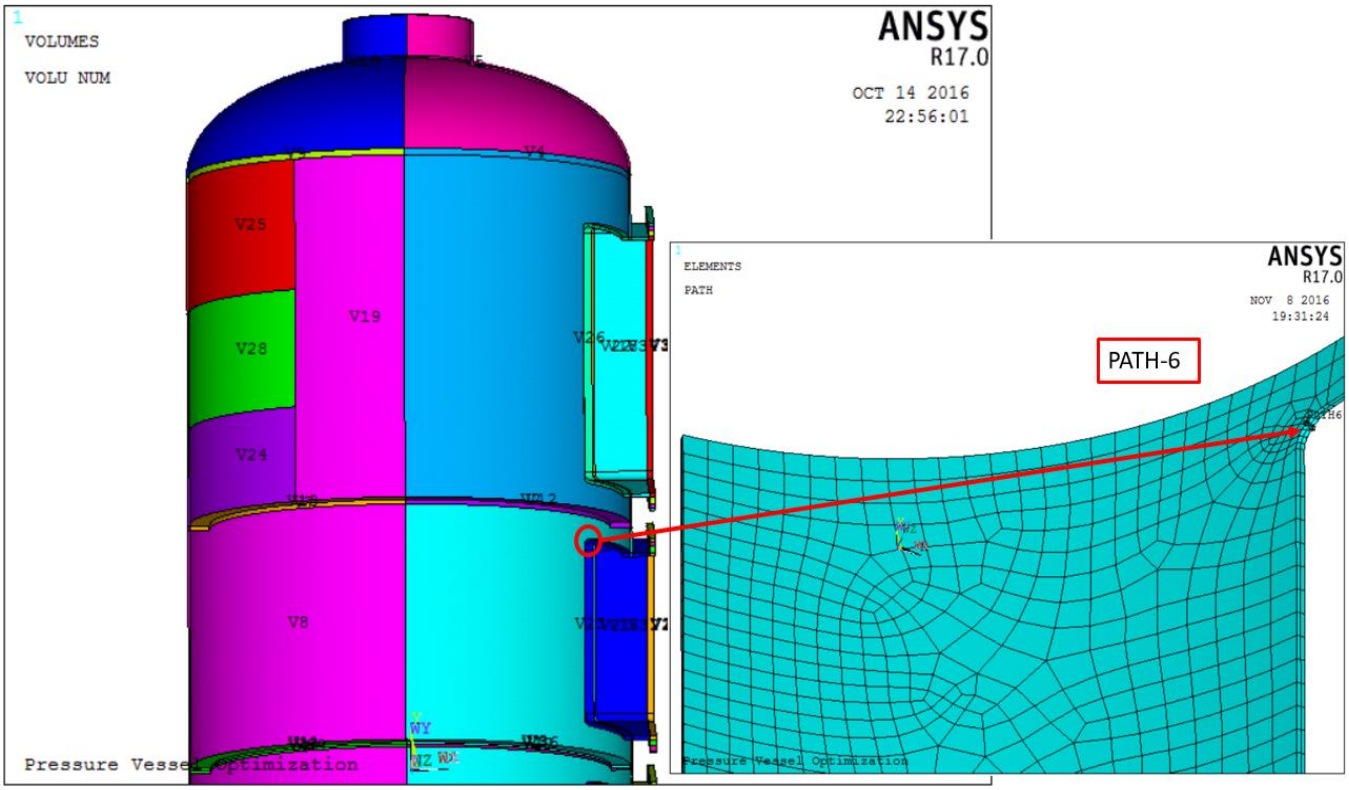

Figure 41: Path-6 plot on geometry

Table 18: Path-6 Evaluation

Load Condition	Allowable Stress S_m (MPa)	ANSYS linearization Type of stress	Stress Classification symbol	Equivalent Stress Intensity SINT (MPa)	Stress Control Value	Evaluation Result
Design Conditions A	137	MEMBRANE	$S_I\ (P_m)$	N/A	$1.0\times S_m$=137	N/A
			$S_{II}\ (P_L)$	61.36	$1.5\times S_m$=205.5	PASS
		MEMBRANE PLUS BENDING	$S_{IV}\ (P_L + P_b + Q)$	128.2	$3\times S_m$=411	PASS

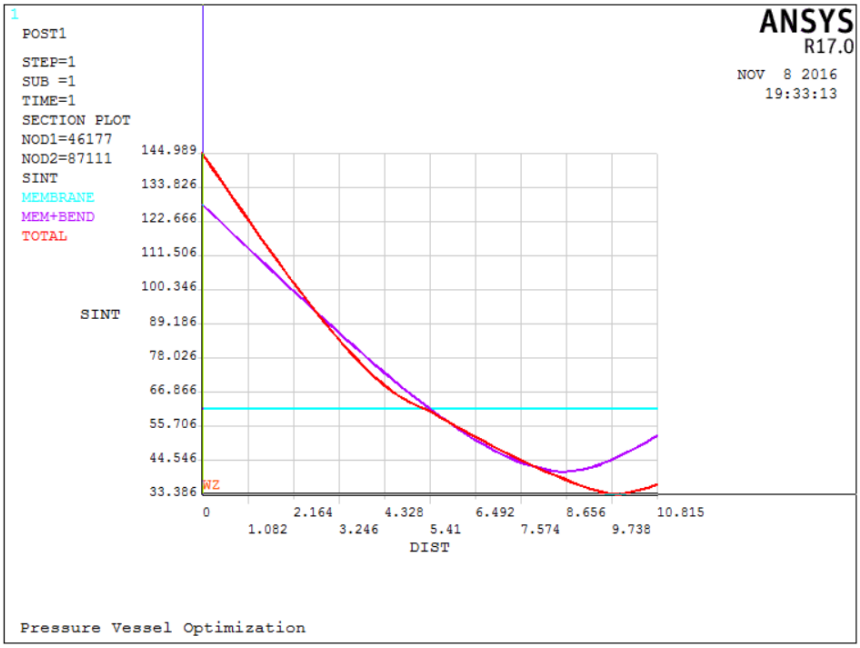

Figure 42: Stress variation through the thickness along Path-6

Table 19: ANSYS Path-6 Linearized Results

** MEMBRANE **

SX	SY	SZ	SXY	SYZ	SXZ
60.46	62.08	64.25	-7.089	1.093	29.77

S1	S2	S3	SINT	SEQV
92.73	62.69	31.38	61.36	53.14

** BENDING ** I=INSIDE C=CENTER O=OUTSIDE

	SX	SY	SZ	SXY	SYZ	SXZ
I	60.39	54.16	29.45	-22.86	-8.220	24.70
C	0.000	0.000	0.000	0.000	0.000	0.000
O	-60.39	-54.16	-29.45	22.86	8.220	-24.70

	S1	S2	S3	SINT	SEQV
I	90.14	38.60	15.26	74.89	66.37
C	0.000	0.000	0.000	0.000	0.000
O	-15.26	-38.60	-90.14	74.89	66.37

** MEMBRANE PLUS BENDING ** I=INSIDE C=CENTER O=OUTSIDE

	SX	SY	SZ	SXY	SYZ	SXZ
I	120.8	116.2	93.71	-29.95	-7.127	54.47
C	60.46	62.08	64.25	-7.089	1.093	29.77
O	0.7349E-01	7.923	34.80	15.77	9.313	5.068

	S1	S2	S3	SINT	SEQV
I	176.7	105.7	48.44	128.2	111.3
C	92.73	62.69	31.38	61.36	53.14
O	40.31	14.81	-12.33	52.64	45.59

** PEAK ** I=INSIDE C=CENTER O=OUTSIDE

	SX	SY	SZ	SXY	SYZ	SXZ
I	10.40	-2.494	-10.89	-7.854	2.528	2.512
C	-9.352	1.891	10.68	8.754	-3.113	-1.899
O	9.817	-2.549	-10.59	-8.200	2.894	2.628

	S1	S2	S3	SINT	SEQV
I	14.17	-4.470	-12.68	26.86	23.84
C	12.83	4.519	-14.14	26.97	23.92
O	13.95	-4.379	-12.89	26.84	23.76

** TOTAL ** I=INSIDE C=CENTER O=OUTSIDE

	SX	SY	SZ	SXY	SYZ	SXZ
I	131.2	113.8	82.82	-37.81	-4.600	56.99
C	51.11	63.98	74.93	1.666	-2.021	27.87
O	9.891	5.374	24.21	7.575	12.21	7.696

	S1	S2	S3	SINT	SEQV	TEMP
I	185.6	101.6	40.60	145.0	126.1	0.000
C	93.35	64.16	32.51	60.84	52.70	
O	34.53	6.918	-1.972	36.50	32.97	0.000

4.5.7 Path-7

Path-7 is the path along Rectangular Nozzle thickness at the corner where shell body of the pressure vessel connects smaller rectangular Nozzle N-2. Similar to the above described path-6, this path also lies near the singularity and therefore the allowable limit for total membrane plus bending stress along this path is $3\times Sm$.

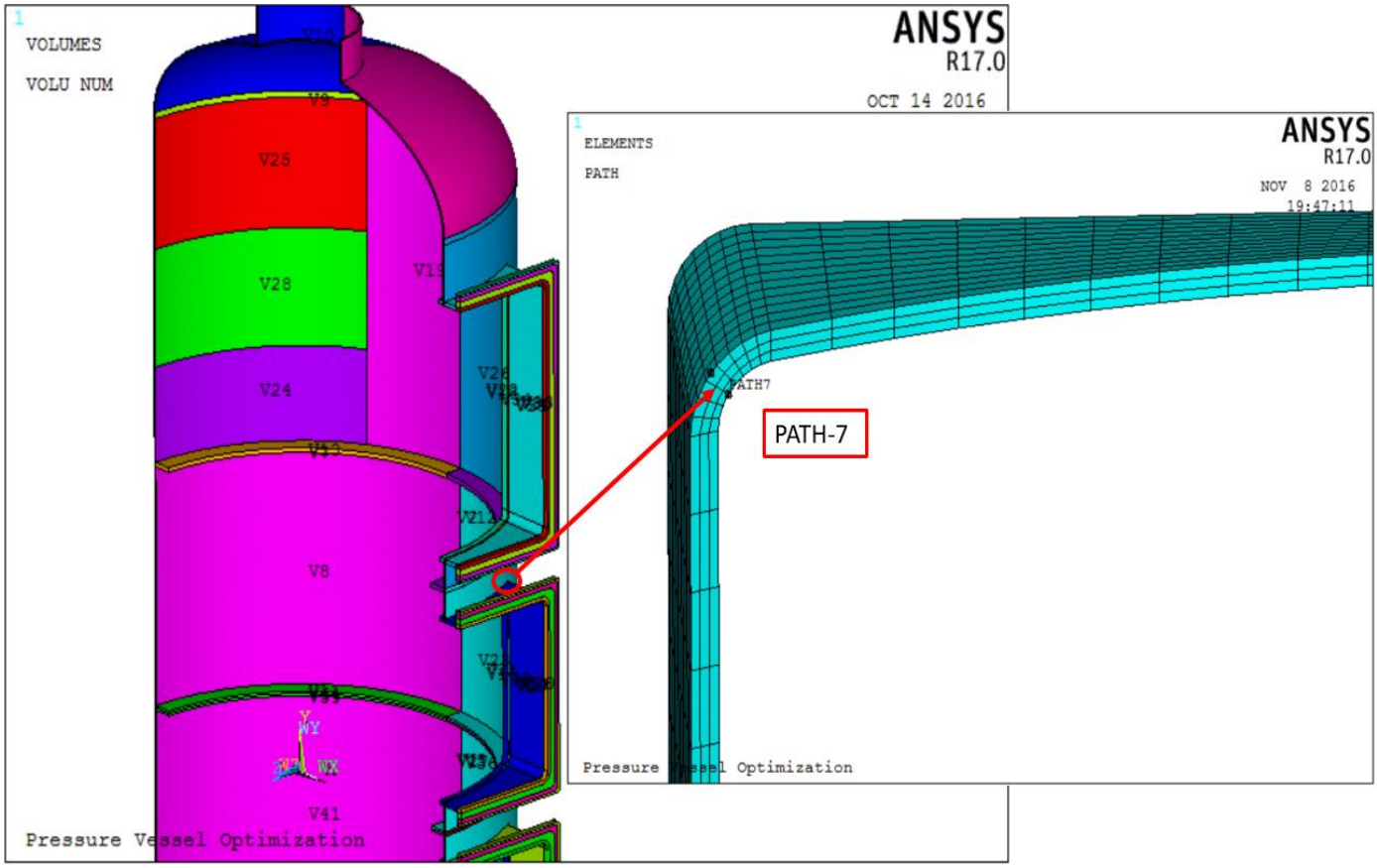

Figure 43: Path-7 plot on geometry

Table 20: Path-7 Evaluation

Load Condition	Allowable Stress S_m (MPa)	ANSYS linearization Type of stress	Stress Classification symbol	Equivalent Stress Intensity SINT (MPa)	Stress Control Value	Evaluation Result
Design Conditions A	137	MEMBRANE	$S_I\ (P_m)$	N/A	$1.0\times S_m$=137	N/A
			$S_{II}\ (P_L)$	109.5	$1.5\times S_m$=205.5	PASS
		MEMBRANE PLUS BENDING	$S_{IV}\ (P_L + P_b + Q)$	169.1	$3\times S_m$=411	PASS

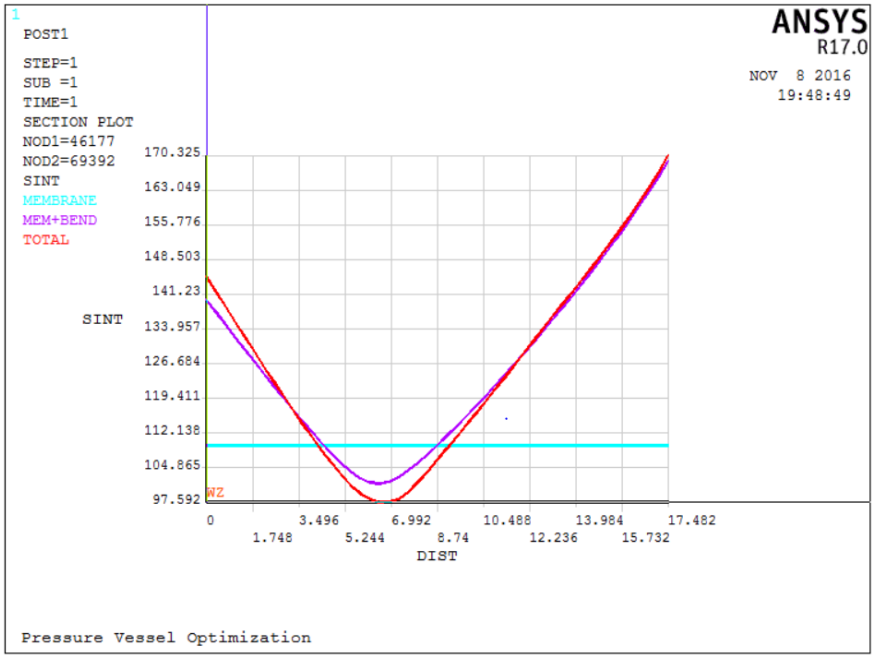

Figure 44: Stress variation through the thickness along Path-7

Table 21: ANSYS Path-7 Linearized Results

** MEMBRANE **						
	SX	SY	SZ	SXY	SYZ	SXZ
	41.37	82.30	47.82	-0.4623	24.15	45.47
	S1	S2	S3	SINT	SEQV	
	105.1	70.74	-4.375	109.5	96.99	
** BENDING ** I=INSIDE C=CENTER O=OUTSIDE						
	SX	SY	SZ	SXY	SYZ	SXZ
I	67.63	12.60	18.90	-34.91	-33.32	10.87
C	0.000	0.000	0.000	0.000	0.000	0.000
O	-67.63	-12.60	-18.90	34.91	33.32	-10.87
	S1	S2	S3	SINT	SEQV	
I	93.29	28.07	-22.23	115.5	100.3	
C	0.000	0.000	0.000	0.000	0.000	
O	22.23	-28.07	-93.29	115.5	100.3	
** MEMBRANE PLUS BENDING ** I=INSIDE C=CENTER O=OUTSIDE						
	SX	SY	SZ	SXY	SYZ	SXZ
I	109.0	94.89	66.72	-35.38	-9.166	56.34
C	41.37	82.30	47.82	-0.4623	24.15	45.47
O	-26.27	69.70	28.92	34.45	57.47	34.60
	S1	S2	S3	SINT	SEQV	
I	165.1	80.49	25.04	140.0	122.2	
C	105.1	70.74	-4.375	109.5	96.99	
O	125.6	-9.702	-43.52	169.1	155.0	
** PEAK ** I=INSIDE C=CENTER O=OUTSIDE						
	SX	SY	SZ	SXY	SYZ	SXZ
I	22.25	18.86	16.10	-2.429	4.567	0.6416
C	-14.79	-12.03	-10.72	1.314	-3.064	-0.6633
O	21.90	19.26	17.72	2.515	7.559	-4.240
	S1	S2	S3	SINT	SEQV	
I	24.00	20.90	12.31	11.69	10.49	
C	-7.973	-14.13	-15.43	7.458	6.899	
O	26.41	23.41	9.066	17.34	16.05	
** TOTAL ** I=INSIDE C=CENTER O=OUTSIDE						
	SX	SY	SZ	SXY	SYZ	SXZ
I	131.2	113.8	82.82	-37.81	-4.600	56.99
C	26.58	70.27	37.10	0.8514	21.09	44.81
O	-4.367	88.96	46.64	36.97	65.02	30.36
	S1	S2	S3	SINT	SEQV	TEMP
I	185.6	101.6	40.60	145.0	126.1	0.000
C	90.98	58.41	-15.44	106.4	94.44	
O	150.9	-0.1921	-19.45	170.3	161.6	0.000

4.5.8 Path-8

Path-8 is the path along the thickness of the rectangular Nozzle at the middle section where cylindrical shell body of the vessel connects the Nozzle N-2. This path lies far away from the singularity. The average membrane stress and membrane plus bending stress along this path are classified as primary and hence checked against the $1.5\times Sm$ limit.

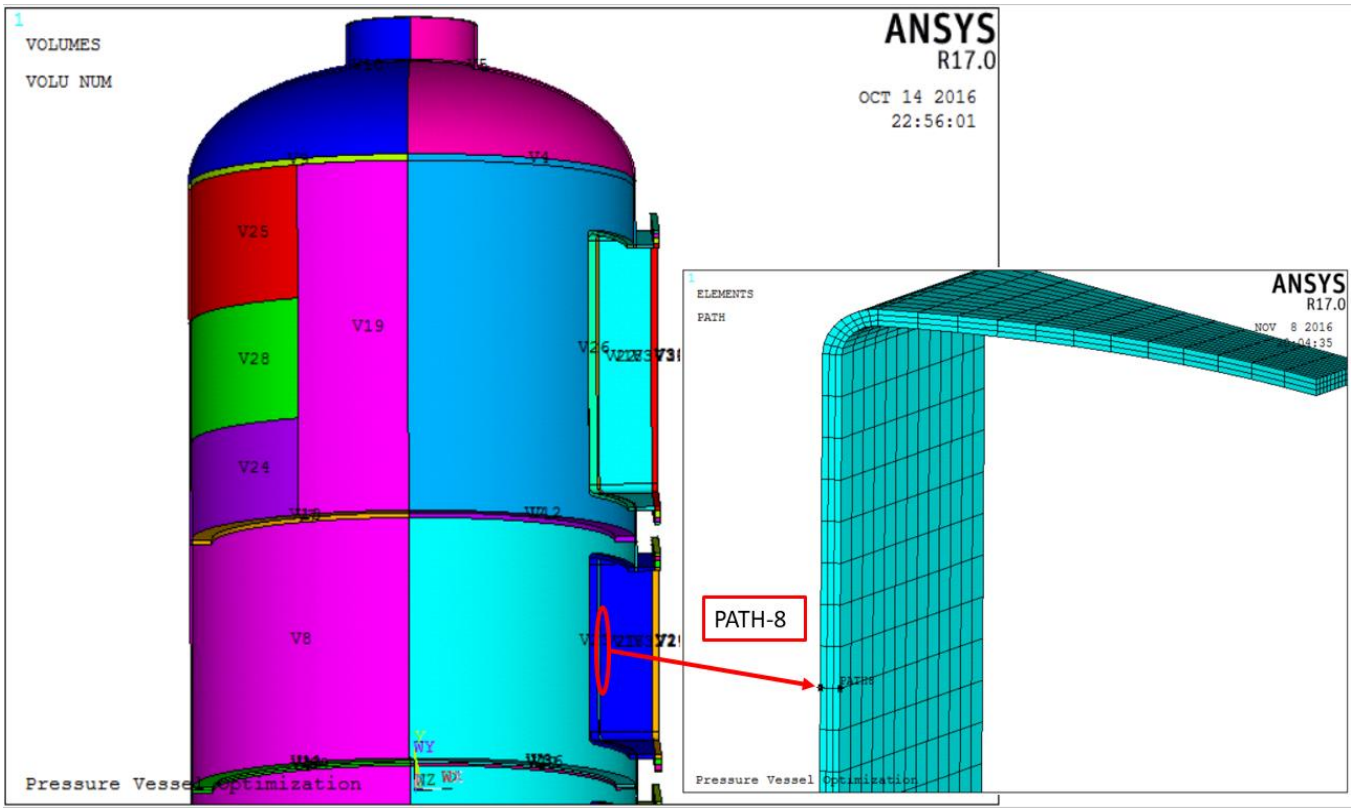

Figure 45: Path-8 plot on geometry

Table 22: Path-8 Evaluation

Load Condition	Allowable Stress S_m (MPa)	ANSYS linearization Type of stress	Stress Classification symbol	Equivalent Stress Intensity SINT (MPa)	Stress Control Value	Evaluation Result
Design Conditions A	137	MEMBRANE	$S_I\ (P_m)$	N/A	$1.0\times S_m$=137	N/A
			$S_{II}\ (P_L)$	16.72	$1.5\times S_m$=205.5	PASS
		MEMBRANE PLUS BENDING	$S_{III}\ (P_L + P_b)$	26.88	$1.5\times S_m$=205.5	PASS

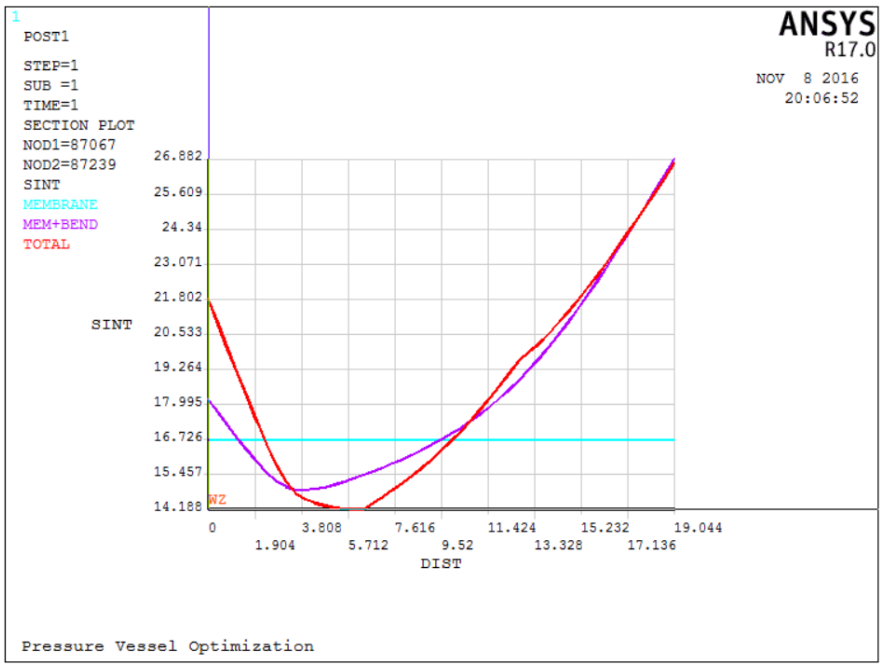

Figure 46: Stress variation through the thickness along Path-8

Table 23: ANSYS Path-8 Linearized Results

** MEMBRANE **						
	SX	SY	SZ	SXY	SYZ	SXZ
	-3.254	-16.28	-3.132	0.6791	0.1810	-3.579
	S1	S2	S3	SINT	SEQV	
	0.3934	-6.734	-16.33	16.72	14.53	
** BENDING ** I=INSIDE C=CENTER O=OUTSIDE						
	SX	SY	SZ	SXY	SYZ	SXZ
I	-15.40	-1.571	-5.353	0.1213	0.2806	-3.850
C	0.000	0.000	0.000	0.000	0.000	0.000
O	15.40	1.571	5.353	-0.1213	-0.2806	3.850
	S1	S2	S3	SINT	SEQV	
I	-1.548	-4.068	-16.70	15.16	14.07	
C	0.000	0.000	0.000	0.000	0.000	
O	16.70	4.068	1.548	15.16	14.07	
** MEMBRANE PLUS BENDING ** I=INSIDE C=CENTER O=OUTSIDE						
	SX	SY	SZ	SXY	SYZ	SXZ
I	-18.65	-17.85	-8.485	0.8004	0.4616	-7.429
C	-3.254	-16.28	-3.132	0.6791	0.1810	-3.579
O	12.14	-14.71	2.221	0.5578	-0.9958E-01	0.2705
	S1	S2	S3	SINT	SEQV	
I	-4.567	-17.68	-22.74	18.18	16.25	
C	0.3934	-6.734	-16.33	16.72	14.53	
O	12.16	2.214	-14.72	26.88	23.54	
** PEAK ** I=INSIDE C=CENTER O=OUTSIDE						
	SX	SY	SZ	SXY	SYZ	SXZ
I	-0.4023	-0.7846	-2.342	0.5809E-01	0.1740	-2.583
C	0.3842	0.4435	1.160	-0.2939E-01	-0.6870E-01	0.7574
O	-1.171	-1.010	-2.334	0.5988E-01	0.1019	-0.4812
	S1	S2	S3	SINT	SEQV	
I	1.388	-0.7765	-4.140	5.528	4.825	
C	1.628	0.4391	-0.7901E-01	1.707	1.516	
O	-0.9779	-1.021	-2.516	1.538	1.517	
** TOTAL ** I=INSIDE C=CENTER O=OUTSIDE						
	SX	SY	SZ	SXY	SYZ	SXZ
I	-19.05	-18.64	-10.83	0.8585	0.6355	-10.01
C	-2.870	-15.84	-1.972	0.6497	0.1123	-2.822
O	10.97	-15.72	-0.1129	0.6177	0.2311E-02	-0.2107
	S1	S2	S3	SINT	SEQV	TEMP
I	-4.117	-18.48	-25.92	21.80	19.20	0.000
C	0.4430	-5.248	-15.87	16.32	14.35	
O	10.99	-0.1169	-15.73	26.72	23.25	0.000

4.5.9 Path-9

Path-9 is the path along the thickness of the rectangular Nozzle around the middle section where cylindrical shell body of the vessel connects the upper side of nozzle N-2. Since this path lies far from the singularity, the average membrane stress and membrane plus bending stress along this path are classified as primary and hence checked against the $1.5 \times Sm$ limit.

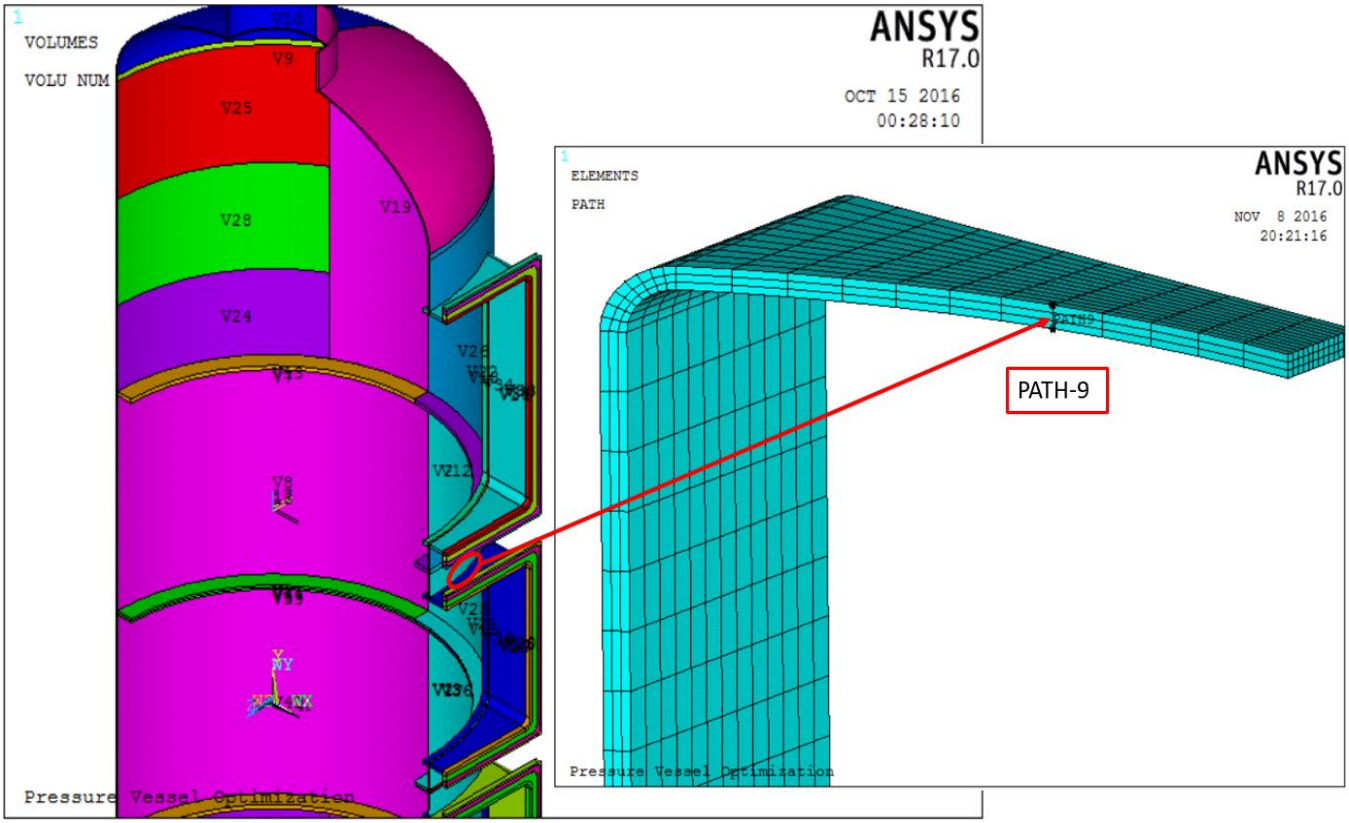

Figure 47: Path-9 plot on geometry

Table 24: Path-9 Evaluation

Load Condition	Allowable Stress S_m (MPa)	ANSYS linearization Type of stress	Stress Classification symbol	Equivalent Stress Intensity SINT (MPa)	Stress Control Value	Evaluation Result
Design Conditions A	137	MEMBRANE	$S_I\ (P_m)$	N/A	$1.0 \times S_m$=137	N/A
			$S_{II}\ (P_L)$	44.89	$1.5 \times S_m$=205.5	PASS
		MEMBRANE PLUS BENDING	$S_{III}\ (P_L + P_b)$	54.67	$1.5 \times S_m$=205.5	PASS

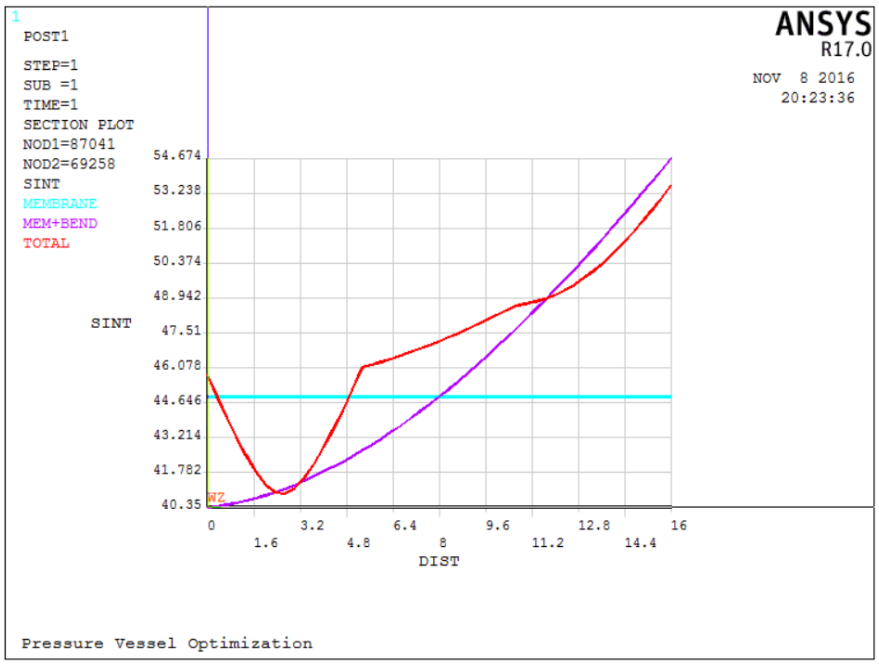

Figure 48: Stress variation through the thickness along Path-9

Table 25: ANSYS Path-9 Linearized Results

** MEMBRANE **						
	SX	SY	SZ	SXY	SYZ	SXZ
	1.009	5.633	43.48	2.930	2.206	4.874
	S1	S2	S3	SINT	SEQV	
	44.20	6.614	-0.6902	44.89	41.72	
	** BENDING ** I=INSIDE C=CENTER O=OUTSIDE					
	SX	SY	SZ	SXY	SYZ	SXZ
I	12.12	9.844	7.640	-1.960	4.996	-6.495
C	0.000	0.000	0.000	0.000	0.000	0.000
O	-12.12	-9.844	-7.640	1.960	-4.996	6.495
	S1	S2	S3	SINT	SEQV	
I	19.07	8.789	1.740	17.34	15.10	
C	0.000	0.000	0.000	0.000	0.000	
O	-1.740	-8.789	-19.07	17.34	15.10	
	** MEMBRANE PLUS BENDING ** I=INSIDE C=CENTER O=OUTSIDE					
	SX	SY	SZ	SXY	SYZ	SXZ
I	13.13	15.48	51.12	0.9695	7.202	-1.621
C	1.009	5.633	43.48	2.930	2.206	4.874
O	-11.11	-4.211	35.84	4.890	-2.789	11.37
	S1	S2	S3	SINT	SEQV	
I	52.57	14.93	12.22	40.35	39.07	
C	44.20	6.614	-0.6902	44.89	41.72	
O	38.51	-1.833	-16.16	54.67	49.10	
	** PEAK ** I=INSIDE C=CENTER O=OUTSIDE					
	SX	SY	SZ	SXY	SYZ	SXZ
I	1.253	4.381	1.616	-5.998	4.261	0.2797E-01
C	-0.1896	-1.997	-0.6305	2.587	-1.729	-0.4014E-01
O	-0.4942	3.607	0.9057	-4.350	2.655	0.1326
	S1	S2	S3	SINT	SEQV	
I	10.38	1.522	-4.650	15.03	13.08	
C	2.092	-0.5366	-4.373	6.466	5.632	
O	7.149	0.6761	-3.807	10.96	9.540	
	** TOTAL ** I=INSIDE C=CENTER O=OUTSIDE					
	SX	SY	SZ	SXY	SYZ	SXZ
I	14.38	19.86	52.74	-5.029	11.46	-1.593
C	0.8196	3.635	42.85	5.517	0.4772	4.834
O	-11.60	-0.6040	36.75	0.5401	-0.1345	11.50
	S1	S2	S3	SINT	SEQV	TEMP
I	56.56	19.64	10.78	45.78	42.06	0.000
C	43.43	7.614	-3.739	47.17	42.64	
O	39.35	-0.5813	-14.22	53.57	48.22	0.000

4.5.10 Path-10

Path-10 is the path through cylindrical shell of the vessel, in the section between the N1 nozzle and N2 nozzle. This path is remote from the singularity region. The stresses along this path are classified as primary and checked against the $1.5 \times Sm$ limit. This main reason for evaluating stresses along this path is to check the strength of cylindrical shell body of the pressure vessel.

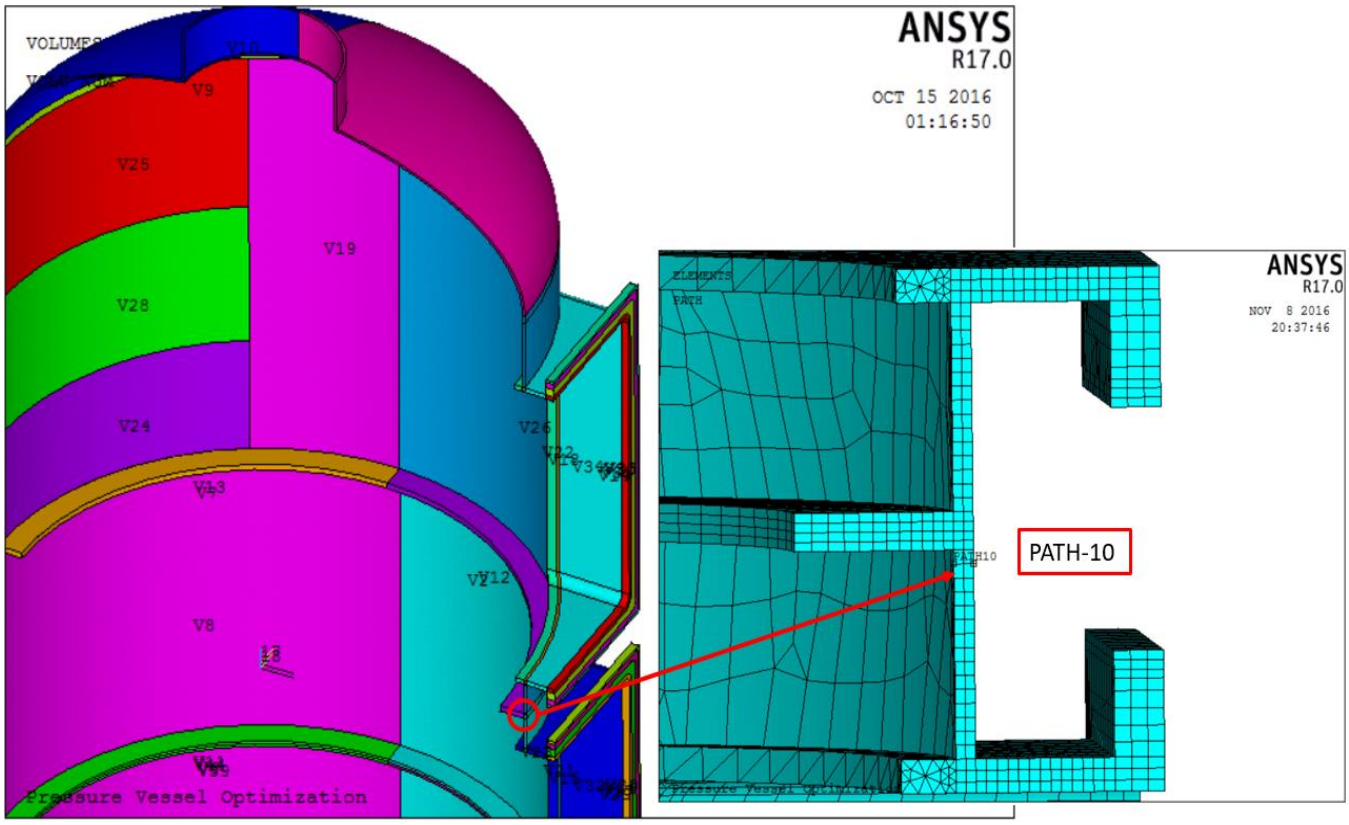

Figure 49: Path-10 plot on geometry

Table 26: Path-10 Evaluation

Load Condition	Allowable Stress S_m (MPa)	ANSYS linearization Type of stress	Stress Classification symbol	Equivalent Stress Intensity SINT (MPa)	Stress Control Value	Evaluation Result
Design Conditions A	137	MEMBRANE	S_I (P_m)	N/A	$1.0 \times S_m$=137	N/A
			S_{II} (P_L)	7.97	$1.5 \times S_m$=205.5	PASS
		MEMBRANE PLUS BENDING	S_{III} ($P_L + P_b$)	57.81	$1.5 \times S_m$=205.5	PASS

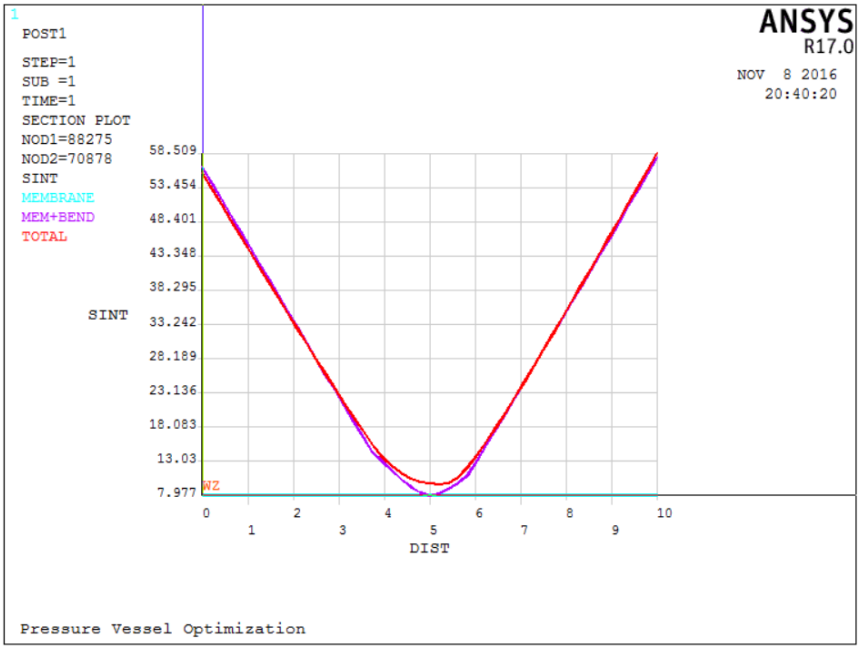

Figure 50: Stress variation through the thickness along Path-10

Table 27: ANSYS Path-10 Linearized Results

```
** MEMBRANE **
   SX        SY        SZ        SXY       SYZ       SXZ
 0.3912     1.368     6.841    -1.950    -0.1216   -0.6912E-01
   S1        S2        S3        SINT      SEQV
 6.844     2.889    -1.133     7.977     6.908

        ** BENDING **  I=INSIDE C=CENTER O=OUTSIDE
   SX        SY        SZ        SXY       SYZ       SXZ
I  3.060    -53.77    -20.58    -2.311    0.2335    0.1131
C  0.000     0.000     0.000     0.000     0.000     0.000
O -3.060     53.77     20.58     2.311    -0.2335   -0.1131
   S1        S2        S3        SINT      SEQV
I  3.155    -20.58    -53.86     57.02     49.61
C  0.000     0.000     0.000     0.000     0.000
O  53.86     20.58    -3.155     57.02     49.61

        ** MEMBRANE PLUS BENDING **  I=INSIDE C=CENTER O=OUTSIDE
   SX        SY        SZ        SXY       SYZ       SXZ
I  3.451    -52.40    -13.74    -4.261    0.1119    0.4395E-01
C 0.3912     1.368     6.841    -1.950    -0.1216   -0.6912E-01
O -2.669     55.14     27.42    0.3612    -0.3552    -0.1822
   S1        S2        S3        SINT      SEQV
I  3.775    -13.74    -52.72     56.50     50.09
C  6.844     2.889    -1.133     7.977     6.908
O  55.14     27.42    -2.672     57.81     50.08

        ** PEAK **  I=INSIDE C=CENTER O=OUTSIDE
   SX        SY        SZ        SXY       SYZ       SXZ
I -1.932    -1.573    -1.023     2.549    0.1941E-01 -0.4298E-01
C  1.933     1.550     1.014    -2.550    -0.1931E-01  0.4303E-01
O -1.935    -1.526    -1.005     2.551    0.1921E-01 -0.4308E-01
   S1        S2        S3        SINT      SEQV
I 0.8031    -1.022    -4.308     5.111     4.486
C  4.299     1.013    -0.8161    5.115     4.489
O 0.8290    -1.005    -4.290     5.119     4.492

        ** TOTAL **  I=INSIDE C=CENTER O=OUTSIDE
   SX        SY        SZ        SXY       SYZ       SXZ
I  1.520    -53.97    -14.77    -1.712    0.1313    0.9701E-03
C  2.324     2.917     7.855    -4.500    -0.1410   -0.2609E-01
O -4.604     53.61     26.42     2.912    -0.3360    -0.2253
   S1        S2        S3        SINT      SEQV      TEMP
I  1.572    -14.77    -54.03     55.60     49.49     0.000
C  7.866     7.121    -1.890     9.757     9.406
O  53.76     26.42    -4.750     58.51     50.71     0.000
```

4.5.11 Path-11

Path-11 is the path created through the N-1 nozzle thickness at the joint between the flange and N-1 nozzle. The membrane stress intensity linearized along this path is classified as primary local stress and thereby will be verified against the ASME local stress limits which is equal to $1.5\times S_m$(Allowable stress). For design to be safe, the linearized membrane stress along this path should be less than $1.5\times S_m$(Allowable stress).

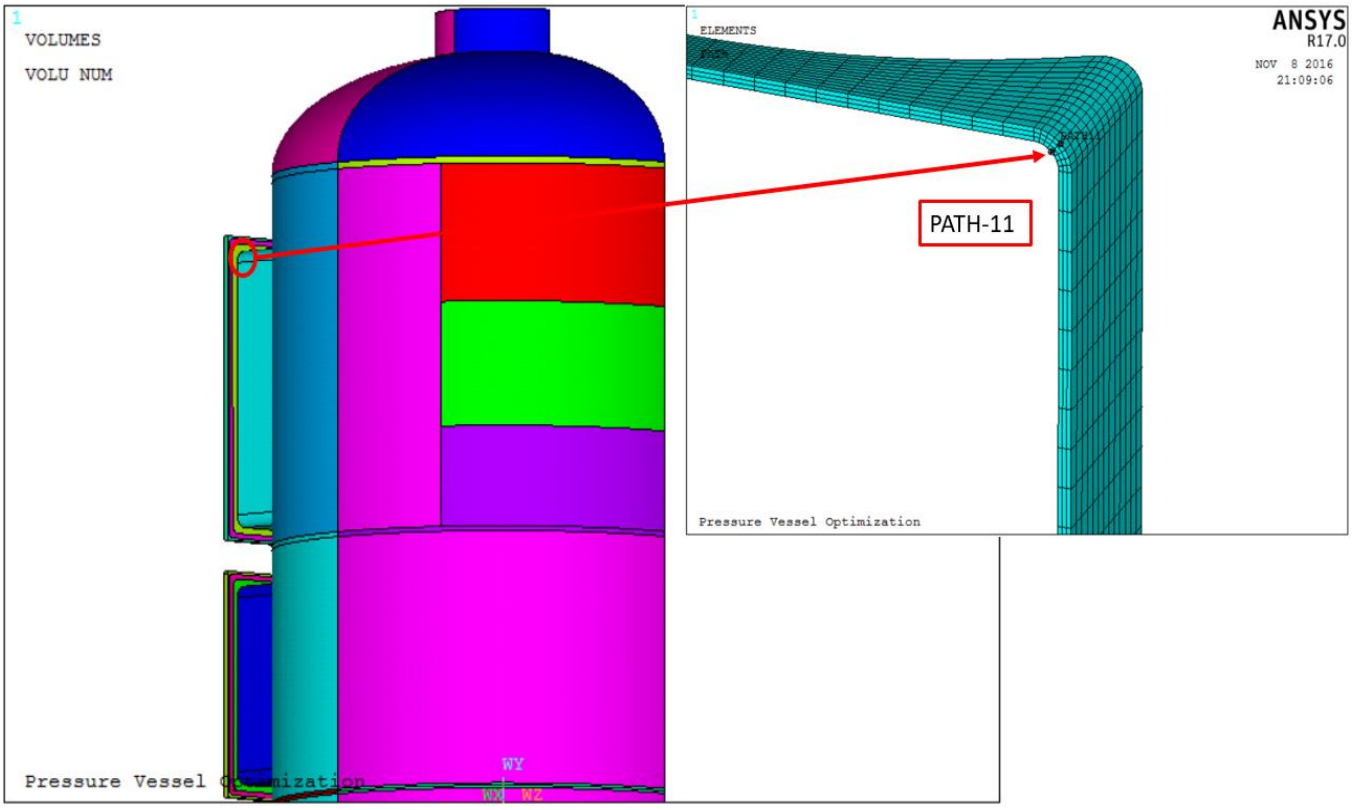

Figure 51: Path-11 plot on geometry

Table 28: Path-11 Evaluation

Load Condition	Allowable Stress S_m (MPa)	ANSYS linearization Type of stress	Stress Classification symbol	Equivalent Stress Intensity SINT (MPa)	Stress Control Value	Evaluation Result
Design Conditions A	137	MEMBRANE	$S_I\ (P_m)$	N/A	$1.0\times S_m$=137	N/A
			$S_{II}\ (P_L)$	46.34	$1.5\times S_m$=205.5	PASS
		MEMBRANE PLUS BENDING	$S_{III}\ (P_L + P_b)$	77.29	$1.5\times S_m$=205.5	PASS

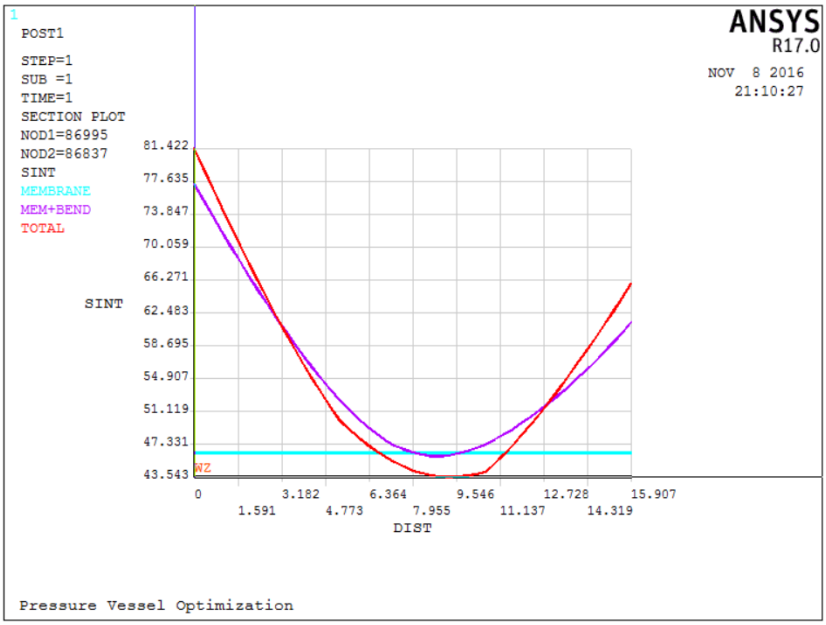

Figure 52: Stress variation through the thickness along Path-11

Table 29: ANSYS Path-11 Linearized Results:

** MEMBRANE **

SX	SY	SZ	SXY	SYZ	SXZ
4.956	25.23	37.89	3.750	7.894	-13.70

S1	S2	S3	SINT	SEQV
44.85	24.70	-1.489	46.34	40.25

** BENDING ** I=INSIDE C=CENTER O=OUTSIDE

	SX	SY	SZ	SXY	SYZ	SXZ
I	-44.60	-7.815	-22.83	-0.2198	13.01	16.07
C	0.000	0.000	0.000	0.000	0.000	0.000
O	44.60	7.815	22.83	0.2198	-13.01	-16.07

	S1	S2	S3	SINT	SEQV
I	1.257	-22.45	-54.04	55.30	48.05
C	0.000	0.000	0.000	0.000	0.000
O	54.04	22.45	-1.257	55.30	48.05

** MEMBRANE PLUS BENDING ** I=INSIDE C=CENTER O=OUTSIDE

	SX	SY	SZ	SXY	SYZ	SXZ
I	-39.64	17.41	15.06	3.530	20.91	2.370
C	4.956	25.23	37.89	3.750	7.894	-13.70
O	49.56	33.04	60.71	3.969	-5.120	-29.77

	S1	S2	S3	SINT	SEQV
I	37.41	-4.691	-39.88	77.29	67.02
C	44.85	24.70	-1.489	46.34	40.25
O	86.21	32.26	24.84	61.37	58.01

** PEAK ** I=INSIDE C=CENTER O=OUTSIDE

	SX	SY	SZ	SXY	SYZ	SXZ
I	2.126	3.863	6.894	0.1707E-01	0.8942	0.2951
C	-2.300	-1.830	-4.067	-0.5594	-0.5183	0.3021
O	7.073	3.458	9.376	2.220	1.179	-1.504

	S1	S2	S3	SINT	SEQV
I	7.154	3.621	2.107	5.048	4.486
C	-1.327	-2.671	-4.199	2.872	2.489
O	10.12	7.788	1.999	8.120	7.242

** TOTAL ** I=INSIDE C=CENTER O=OUTSIDE

	SX	SY	SZ	SXY	SYZ	SXZ
I	-37.52	21.28	21.95	3.547	21.80	2.665
C	2.657	23.40	33.82	3.190	7.376	-13.40
O	56.63	36.50	70.09	6.190	-3.941	-31.27

	S1	S2	S3	SINT	SEQV	TEMP
I	43.66	-0.1788	-37.77	81.42	70.58	0.000
C	40.81	22.56	-3.494	44.30	38.56	
O	96.16	36.70	30.36	65.80	62.87	0.000

4.5.12 Path-12

Path-12 is a path created through the flange thickness at the joint between the flange and N-1 nozzle. This path is constructed on the flange at nozzle N-1 to check the safe design of the flange component at the nozzle opening. This path is far from the singularity. The average membrane stress and membrane plus bending stress along this path are classified as primary and checked against the $1.5 \times Sm$ limit.

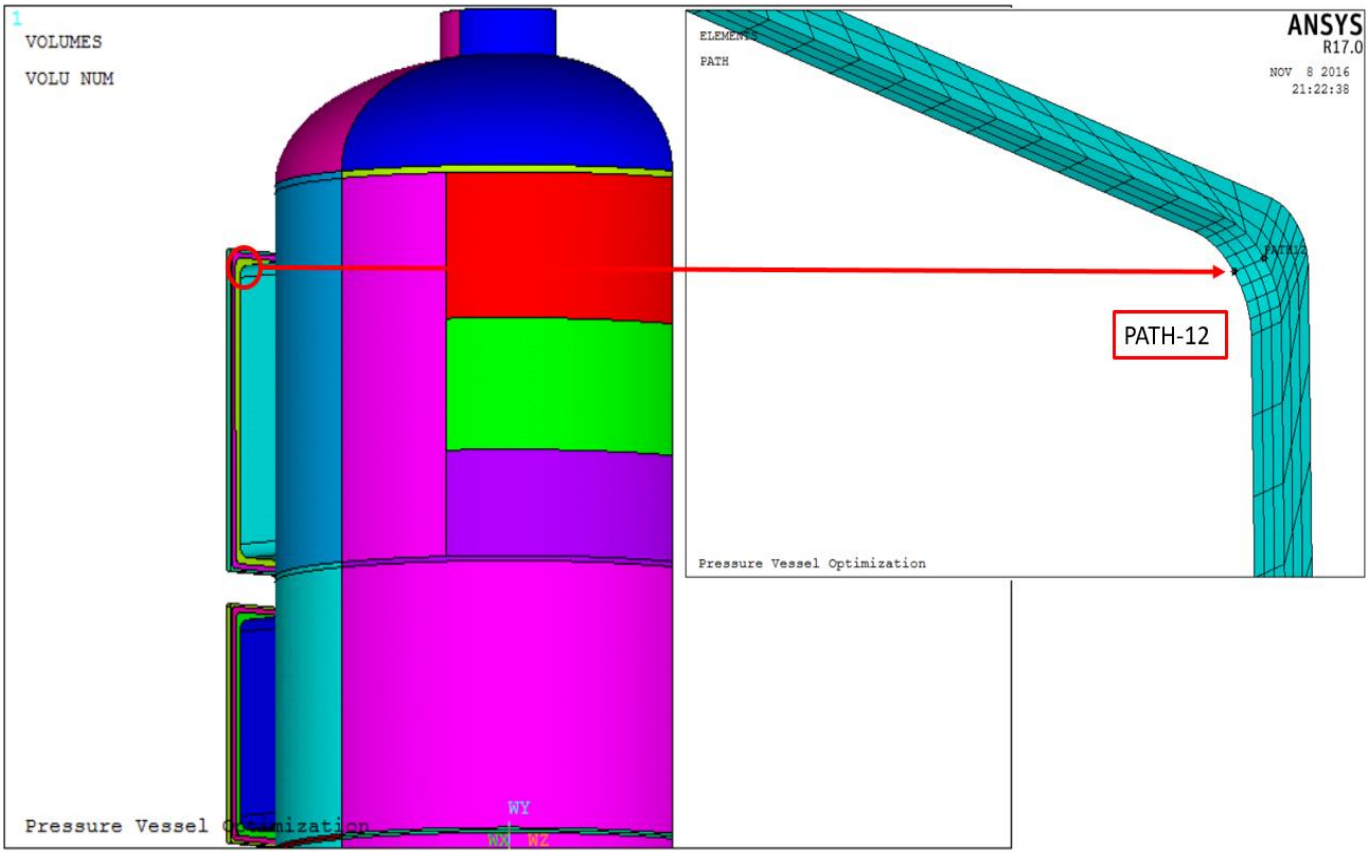

Figure 53: Path-12 plot on geometry

Table 30: Path-12 Evaluation

Load Condition	Allowable Stress S_m (MPa)	ANSYS linearization Type of stress	Stress Classification symbol	Equivalent Stress Intensity SINT (MPa)	Stress Control Value	Evaluation Result
Design Conditions A	137	MEMBRANE	S_I (P_m)	N/A	$1.0 \times S_m$=137	N/A
			S_{II} (P_L)	16.67	$1.5 \times S_m$=205.5	PASS
		MEMBRANE PLUS BENDING	S_{III} ($P_L + P_b$)	47.77	$1.5 \times S_m$=205.5	PASS

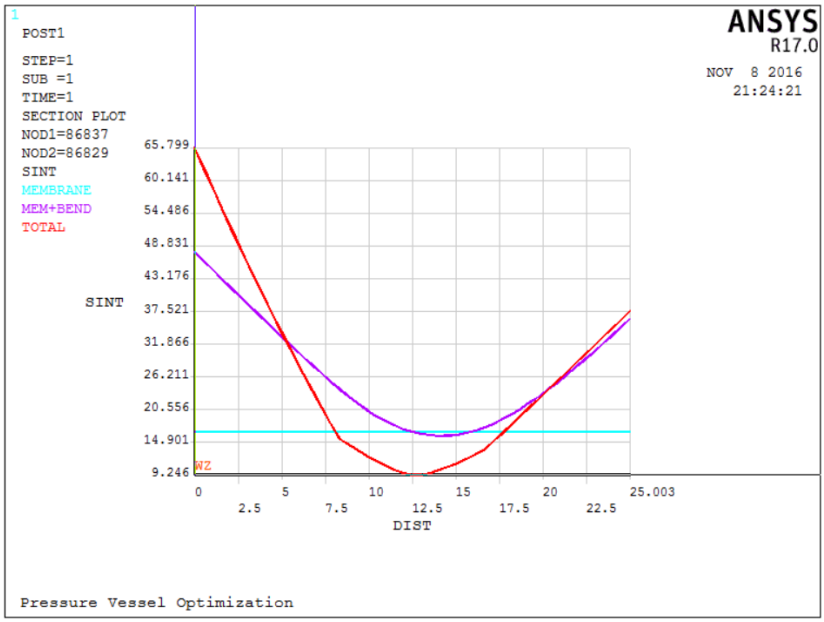

Figure 54: Stress variation through the thickness along Path-12

Table 31: ANSYS Path-12 Linearized Results

** MEMBRANE **						
	SX	SY	SZ	SXY	SYZ	SXZ
	17.19	5.843	9.425	1.558	-2.689	-5.877
	S1	S2	S3	SINT	SEQV	
	20.82	7.482	4.152	16.67	15.28	
** BENDING ** I=INSIDE C=CENTER O=OUTSIDE						
	SX	SY	SZ	SXY	SYZ	SXZ
I	27.76	23.10	49.42	3.156	4.190	-13.86
C	0.000	0.000	0.000	0.000	0.000	0.000
O	-27.76	-23.10	-49.42	-3.156	-4.190	13.86
	S1	S2	S3	SINT	SEQV	
I	56.35	26.72	17.20	39.15	35.36	
C	0.000	0.000	0.000	0.000	0.000	
O	-17.20	-26.72	-56.35	39.15	35.36	
** MEMBRANE PLUS BENDING ** I=INSIDE C=CENTER O=OUTSIDE						
	SX	SY	SZ	SXY	SYZ	SXZ
I	44.95	28.94	58.84	4.714	1.501	-19.74
C	17.19	5.843	9.425	1.558	-2.689	-5.877
O	-10.57	-17.26	-39.99	-1.599	-6.880	7.984
	S1	S2	S3	SINT	SEQV	
I	72.87	34.76	25.11	47.77	43.75	
C	20.82	7.482	4.152	16.67	15.28	
O	-7.349	-16.94	-43.53	36.19	32.47	
** PEAK ** I=INSIDE C=CENTER O=OUTSIDE						
	SX	SY	SZ	SXY	SYZ	SXZ
I	11.67	7.558	11.25	1.476	-5.441	-11.53
C	-5.321	-2.610	-4.007	-0.6885	1.856	4.740
O	9.610	2.883	4.783	1.278	-1.981	-7.428
	S1	S2	S3	SINT	SEQV	
I	24.43	7.180	-1.129	25.56	22.58	
C	0.4475	-2.515	-9.871	10.32	9.202	
O	15.39	2.708	-0.8267	16.22	14.77	
** TOTAL ** I=INSIDE C=CENTER O=OUTSIDE						
	SX	SY	SZ	SXY	SYZ	SXZ
I	56.63	36.50	70.09	6.190	-3.941	-31.27
C	11.87	3.233	5.418	0.8692	-0.8337	-1.137
O	-0.9637	-14.37	-35.21	-0.3206	-8.861	0.5558
	S1	S2	S3	SINT	SEQV	TEMP
I	96.16	36.70	30.36	65.80	62.87	0.000
C	12.18	5.419	2.926	9.249	8.289	
O	-0.9354	-11.14	-38.47	37.54	33.62	0.000

4.5.13 Path-13

Path-13 is a path through the nozzle thickness at the joint between the flange and N-2 small nozzle. This path is created on nozzle N-2. Similar to path-11, this path is also far from the singularity. Thus, the average membrane stress and membrane plus bending stress along this path are classified as primary and hence checked against the $1.5\times Sm$ limit.

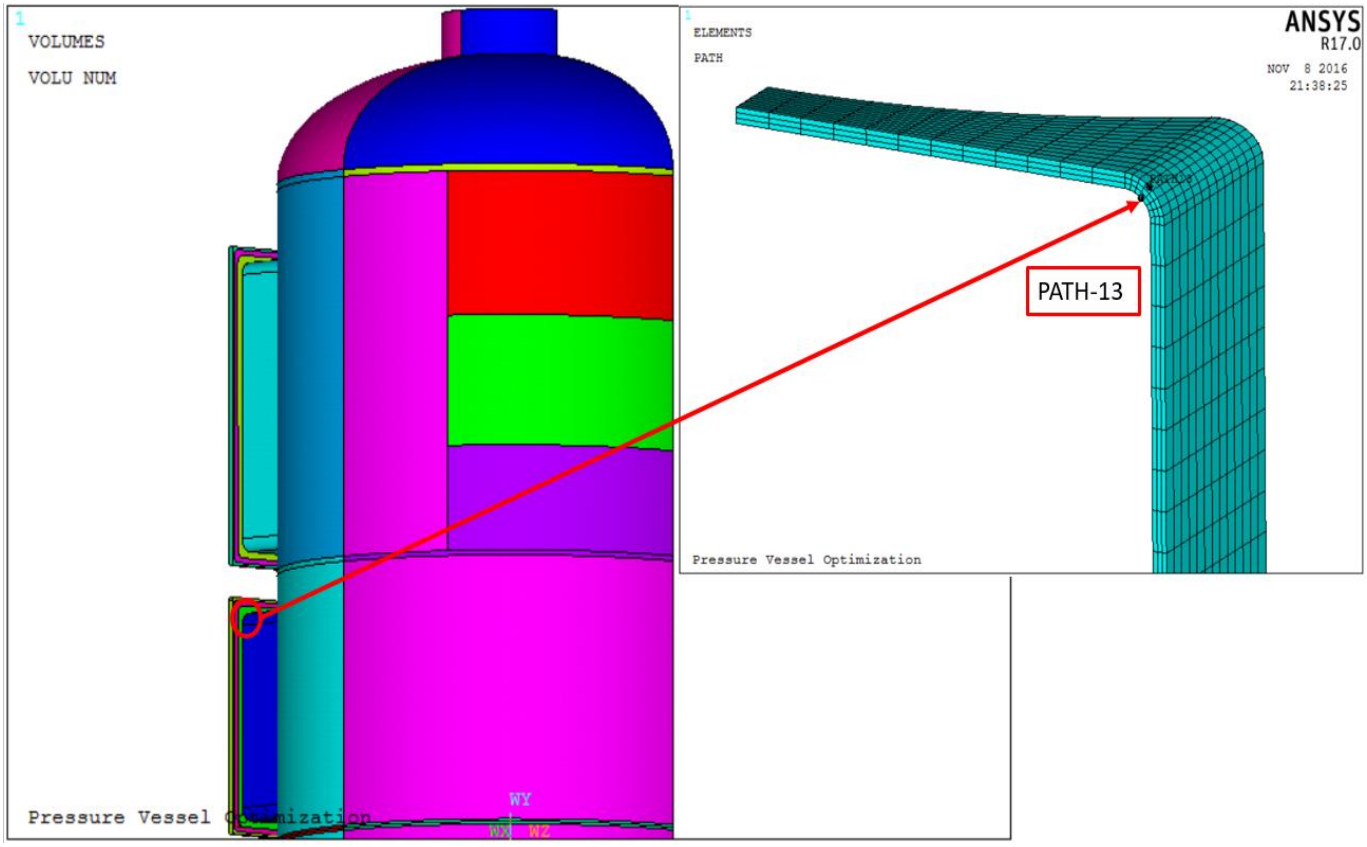

Figure 55: Path-13 plot on geometry

Table 32: Path-13 Evaluation

Load Condition	Allowable Stress S_m (MPa)	ANSYS linearization Type of stress	Stress Classification symbol	Equivalent Stress Intensity SINT (MPa)	Stress Control Value	Evaluation Result
Design Conditions A	137	MEMBRANE	$S_I\ (P_m)$	N/A	$1.0\times S_m$=137	N/A
			$S_{II}\ (P_L)$	36.10	$1.5\times S_m$=205.5	PASS
		MEMBRANE PLUS BENDING	$S_{III}\ (P_L + P_b)$	64.37	$1.5\times S_m$=205.5	PASS

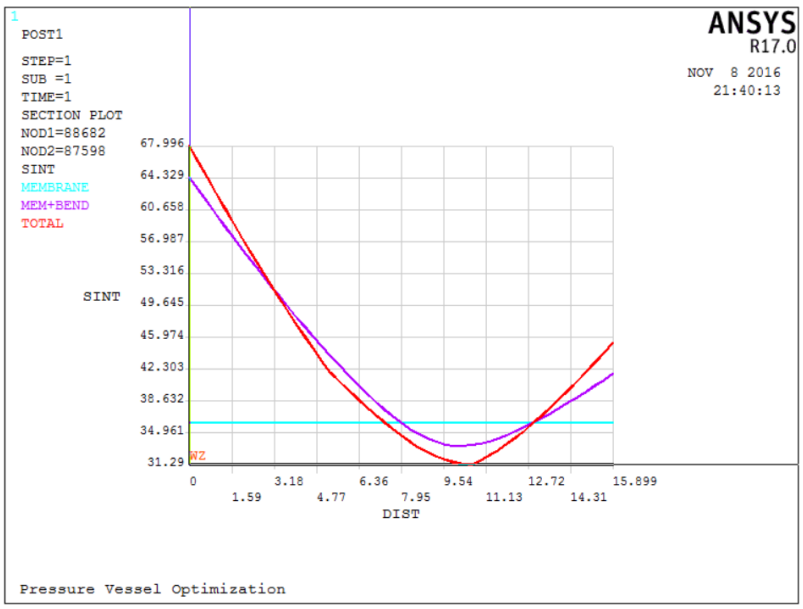

Figure 56: Stress variation through the thickness along Path-13

Table 33: ANSYS Path-13 Linearized Results

** MEMBRANE **						
	SX	SY	SZ	SXY	SYZ	SXZ
	3.937	22.68	30.61	6.055	6.370	-8.649
	S1	S2	S3	SINT	SEQV	
	34.99	23.36	-1.117	36.10	31.92	
	** BENDING ** I=INSIDE C=CENTER O=OUTSIDE					
	SX	SY	SZ	SXY	SYZ	SXZ
I	-34.37	-10.50	-12.24	-3.929	11.87	9.308
C	0.000	0.000	0.000	0.000	0.000	0.000
O	34.37	10.50	12.24	3.929	-11.87	-9.308
	S1	S2	S3	SINT	SEQV	
I	0.9163	-17.98	-40.04	40.95	35.50	
C	0.000	0.000	0.000	0.000	0.000	
O	40.04	17.98	-0.9163	40.95	35.50	
	** MEMBRANE PLUS BENDING ** I=INSIDE C=CENTER O=OUTSIDE					
	SX	SY	SZ	SXY	SYZ	SXZ
I	-30.43	12.18	18.37	2.127	18.24	0.6589
C	3.937	22.68	30.61	6.055	6.370	-8.649
O	38.31	33.18	42.84	9.984	-5.504	-17.96
	S1	S2	S3	SINT	SEQV	
I	33.83	-3.174	-30.54	64.37	55.96	
C	34.99	23.36	-1.117	36.10	31.92	
O	62.63	30.82	20.88	41.76	37.78	
	** PEAK ** I=INSIDE C=CENTER O=OUTSIDE					
	SX	SY	SZ	SXY	SYZ	SXZ
I	1.789	3.470	5.397	-0.3364	0.8467	0.3462
C	-1.914	-1.813	-3.068	-0.2890	-0.4501	0.1575
O	5.809	3.778	6.850	1.467	0.9518	-0.9577
	S1	S2	S3	SINT	SEQV	
I	5.727	3.277	1.651	4.076	3.553	
C	-1.445	-2.135	-3.216	1.771	1.546	
O	7.422	6.402	2.614	4.808	4.388	
	** TOTAL ** I=INSIDE C=CENTER O=OUTSIDE					
	SX	SY	SZ	SXY	SYZ	SXZ
I	-28.64	15.65	23.77	1.790	19.09	1.005
C	2.023	20.87	27.54	5.766	5.920	-8.491
O	44.12	36.96	49.69	11.45	-4.552	-18.91
	S1	S2	S3	SINT	SEQV	TEMP
I	39.28	0.2136	-28.72	68.00	59.10	0.000
C	31.82	21.41	-2.801	34.62	30.77	
O	69.75	36.59	24.43	45.32	40.63	0.000

4.5.14 Path-14

Path-14 is a path through the flange thickness at the joint between the flange and N-2 small nozzle. This path is constructed on the flange connected to nozzle N-2. This path lies far from the singularity. The average membrane stress and membrane plus bending stress along this path are classified as primary and hence checked against the $1.5\times Sm$ limit.

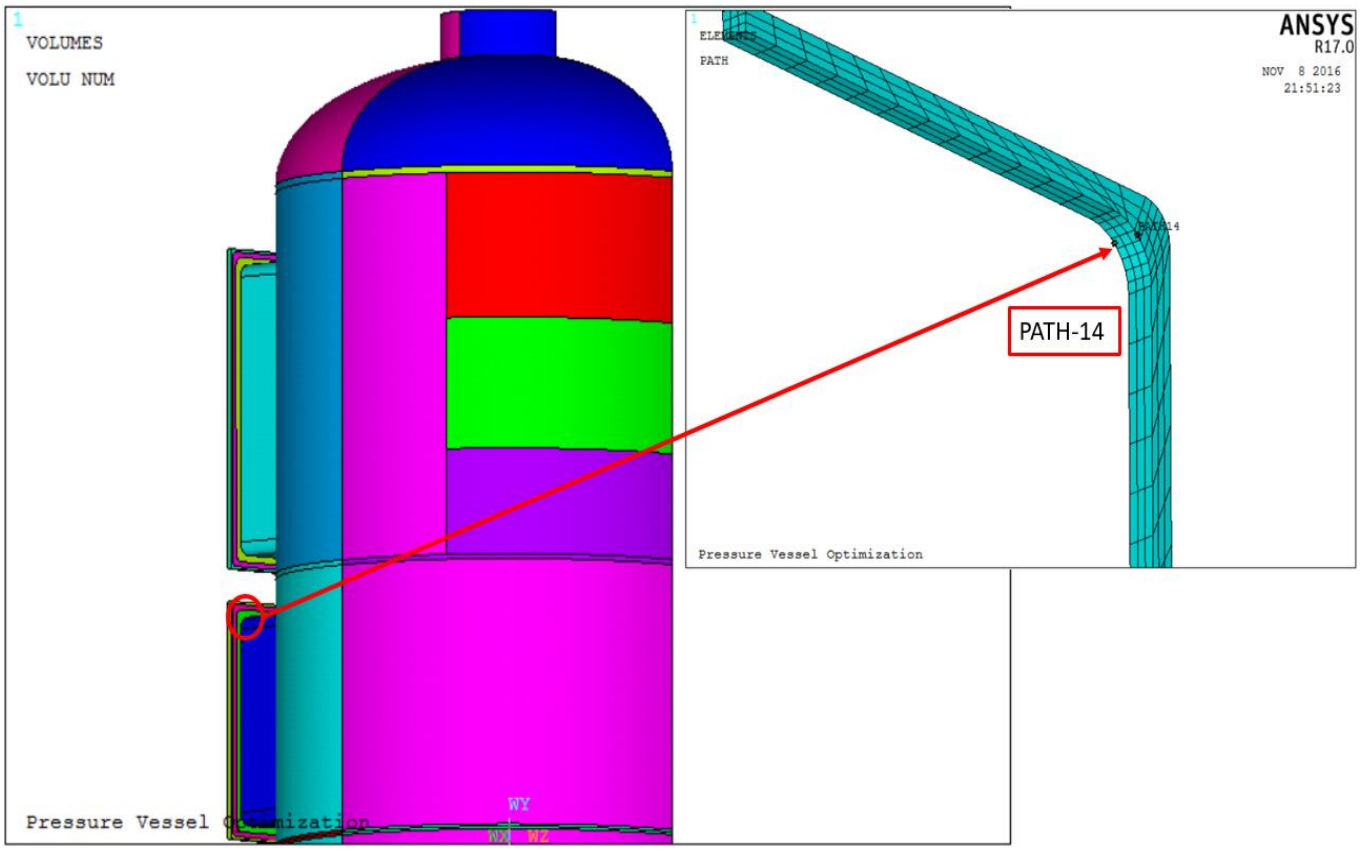

Figure 57: Path-14 plot on geometry

Table 34: Path-14 Evaluation

Load Condition	Allowable Stress S_m (MPa)	ANSYS linearization Type of stress	Stress Classification symbol	Equivalent Stress Intensity SINT (MPa)	Stress Control Value	Evaluation Result
Design Conditions A	137	MEMBRANE	S_I (P_m)	N/A	$1.0\times S_m$=137	N/A
			S_{II} (P_L)	10.39	$1.5\times S_m$=205.5	PASS
		MEMBRANE PLUS BENDING	S_{III} ($P_L + P_b$)	30.87	$1.5\times S_m$=205.5	PASS

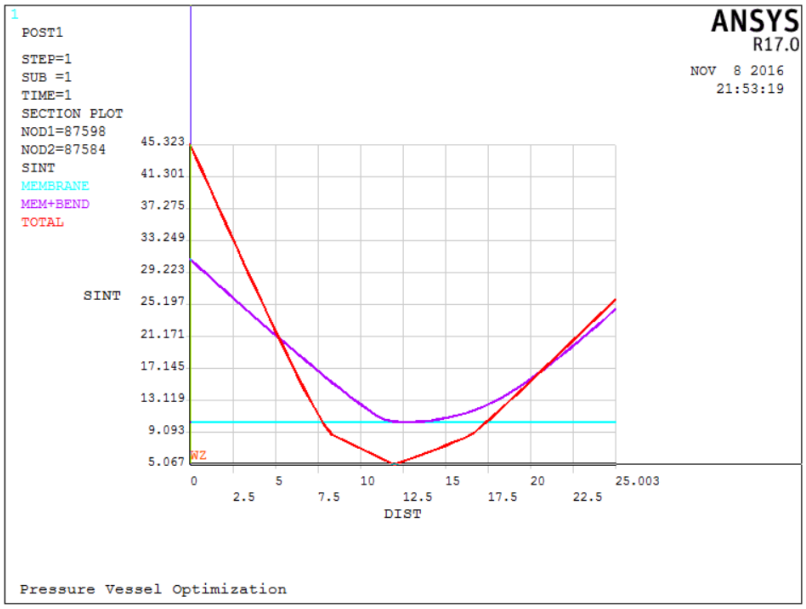

Figure 58: Stress variation through the thickness along Path-14

Table 35: ANSYS Path-14 Linearized Results

** MEMBRANE **						
	SX	SY	SZ	SXY	SYZ	SXZ
	13.53	8.496	7.175	2.834	-1.757	-3.007
	S1	S2	S3	SINT	SEQV	
	16.15	7.302	5.756	10.39	9.709	
** BENDING ** I=INSIDE C=CENTER O=OUTSIDE						
	SX	SY	SZ	SXY	SYZ	SXZ
I	21.77	20.89	35.27	5.364	1.484	-8.430
C	0.000	0.000	0.000	0.000	0.000	0.000
O	-21.77	-20.89	-35.27	-5.364	-1.484	8.430
	S1	S2	S3	SINT	SEQV	
I	39.38	24.96	13.59	25.79	22.39	
C	0.000	0.000	0.000	0.000	0.000	
O	-13.59	-24.96	-39.38	25.79	22.39	
** MEMBRANE PLUS BENDING ** I=INSIDE C=CENTER O=OUTSIDE						
	SX	SY	SZ	SXY	SYZ	SXZ
I	35.30	29.38	42.45	8.198	-0.2730	-11.44
C	13.53	8.496	7.175	2.834	-1.757	-3.007
O	-8.233	-12.39	-28.10	-2.529	-3.241	5.423
	S1	S2	S3	SINT	SEQV	
I	52.08	33.84	21.21	30.87	26.88	
C	16.15	7.302	5.756	10.39	9.709	
O	-5.300	-13.57	-29.85	24.55	21.64	
** PEAK ** I=INSIDE C=CENTER O=OUTSIDE						
	SX	SY	SZ	SXY	SYZ	SXZ
I	8.815	7.575	7.246	3.254	-4.279	-7.477
C	-4.075	-2.668	-2.542	-1.385	1.459	3.112
O	7.486	3.098	2.926	2.282	-1.555	-4.970
	S1	S2	S3	SINT	SEQV	
I	18.19	5.119	0.3269	17.86	16.01	
C	-0.5947E-01	-1.865	-7.360	7.300	6.586	
O	11.57	2.201	-0.2649	11.84	10.82	
** TOTAL ** I=INSIDE C=CENTER O=OUTSIDE						
	SX	SY	SZ	SXY	SYZ	SXZ
I	44.12	36.96	49.69	11.45	-4.552	-18.91
C	9.459	5.828	4.633	1.450	-0.2985	0.1054
O	-0.7466	-9.294	-25.17	-0.2474	-4.796	0.4522
	S1	S2	S3	SINT	SEQV	TEMP
I	69.75	36.59	24.43	45.32	40.63	0.000
C	9.967	5.444	4.510	5.457	5.055	
O	-0.7235	-7.976	-26.51	25.79	23.04	0.000

4.5.15 Paths-15,16,17,18,19 and 20

With stress linearization approach, it is preferred to have a stress classification line passing through the stress singularity point in order to completely capture the effects of local stress concentrations in this region. But, since our pressure vessel model contains filleted corner, we cannot pin-point the exact location of the singularity. Thus, we cannot be assured whether the paths path-2 and path-3 created above passes through the singularity. Hence, as a precautionary measure and to ensure safe design of the pressure vessel, a few more paths were created around the maximum stress region. Paths-15,17,19 were created through the thickness of the cylindrical shell body of the vessel whereas Paths-16,18,20 were created through the thickness of Nozzle N-1. The stress analysis results and verifications performed along these paths are shown below. The linearized membrane plus bending stress along these paths are classified as secondary and thereby will be verified against the ASME local stress limits which is equal to 3×Sm (Allowable stress).

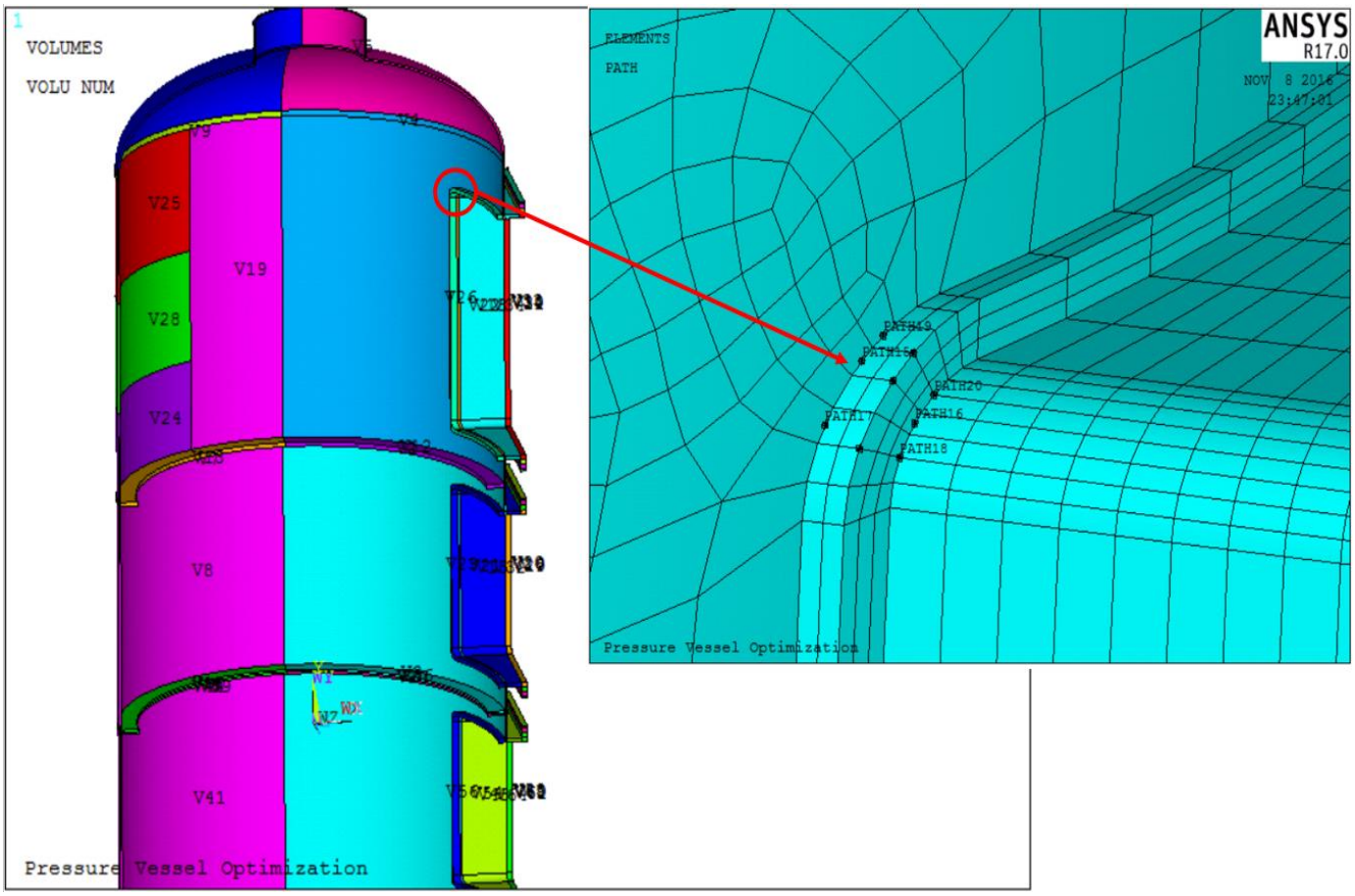

Figure 59: Additional paths created near the stress singularity region

Table 36: Path-15 Evaluation

Load Condition	Allowable Stress S_m (MPa)	ANSYS linearization Type of stress	Stress Classification symbol	Equivalent Stress Intensity SINT (MPa)	Stress Control Value	Evaluation Result
Design Conditions A	137	MEMBRANE	S_I (P_m)	N/A	1.0×S_m=137	N/A
			S_{II} (P_L)	96.24	1.5×S_m=205.5	PASS
		MEMBRANE PLUS BENDING	S_{IV} $(P_L + P_b + Q)$	198.1	3×S_m=411	PASS

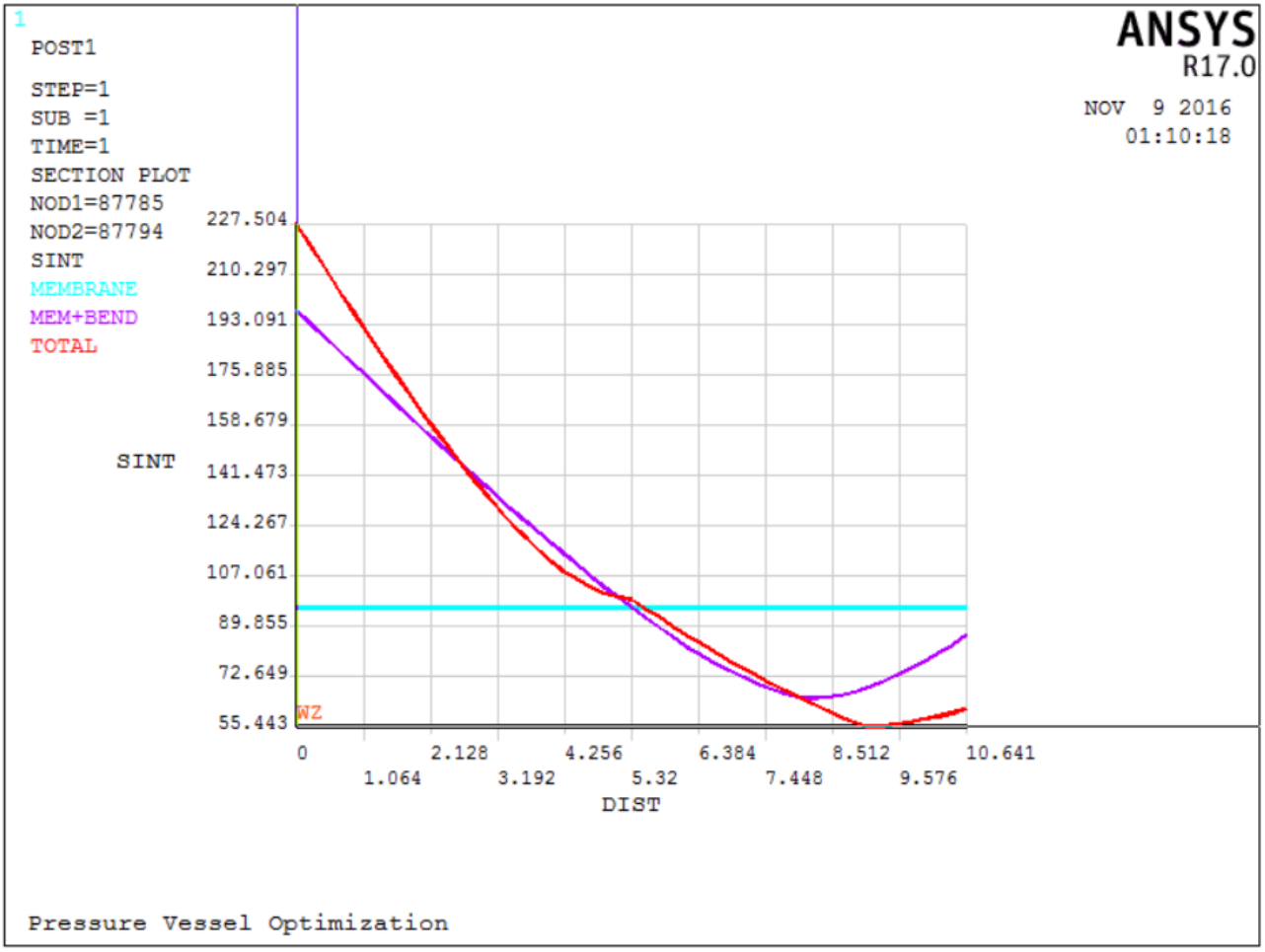

Figure 60: Stress variation through the thickness along Path-15

Table 37: Path-16 Evaluation

Load Condition	Allowable Stress S_m (MPa)	ANSYS linearization Type of stress	Stress Classification symbol	Equivalent Stress Intensity SINT (MPa)	Stress Control Value	Evaluation Result
Design Conditions A	137	MEMBRANE	S_I (P_m)	N/A	1.0×S_m=137	N/A
			S_{II} (P_L)	158.1	1.5×S_m=205.5	PASS
		MEMBRANE PLUS BENDING	S_{IV} $(P_L + P_b + Q)$	240.1	3×S_m=411	PASS

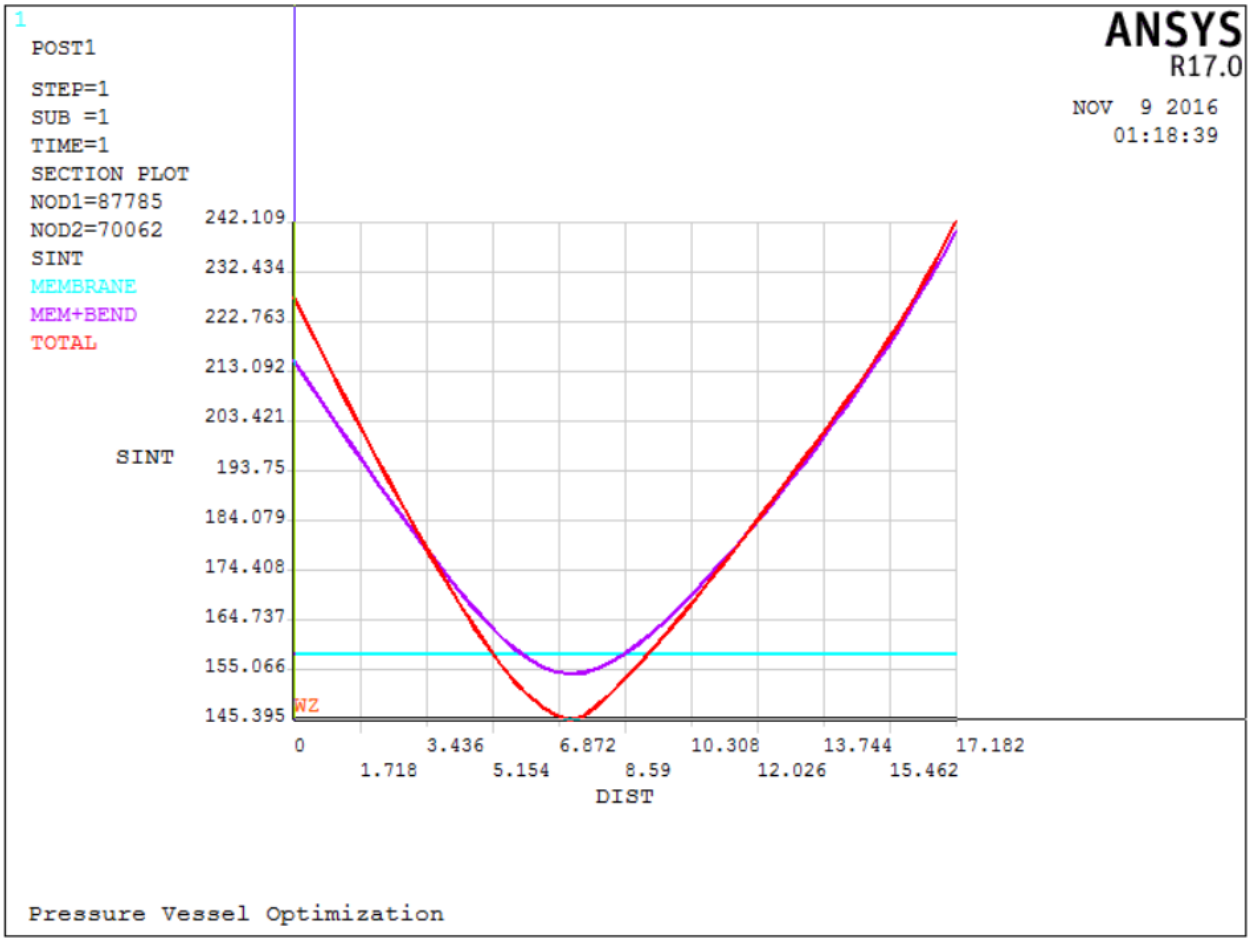

Figure 61: Stress variation through the thickness along Path-16

Table 38: Path-17 Evaluation

Load Condition	Allowable Stress S_m (MPa)	ANSYS linearization Type of stress	Stress Classification symbol	Equivalent Stress Intensity SINT (MPa)	Stress Control Value	Evaluation Result
Design Conditions A	137	MEMBRANE	S_I (P_m)	N/A	1.0×S_m=137	N/A
			S_{II} (P_L)	129.5	1.5×S_m=205.5	PASS
		MEMBRANE PLUS BENDING	S_{IV} $(P_L + P_b + Q)$	227.7	3×S_m=411	PASS

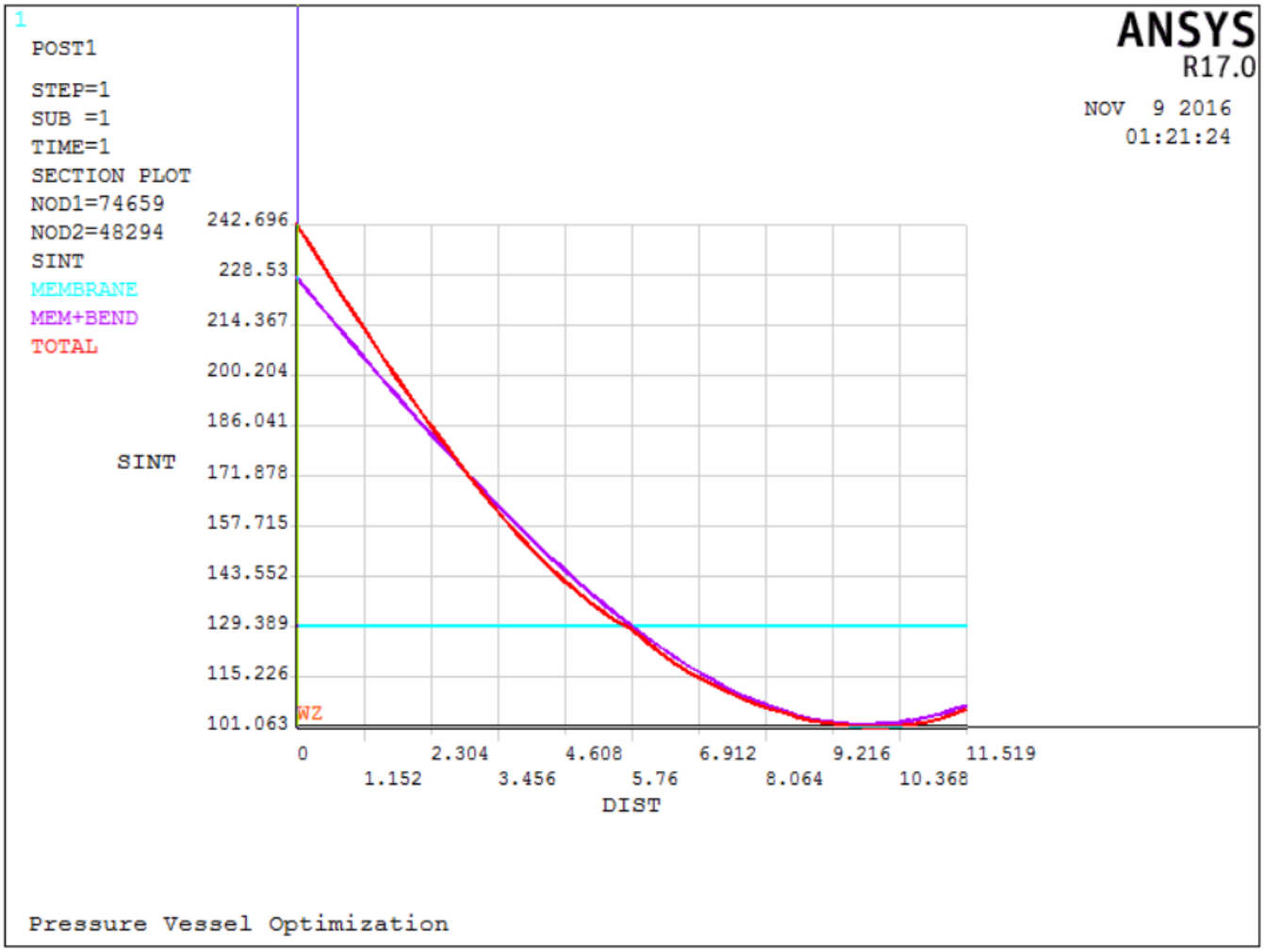

Figure 62: Stress variation through the thickness along Path-17

Table 39: Path-18 Evaluation

Load Condition	Allowable Stress S_m (MPa)	ANSYS linearization Type of stress	Stress Classification symbol	Equivalent Stress Intensity SINT (MPa)	Stress Control Value	Evaluation Result
Design Conditions A	137	MEMBRANE	S_I (P_m)	N/A	1.0×S_m=137	N/A
			S_{II} (P_L)	151.1	1.5×S_m=205.5	PASS
		MEMBRANE PLUS BENDING	S_{IV} $(P_L + P_b + Q)$	225.1	3×S_m=411	PASS

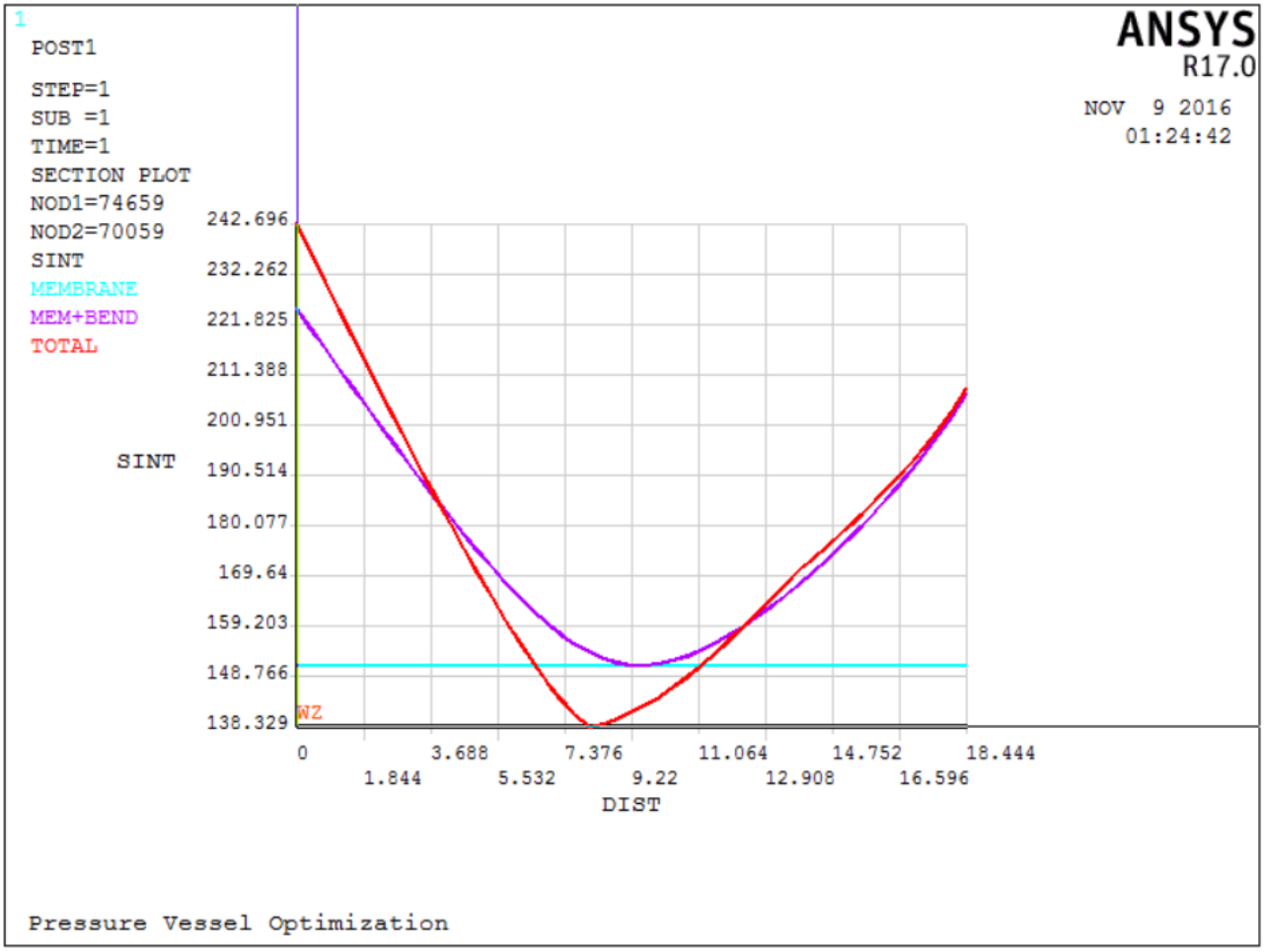

Figure 63: Stress variation through the thickness along Path-18

Table 40: Path-19 Evaluation

Load Condition	Allowable Stress S_m (MPa)	ANSYS linearization Type of stress	Stress Classification symbol	Equivalent Stress Intensity SINT (MPa)	Stress Control Value	Evaluation Result
Design Conditions A	137	MEMBRANE	S_I (P_m)	N/A	1.0×S_m=137	N/A
			S_{II} (P_L)	78.53	1.5×S_m=205.5	PASS
		MEMBRANE PLUS BENDING	S_{IV} $(P_L + P_b + Q)$	174.3	3×S_m=411	PASS

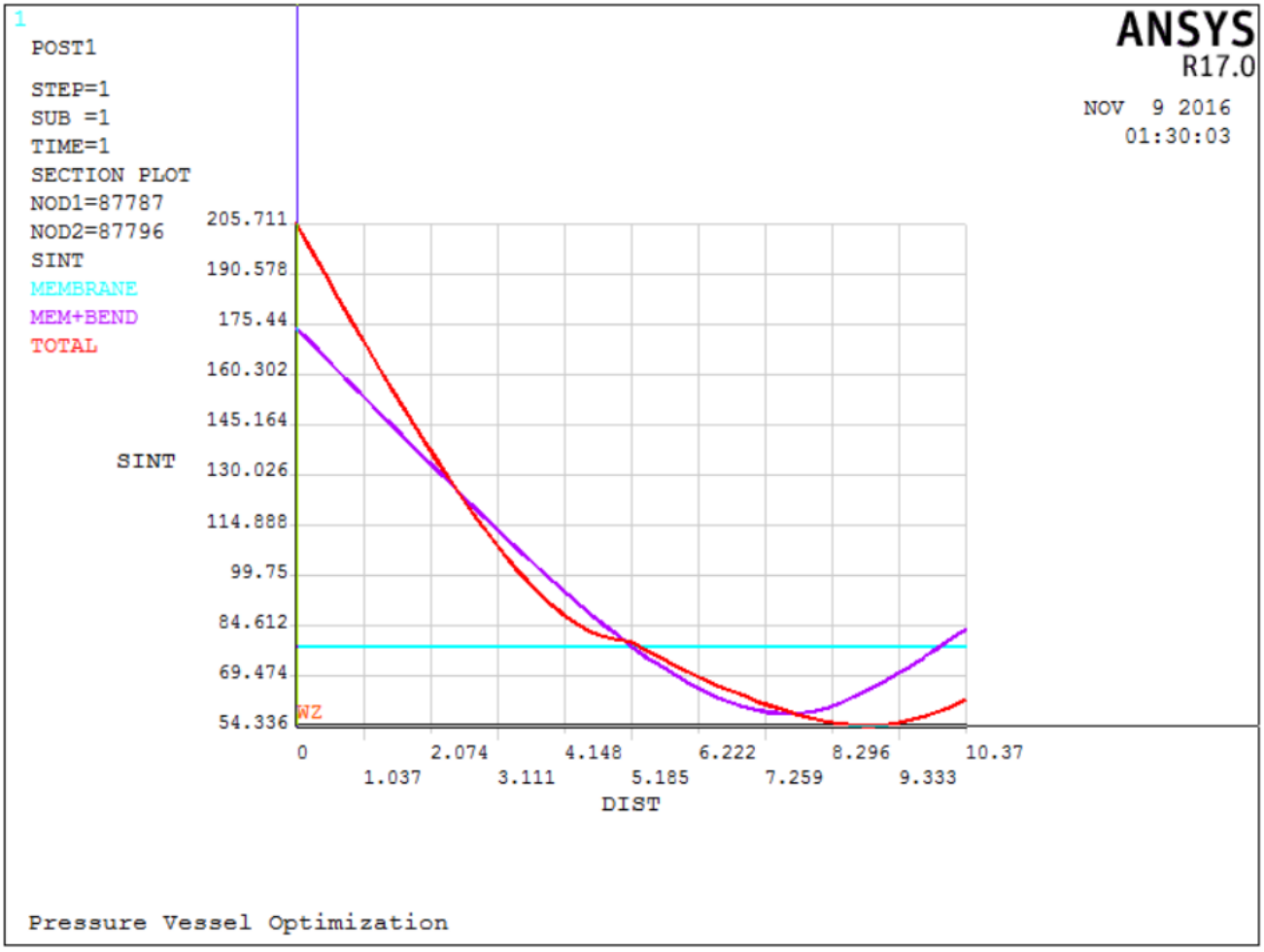

Figure 64: Stress variation through the thickness along Path-19

Table 41: Path-20 Evaluation

Load Condition	Allowable Stress S_m (MPa)	ANSYS linearization Type of stress	Stress Classification symbol	Equivalent Stress Intensity SINT (MPa)	Stress Control Value	Evaluation Result
Design Conditions A	137	MEMBRANE	S_I (P_m)	N/A	1.0×S_m=137	N/A
			S_{II} (P_L)	159.4	1.5×S_m=205.5	PASS
		MEMBRANE PLUS BENDING	S_{IV} $(P_L + P_b + Q)$	249.1	3×S_m=411	PASS

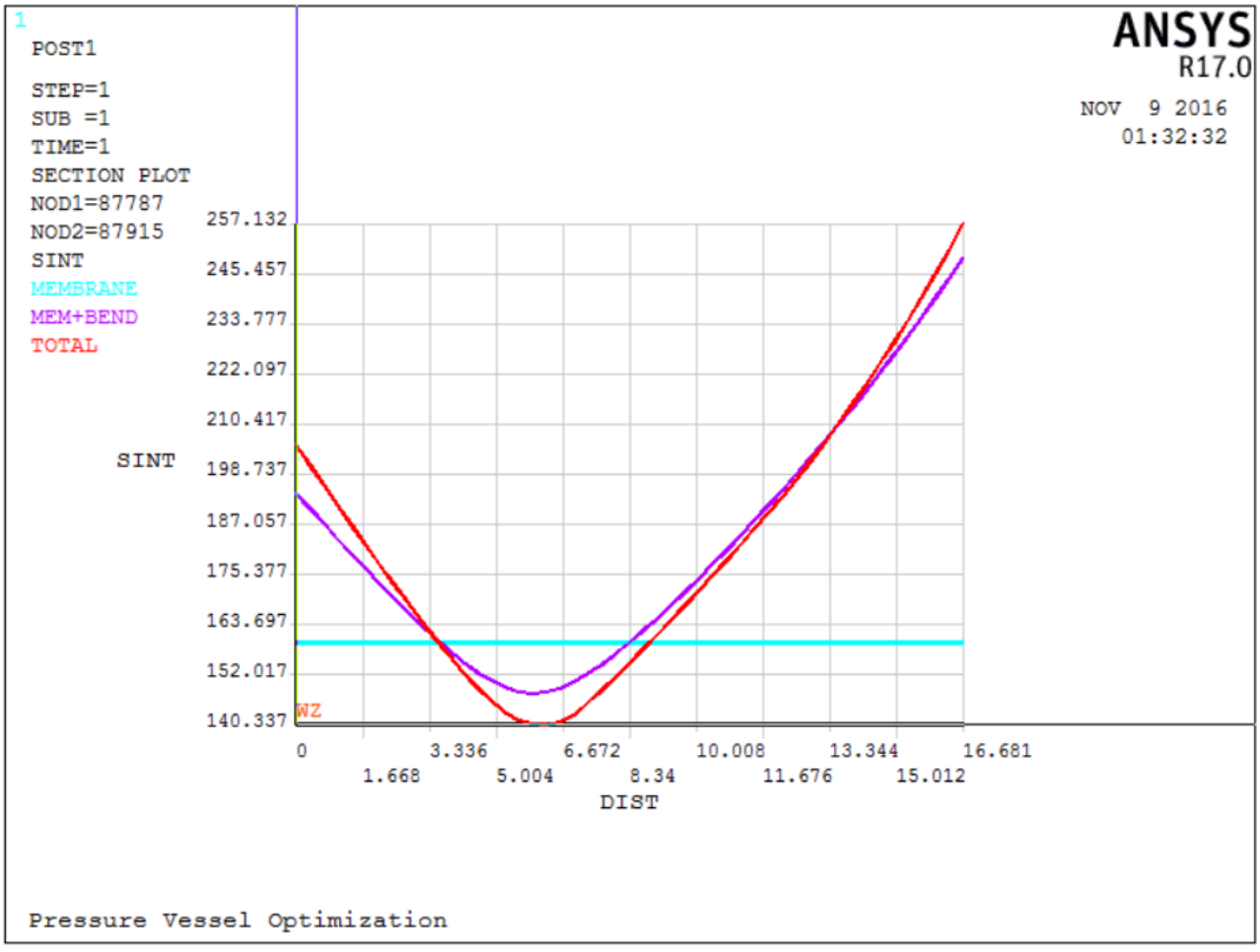

Figure 65: Stress variation through the thickness along Path-20

4.6 Summary of Stress Analysis Results

Table 42: Stress Verification

Path	Stress		Allowable Stress (MPa)		Calculated Stress (MPa)
	Type	Category			
PATH-1	Membrane	P_L	1.5×S_m	205.5	59.85
	Membrane Plus Bending	$P_L + P_b$	1.5×S_m	205.5	73.26
PATH-2	Membrane	P_L	1.5×S_m	205.5	105.1
	Membrane Plus Bending	$P_L + P_b + Q$	3×S_m	411	206.6
PATH-3	Membrane	P_L	1.5×S_m	205.5	157.1
	Membrane Plus Bending	$P_L + P_b + Q$	3×S_m	411	235.0
PATH-4	Membrane	P_L	1.5×S_m	205.5	45.48
	Membrane Plus Bending	$P_L + P_b$	1.5×S_m	205.5	59.05
PATH-5	Membrane	P_L	1.5×S_m	205.5	73.18
	Membrane Plus Bending	$P_L + P_b$	1.5×S_m	205.5	80.24
PATH-6	Membrane	P_L	1.5×S_m	205.5	61.36
	Membrane Plus Bending	$P_L + P_b + Q$	3×S_m	411	128.2
PATH-7	Membrane	P_L	1.5×S_m	205.5	109.5
	Membrane Plus Bending	$P_L + P_b + Q$	3×S_m	411	169.1
PATH-8	Membrane	P_L	1.5×S_m	205.5	16.72
	Membrane Plus Bending	$P_L + P_b$	1.5×S_m	205.5	26.88
PATH-9	Membrane	P_L	1.5×S_m	205.5	44.89
	Membrane Plus Bending	$P_L + P_b$	1.5×S_m	205.5	54.67
PATH-10	Membrane	P_L	1.5×S_m	205.5	7.97
	Membrane Plus Bending	$P_L + P_b$	1.5×S_m	205.5	57.81
PATH-11	Membrane	P_L	1.5×S_m	205.5	46.34
	Membrane Plus Bending	$P_L + P_b$	1.5×S_m	205.5	77.29
PATH-12	Membrane	P_L	1.5×S_m	205.5	16.67
	Membrane Plus Bending	$P_L + P_b$	1.5×S_m	205.5	47.77
PATH-13	Membrane	P_L	1.5×S_m	205.5	36.10
	Membrane Plus Bending	$P_L + P_b$	1.5×S_m	205.5	64.37
PATH-14	Membrane	P_L	1.5×S_m	205.5	10.39
	Membrane Plus Bending	$P_L + P_b$	1.5×S_m	205.5	30.87
PATH-15	Membrane	P_L	1.5×S_m	205.5	96.24
	Membrane Plus Bending	$P_L + P_b + Q$	3×S_m	411	198.1
PATH-16	Membrane	P_L	1.5×S_m	205.5	158.1
	Membrane Plus Bending	$P_L + P_b + Q$	3×S_m	411	240.1
PATH-17	Membrane	P_L	1.5×S_m	205.5	129.5
	Membrane Plus Bending	$P_L + P_b + Q$	3×S_m	411	227.7
PATH-18	Membrane	P_L	1.5×S_m	205.5	151.1
	Membrane Plus Bending	$P_L + P_b + Q$	3×S_m	411	225.1
PATH-19	Membrane	P_L	1.5×S_m	205.5	78.53
	Membrane Plus Bending	$P_L + P_b + Q$	3×S_m	411	174.3
PATH-20	Membrane	P_L	1.5×S_m	205.5	159.4
	Membrane Plus Bending	$P_L + P_b + Q$	3×S_m	411	249.1

From the stress analysis of the initial design, it is observed that the maximum membrane and membrane plus bending stress occurs along path-20 whereas minimum membrane stress occurs at path-10 and minimum membrane plus bending stress is found along path-8. We did expect the maximum stress values along path-20, as this path/SCL was created in the high stress region of the model. Note that, stress analysis was performed on nominal design of the pressure vessel model with shell thickness of 10 mm and flange thickness of 16 mm. The above stress verification results demonstrates that linearized stresses evaluated along all the paths are well-within the allowable limits and hence this design of the pressure vessel model is legitimate and safe. Although the initial design is valid, it is not the best fit solution as the weight of the pressure vessel can be further reduced while it can still sustain stresses within the allowable limits. Thus, a volume/weight minimizing optimization was carried out by varying the shell thickness and flange thickness of the vessel. When we seek the optimal design for weight reduction of this pressure vessel model, the above-mentioned stress linearization and classification approach is followed and the stress verifications as specified by the ASME Pressure vessel code are evaluated for every optimization search iteration. Note that, the linearization paths creation is also automated through the APDL script file such that the paths are recreated in the same location of the geometry every time the design parameters changes. This allows us to evaluate the stresses along the same locations in the model for every search iteration in the optimization loop. The details of the optimization problem formulation for the pressure vessel model in MATLAB are discussed in the next chapter.

CHAPTER 5: MATLAB Optimization

From the general standpoint of searching for the best available design, optimization can be defined as follows. Mathematical optimization is the process of maximizing and/or minimizing one or more objectives without violating specified design constraints, by regulating a set of variable parameters that influence both the objectives and the design constraints. It is important to realize that in order to apply mathematical optimization, you need to express the objective(s) and the design constraint(s) as quantitative functions of the variable parameters. These variable parameters are also known as design variables or decision variables.

MATLAB Optimization tool provides some very powerful functions for finding parameters that minimize or maximize objectives while satisfying constraints. Based on the problem in hand, these optimization solvers can be used along with a suitable algorithm to find the optimal solution. The

tool includes solvers for linear programming, mixed-integer linear programming, quadratic programming, nonlinear optimization, and nonlinear least squares. We can use these solvers to find optimal solutions to continuous and discrete problems, perform tradeoff analyses, and incorporate optimization methods into algorithms and applications.

5.1 Optimization Problem Formulation in MATLAB

A general structural optimization problem can be mathematically formulated using the following set of equations:

$$\min f(x)$$

subject to

$$g(x) \leq 0$$

$$h(x) = 0$$

where

$$x_L \leq x \leq x_U$$

The function f(x) represents the objective function or the cost function, which we would like to minimize or maximize. The function g(x) represents a vector of inequality constraints evaluated at x and the function h(x) represents a vector of equality constraints evaluated at x. The vector x represents the vector of real-valued design variables. These are the quantities that we can change in the design to improve its behavior. The constraints on the design variables, x_L and x_U, are called side constraints. Design variables cannot be chosen arbitrarily; they must satisfy certain specific functional requirements to produce an acceptable design. For example, in this pressure vessel design, the variables selected by the optimization algorithm should be such that the design passes the stress verifications in order to be considered as an acceptable design. These restrictions that must be satisfied in a design are called design constraints. Design constraints are classified into two; one that represent limitations on the behavior or performance of the system and one that pose physical limitations on the design variables. While the former is referred to as behavior or functional constraint, the latter is known as geometric or side constraints. An efficient and accurate solution to the above stated optimization problem depends not only on the size of the problem in terms of the number of constraints and design variables but also on characteristics of the objective function and constraints.

For the pressure vessel model under consideration, the above shown optimization problem can be mathematically formulated as:

$$\text{minimize: Total Weight of the Pressure Vessel} \longrightarrow f(x)$$

subject to

$$\left.\begin{array}{c}\text{Primary Membrane Stress } P_L \leq 205.5 \text{ MPa} \\ \text{Primary Membrane Plus Bending Stress } P_L + P_b \leq 205.5 \text{ MPa} \\ \text{Primary Membrane Plus Bending + Secondary Stress } P_L + P_b + Q \leq 411 \text{ MPa}\end{array}\right\} g(x)$$

$$h(x) = 0$$

where

$$4 \text{ mm} \leq x(1)\text{: shell thickness} \leq 10 \text{ mm}$$
$$16 \text{ mm} \leq x(2)\text{: flange thickness} \leq 30 \text{ mm}$$

Objective Function: The objective function to be minimized is the total weight of the pressure vessel. Like most of the conventional optimization problems, this is also a single objective optimization problem. Instead of the conventional method where the objective in MATLAB is evaluated as a function of design parameters, a scalar value representing the total volume of the pressure vessel structure, obtained from ANSYS FEA is being directly feed into the objective function value.

Design Variables: During design of a Pressure Vessel, several parameters have to be considered to manufacture it efficiently by meeting up the industry requirements. For the analysis of the current pressure vessel equipment, we consider the shell thickness and flange thickness of the vessel as the design parameters. During Optimization, both the design parameters are varied in a specified range. The shell thickness value is varied from 4mm to 10mm, whereas the flange thickness value is varied from 16mm to 30mm. The figure-66 displayed below, shows the design variables used in this optimization problem.

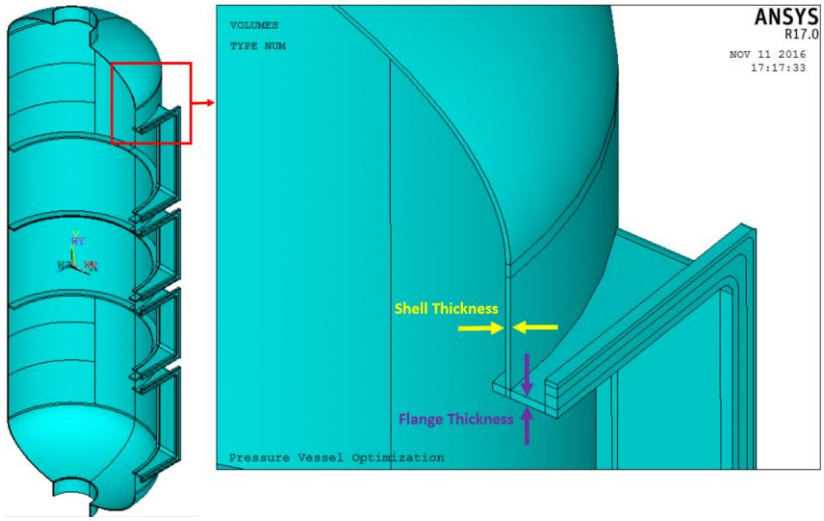

Figure 66: Design Variables

Constraints: In general, almost all engineering problems are constrained. Constraints can be either inequality constraints ($g(x) \leq$ or $g(x) \geq$) or equality constraints ($h(x) = 0$). The feasible region for inequality constraints represents the entire area on the feasible side of the allowable value; for equality constraints, the feasible region is only where the constraint is equal to the allowable value. As discussed in section 4.2, different allowable limits have been specified for membrane and membrane plus bending stress, based on the stress category and path locations. For the current pressure vessel optimization, these stress limits form the inequality design constraints. Note that, this optimization problem does not contain equality constraints. As mentioned earlier, the design should comply with these constraints in order to be considered as a feasible solution.

Side Constraints: Side constraints can be described as the geometrical or physical limitations imposed on the design variables. Since this is a minimization problem, the range of the design variables are the side constraints. In MATLAB, the side constraints are defined by two sets of vectors x_L and x_U where x_L represents a lower bound on the design variables and x_U represents the upper bound on the design variables. Number of elements on each of these vectors must be equal to the number of design variables. A lower bound of 4 mm has been set for the shell thickness because of the geometrical restrictions. When shell thickness has a value lower than 4mm, some of the geometrical entities in the finite element model becomes invalid and thus the analysis can no longer be conducted. An upper bound of 10 mm was set for the shell thickness. Similarly, an a lower bound of 16mm and an upper bound of 30 mm was set for flange thickness.

To formulate an optimization problem in MATLAB, we generally follow these steps:

- Choose an optimization solver.
- Create an objective function, typically the function you want to minimize.
- Create constraints, if any.
- Set options, or use the default options.
- Call the appropriate solver/Algorithm.

5.2 Design Space Exploration

Once we have defined the optimization problem, we are ready to start searching the design space. Prior to optimizing a design, it is useful to employ design space exploration—a quantitative method that help engineers gain a better, more complete understanding of a structure's potential by discovering which design variables will have the greatest impact on the structure's

performance. Design exploration assumes that the optimal design is initially unknown and initially uncharacterizable. The process of design exploration discovers design conditions and through experimentation characterizes what an optimal design looks like. Once this is known, the final solution can then be found through a convergent design optimization algorithm. The essential quantitative method for design space exploration is design-of-experiment (DOE) studies. In a DOE study, an analysis model is automatically evaluated multiple times, with the design variables set to different values in each iteration. The results identify which variable(s) affect the design the most, and which least.

A design of experiments study was conducted for the finite element model of the pressure vessel. This analysis model is automatically evaluated multiple times, with the design variables – shell thickness and flange thickness set to different values in each iteration. The results of DOE process were then used to generate the response of the model. Analyzing response of a system is necessary for visualizing the design space, examining relationships among design variables and their effects on key responses, and rapidly evaluating design alternatives. The figure-67 below depicts the response of the pressure vessel model generated in MATLAB. The plot is based on data created by meshing the space with a 20X20 grid of values for the design parameters, shell and flange thickness. Hence the finite element model of the pressure vessel was evaluated 400 times to generate the results for the contour plot. The shell thickness parameter was varied from 4mm to 10mm, whereas flange thickness parameter was varied from 16mm to 30mm.

It is important to keep in mind that the graphical representation is typically restricted to two variables. For three variables, we need a fourth dimension to resolve the information while three-dimensional contour plots are not easy to illustrate. Sometimes, even the three-dimensional graphical representation does not really enhance our understanding of the problem or solution. But since we are considering only two design variables for the current optimization problem of pressure vessel, we can easily plot and analyze the graphical results.

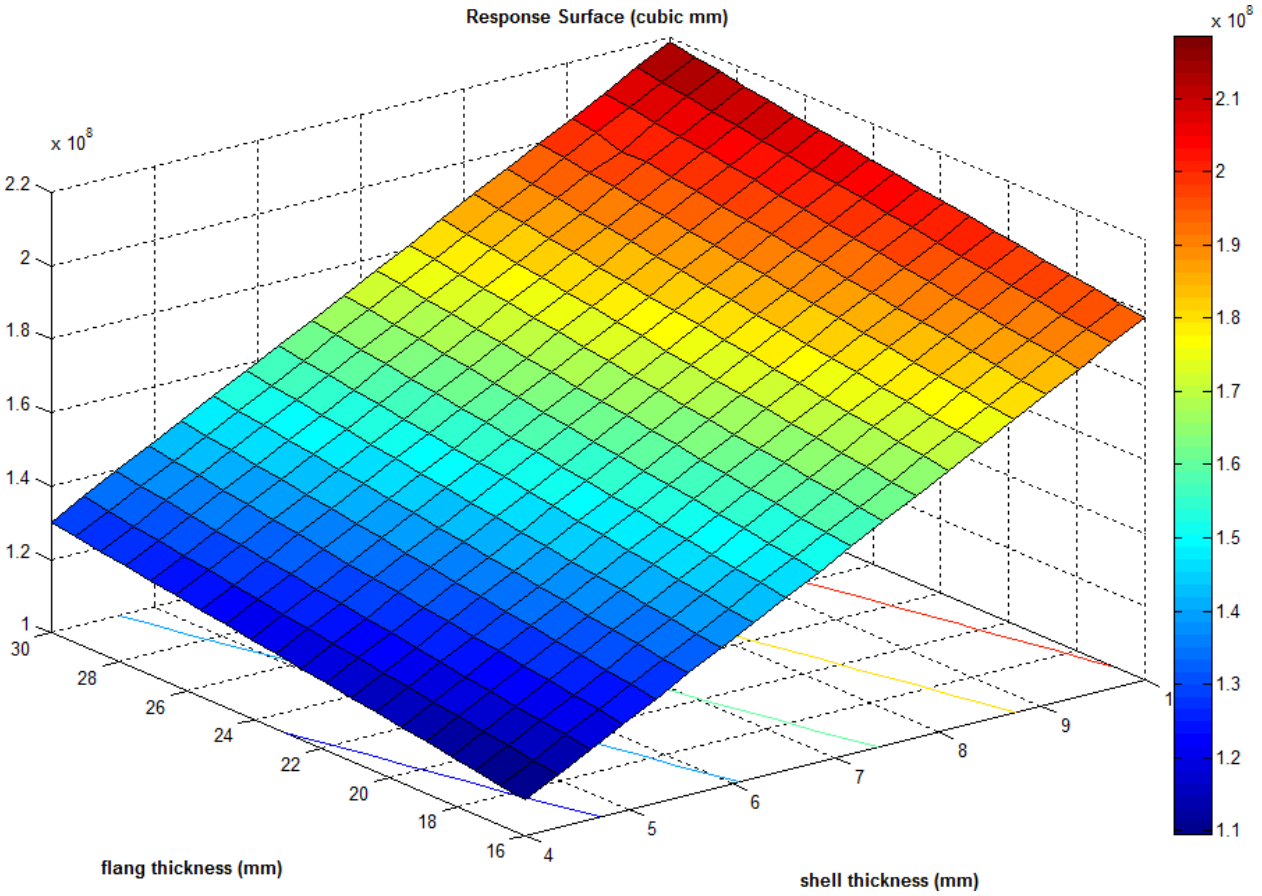

Figure 67: Response of the Pressure Vessel Model

It can be seen from figure-67 that total weight of the pressure vessel reduces linearly with the decrease in shell and flange thickness. Smooth flat continuous surface in the response indicates a linearly varying objective function, weight of the vessel in this case.

The simplest determination of non-linearity or linearity in the model is through a graphical representation of the design functions involved in the problem. In order to determine the feasible design region for our parameters, we need to draw the contours of the objective function and design constraints. Since, as per the DOE results the maximum membrane and membrane plus bending stress occurs along path-17, we will use stress results along this path to draw the constraint contours. The figure-68 below represents the design space created in MATLAB with the same data points which were used to create the response. The membrane and membrane plus bending stress contours are shown on the same plot, drawn in blue and red color respectively. The solid black lines represent contours of the total volume of the pressure vessel, the objective. These contour plots give the insight on the behavior of the objective function with respect to change in the design variables. We can see that weight decreases as we move from

the upper right corner of the design space towards the lower left corner. According to the design space, optimal solution should lie in the range of shell thickness 4mm-4.5mm and flange thickness of 22mm-30mm. This is a feasible region for the optimum solution because the pressure vessel model can sustain the stresses within the allowable stress limits for membrane and membrane plus bending stress, when design parameter values lie in this specific region. If we look closely at figure-68, the possible space for optimal solution is drawn on the design space.

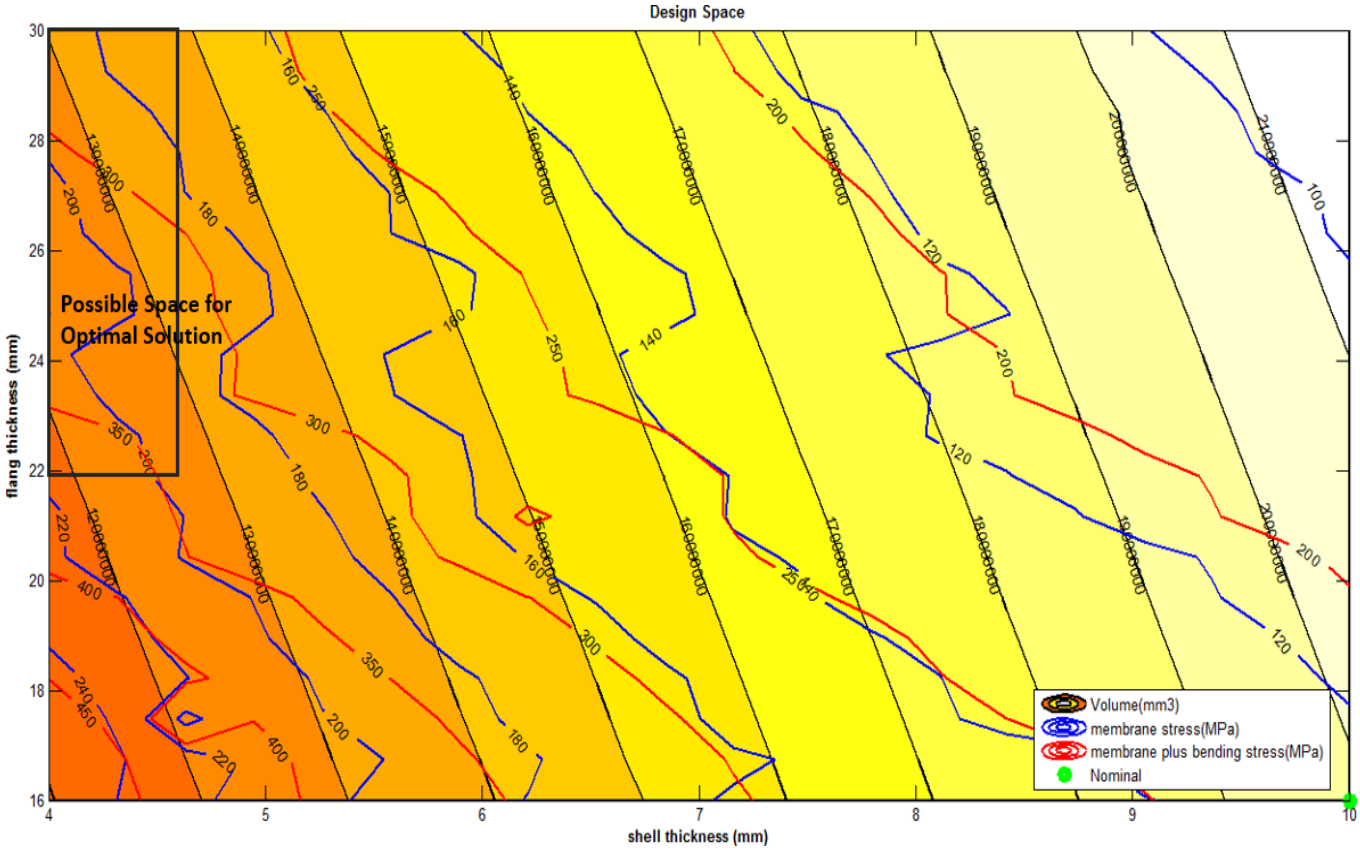

Figure 68: Design Space

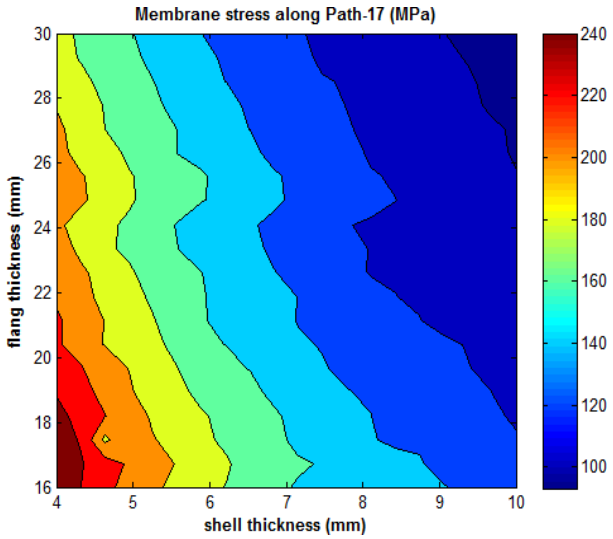

Figure 69: Membrane Stress Contours

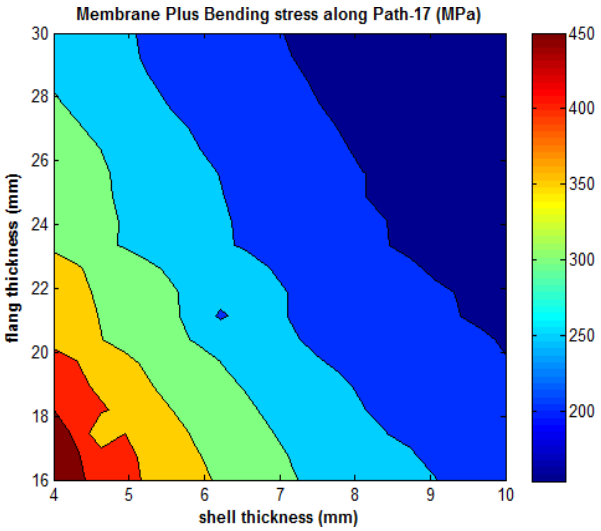

Figure 70: Membrane Plus Bending Stress Contours

Figure-69 and figure-70 represents the stress contours for the linearized membrane and membrane plus bending stress evaluated along path-17. The contours shows the increase in stress with decrease in shell thickness and flange thickness values.

For the nominal value of shell thickness equal to 10 millimeters and flange thickness equal to 16 millimeters, the total volume possessed by the pressure vessel was evaluated to be 198559610 cubic millimeters and the maximum element Von-Mises stress was calculated to be 325.77 MPa. As this is a minimization problem, our aim should be to achieve a lower value for the total weight (objective function) in comparison with the nominal value. Again, remember that the linearized stresses along all the paths must be less than the allowable stress limits to avoid failure.

Individual graphs were plotted to determine the level of influence that each design variable poses on the objective function. The figure-71 shows the variation of the total volume of the vessel with respect to the change in shell thickness while the flange thickness was fixed to the nominal value of 16mm. The figure-72 shows the variation of the total volume of the vessel with respect to the change in flange thickness while the shell thickness was fixed to the nominal value of 10mm. It can be clearly seen from the figures that our design function, i.e., total weight of the pressure vessel is more sensitive to change in shell thickness parameter. This was in-fact expected because shell thickness parameter has more weightage in the model geometry construction in comparison to flange thickness.

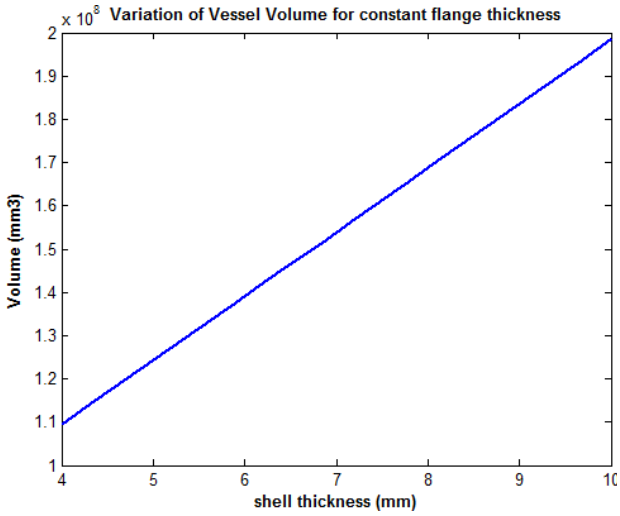

Figure 71: Objective function (Total Volume) vs shell thickness

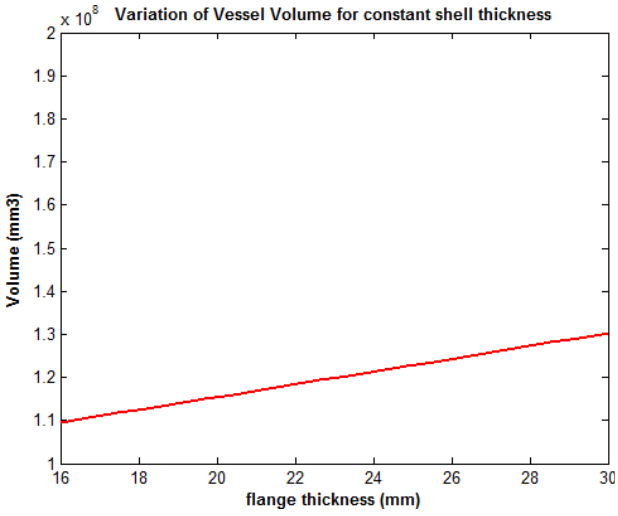

Figure 72: Objective function (Total Volume) vs flange thickness

5.3 MATLAB fmincon function

The MATLAB provides inbuilt functions like fminbnd, fminunc, fminsearch, ga, linprog, quadprog, fmincon, lsqcurvefit, fgoalattain, lsqnonlin, etc which can be used for minimization, multiobjective optimization, and solving least-squares or data-fitting problems. The most difficult part in MATLAB, is to decide which solver and algorithm will produce the best optimal results for the problem in hand. For the current problem, 'fmincon' is the best suitable option because this is a minimization problem which involves a constrained nonlinear multivariable function. fmincon is a MatLab inbuilt nonlinear solver for optimization which best applies to smooth objective functions with smooth constraints. It is a gradient-based method that is designed to work on problems where the objective and constraint functions are both continuous and have continuous first derivatives. It has proved to be a suitable tool to solve many optimization problems in the mechanical engineering field. Like most of the optimization solvers, fmincon only guarantee's finding a local optimum. To run fmincon, we need to define the objective function, constraint function and we also need to specify the initial design variable values. The user can also set the optimization options for fmincon or any other solver in MATLAB by using the 'optimoptions' function.

The fmincon function in MATLAB is called using the command shown below:

```
[Xopt,Fopt] = fmincon(fun,x0,A,b,Aeq,beq,lb,ub,nonlcon,options)
```

where x0, A, b, Aeq, beq, LB, and UB are the input variables that need to be defined before calling fmincon. ‘fun’ is the name of the function file containing the definition of f(x), and ‘nonlcon’ is the name of the function file containing the nonlinear constraints. The variables Xopt and Fopt are the outputs of fmincon, where Xopt is the optimum vector of variables [x1,x2] and Fopt is the minimum value of the objective function. Other output details like exit flag, stopping criteria message and gradient values can also be extracted. A, b, Aeq, and beq: These variables need to be defined only if the problem has linear constraints. In many cases, all constraints (linear and nonlinear) can be defined in the nonlcon.m file, so these variables can simply be defined as empty matrices. LB and UB are the vectors that define lower and upper bounds on the design variables. fmicon starts the optimization at x0 and attempts to find a minimizer x of the function described in fun subjected to the linear and nonlinear, equality and in-equality constraints.

The optimset command can be used to set or change the values of the optimization options. Some of these options are relevant to particular algorithms. The options arguments include algorithms selection, stopping criteria, iteration display settings, step tolerance, constraint tolerance, Max iterations, Max function evaluations, plot functions etc. The function optimset creates an options structure that is passed as an input argument to the optimization solver (fmincon in this case). For the pressure vessel optimization problem, a few options that were changed from their default value are explained below in table-43:

Table 43: fmincon Optimization Options

Option Name	Description	Default Value	Changed Value
Algorithm	Algorithm used by solver (fmincon)	Interior-point	Active-set
DiffMinChange	Minimum change in variables for finite differencing	1e-6	0.1
tolx (Step Tolerance)	Termination tolerance on x, the current point. TolX is a lower bound on the size of a step. If the solver attempts to take a step that is smaller than TolX, the iterations end.	1e-6	1e-4
MaxIter	Maximum number of iterations allowed.	100	10000
MaxFunEvals	Maximum number of function evaluations allowed.	200	10000

PlotFcns	User-defined or built-in plot function that an optimization function calls at each iteration.	{ }	{@optimplotx, @optimplotfval, @optimplotconstrviolation, @optimplotfunccount, @optimplotfirstorderopt, @optimplotstepsize}
Display	Level of display. 'off' displays no output; 'iter' displays output at each iteration; 'final' displays just the final output; 'notify' displays output only if the function does not converge.	off	iter

After defining the above quantities, the function fmincon is called. The function fmincon calls (i) nonlcon.m to evaluate the constraints and (ii) fun.m to evaluate the objective function. fmincon provides five different algorithms options:

1. 'interior-point' (default)
2. 'Trust-region-reflective'
3. 'sqp'
4. 'sqp-legacy'
5. 'active-set'

In the present work, active-set and sqp algorithms are used. Results are discussed at the end. The other algorithms are excluded because either they are time consuming or they are not suitable for the problem in hand. For example, implementing Trust-Region-Reflective Algorithm is very complex process as it requires user specified gradient for both objective and constraint functions. Understanding how these algorithms work requires advanced statistics and machine learning background and since this is beyond the scope of this work, only a brief description of these algorithms is stated below.

Interior- Point: 'interior-point' handles large, sparse problems, as well as small dense problems. The algorithm satisfies bounds at all iterations, and can recover from NaN or Inf results. It is a large-scale algorithm; The algorithm can use special techniques for large-scale problems. For details, see Interior-Point Algorithm in fmincon options

Active-set: 'active-set' can take large steps, which adds speed. The algorithm is effective on some problems with non-smooth constraints. It is not a large-scale algorithm. Lagrange multipliers are directly computed based on the solution of KKT (Karush-Kuhn-Tucker) equations. Constrained quasi-Newton methods guarantee superlinear convergence by accumulating second-order information regarding the KKT equations using a quasi-Newton updating procedure. Like sqp algorithm, a QP sub-problem is solved at each major iteration.

Sqp: 'sqp' satisfies bounds at all iterations. It is not a large-scale algorithm. This method allows us to closely mimic Newton's method for constrained optimization just as is done for unconstrained optimization. At each major iteration, an approximation is made of the Hessian of the Lagrangian function using a quasi-Newton updating method. This is then used to generate a QP subproblem whose solution is used to form a search direction for a line search procedure. This algorithm has proved to be superior in terms of efficiency, accuracy, and percentage of successful solutions, over a large number of test problems.

Trust-region-reflective: 'trust-region-reflective' requires you to provide a gradient, and allows only bounds or linear equality constraints, but not both. Within these limitations, the algorithm handles both large sparse problems and small dense problems efficiently. It is a large-scale algorithm. The algorithm can use special techniques to save memory usage, such as a Hessian multiply function.

As discussed in previous section, the objective function, i.e., total weight of the pressure vessel is more sensitive to change in shell thickness. Hence, to effectively reduce the weight of the vessel, optimization algorithms would try minimize the shell thickness of the vessel as much as possible. On the other hand, since the maximum stress occurs along the corner junction of shell body and nozzle, the algorithms would try maximize the flange thickness in order to comply with the stress constraints.

CHAPTER 6: Integration of ANSYS and MATLAB

In this chapter, the methodology to interface ANSYS and MATLAB is explained in detail. It is worth highlighting that any other finite element software either licensed or opened source may be used to be coupled with MatLab. The requirement to be fulfilled is that the software must allow programming the finite element model by means of a script file in order to be able to automate the proposed optimization methodology shown. This kind of integrated approach is desired in optimization of complex designs because it is completely automated and does not require any

kind of user intervention, until an optimum solution is found. The coupling between MatLab and the finite element software is done by means of a batch command shown below.

```
!"C:\Program Files\ANSYS Inc\v170\ansys\bin\winx64\ANSYS170.exe" -b
-i C:\Users\artik\Desktop\Thesis\PressureVesselModel_script.txt
-o C:\Users\artik\Desktop\Thesis\FEAreport.txt
```

Where -b is the batch command followed by -i and -o which represent the directory for input and output file respectively. The Objective function file “PressureVessel_obj.m” defined in MatLab calls ANSYS to runs in batch mode. This file updates the variables in the Ansys script file “PressureVesselModel_script.txt”, executes ANSYS in batch mode and evaluates the Objective function and stress results.

The main advantage of creating and solving a model by means of APDL script is that the model can be defined in terms of variables, thus creating a parametric model. The variables that are employed to create a parametric model for the pressure vessel are shell thickness and flange thickness. The values of these variables will be varied by the optimization algorithm until a minimum is reached. APDL post-process allows, to store the results of the analyzed model in a text file. Required data are extracted from this text file and are fed to the optimization tool in order to redefine the design variables.

Figure-73 below defines the optimization loop. It can be seen that the information between ANSYS and MatLab is exchanged based on the text files which are overwritten in each loop. It should be noted that all the created files must be placed on the same directory of the hard drive or else the user should set appropriate path for these files.

The optimization loop will flow through the following steps:

- The file “PressureVessel_Optimization.m” is the main file which runs fmincon to evaluate the objective function. (Weight of the pressure Vessel in this case).
- As soon as the main file is run in MATLAB, the objective function file ‘PressureVessel_obj.m’ is called.
- Objective function file runs ANSYS in batch mode by using the above-mentioned command.
- ANSYS script file ‘PressureVesselModel_script.txt’ retrieves the values of shell thickness and flange thickness from MATLAB design variables and the finite element model is solved in ANSYS.

- Results obtained from finite element analysis are stored in a text file “ANYSresults.txt”. These results are extracted in MATLAB to evaluate the Objective function and constraints.
- fmincon algorithm updates the value of design parameters and the loop is repeated until an optimum solution is found.

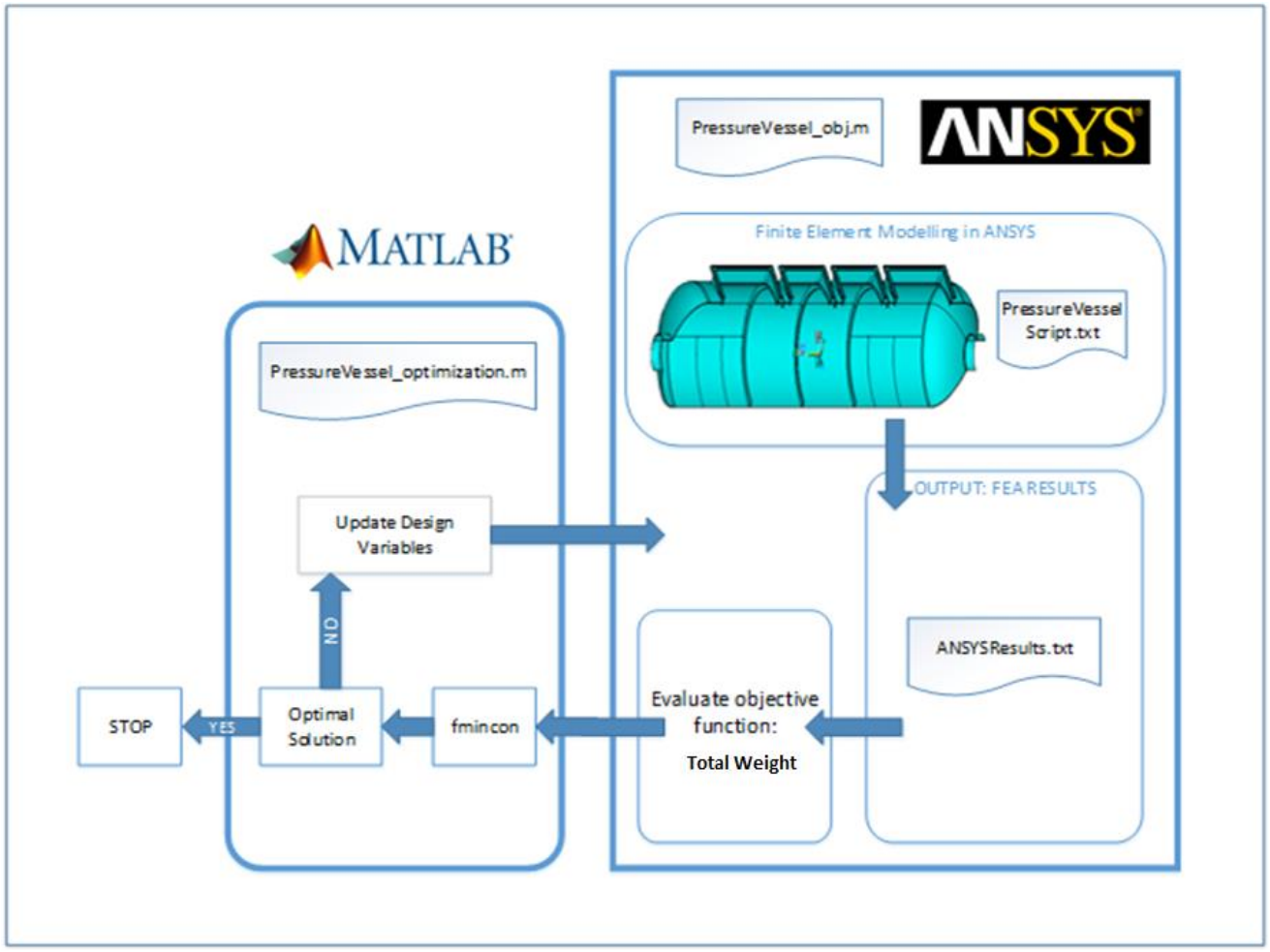

Figure 73: Integration Flow Chart

CHAPTER 7: Results and Conclusion

7.1 Results

Several cases were run by calling fmincon with different initial design variable values and with different step tolerance limits, to check the convergence of the optimal solution. The optimized results obtained by using active-set algorithm were compared with the results given by sqp algorithm. The first three runs were conducted using active-set algorithm whereas all the other runs were performed using sqp algorithm. As shown in table-45 below, the best solution was given

by run-2 in which the total weight of the pressure vessel was reduced by about 39.21%. The convergence of the optimal solution was checked using different initial design variable values and different step tolerance values. From table-44, we can see that a faster convergence is obtained by using lower step tolerance values with a slight decrease in the weight reduction %. The reason behind this is that for tight tolerances, fmincon evaluates more number of points which thereby increases the number of iterations taken to get convergence at the optimal point. Hence the best approach is to start optimization with a low step tolerance value whenever the problem is time consuming and the design space is widely spread. It should be noted that since fmincon is not a global optimization solver, optimized values of the design variables are possible local minimum. The optimization results along with the descriptive iterations for different fmincon runs are shown below:

Fmincon run-1

Initial Design Points: X0= [5 23] where,

X0(1) =shell thickness (Unit: mm)
X0(2) =flange thickness (Unit: mm)

Lower and Upper Bounds on Design parameters: XL=[4 16] XU=[10 30]

Optimization Settings: optimoptions(@fmincon, 'Algorithm', 'active-set', DiffMinChange', 0.1, 'MaxIter', 10000, 'MaxFunEvals', 10000, 'TolX' ,1e-2, 'PlotFcns', {@optimplotx,@optimplotfval,@optimplotconstrviolation,@optimplotfunccount,@optimplotfirstorderopt,@optimplotstepsize}, 'display', 'iter')

Optimized Design Parameters: XOPT= [4.1609 23.0116]

Optimized Objective Function (Minimized Volume): FOPT= 122236730

$$\text{Total Volume Reduction} = \frac{198559610 - 122236730}{198559610} \times 100 = 38.43\%$$

Command Window

New to MATLAB? Watch this Video, see Examples, or read Getting Started.

Iter	F-count	f(x)	Max constraint	Line search steplength	Directional derivative	First-order optimality	Procedure
0	3	1.34561e+08	0				
1	7	1.27761e+08	0	0.5	-1.09e+07	6.07e+06	
2	11	1.24817e+08	0	0.5	-7.56e+06	1.23e+07	
3	16	1.23446e+08	0	0.25	-1.09e+07	3.25e+06	Hessian modi
4	21	1.22589e+08	0	0.25	-1.1e+07	3.46e+06	
5	29	1.22567e+08	0	0.0313	-8.7e+06	5.87e+06	
6	35	1.22275e+08	0	0.125	-7.06e+06	4.48e+06	Hessian modi
7	44	1.22237e+08	0	0.0156	-1.48e+07	2.57e+06	

Local minimum possible. Constraints satisfied.

fmincon stopped because the size of the current search direction is less than twice the selected value of the step size tolerance and constraints are satisfied to within the default value of the constraint tolerance.

Figure 74: fmincon run-1 iterations

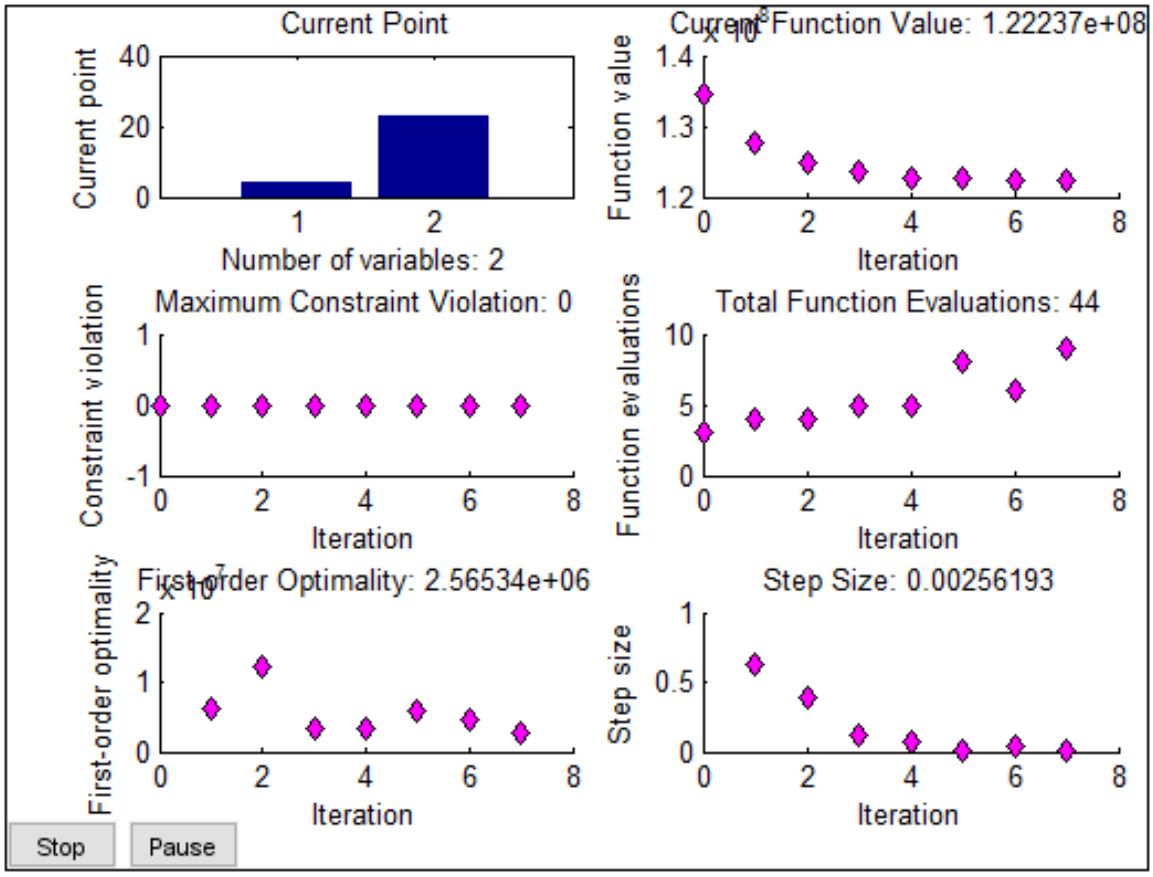

Figure 75: Plot functions for fmincon run-1

Fmincon run-2

Initial Design Points: X0= [4.1 25] where,

X0(1) =shell thickness (Unit: mm)

X0(2) =flange thickness (Unit: mm)

Lower and Upper Bounds on Design parameters: XL=[4 16] XU=[10 30]

Optimization Settings: optimoptions(@fmincon, 'Algorithm', 'active-set', DiffMinChange', 0.1, 'MaxIter', 10000, 'MaxFunEvals', 10000, 'TolX' ,1e-3, 'PlotFcns', {@optimplotx,@optimplotfval,@optimplotconstrviolation,@optimplotfunccount,@optimplotfirstorderopt,@optimplotstepsize}, 'display', 'iter')

Optimized Design Parameters: XOPT= [4.0000 23.5703]

Optimized Objective Function (Minimized Volume): FOPT=120699140

$$\text{Total Volume Reduction} = \frac{198559610 - 120699140}{198559610} \times 100 = 39.21\%$$

Command Window

New to MATLAB? Watch this Video, see Examples, or read Getting Started.

Iter	F-count	f(x)	Max constraint	Line search steplength	Directional derivative	First-order optimality	Procedure
0	3	1.24287e+08	0.02579				Infeasible start point
1	6	1.21012e+08	0.006061	1	-2.68e+06	4.12e+06	
2	9	1.21031e+08	0.001522	1	1.66e+05	8.66e+06	
3	15	1.21021e+08	0	0.125	-1.28e+06	9.91e+06	
4	21	1.21002e+08	0	0.125	-7.77e+06	1.99e+06	
5	25	1.20942e+08	0	0.5	-7.18e+06	2.13e+06	Hessian modified
6	28	1.20868e+08	0	1	-1.48e+07	1.41e+06	
7	36	1.20861e+08	0	0.0313	-1.41e+06	1.48e+06	
8	48	1.20861e+08	0	0.00195	-1.48e+06	1.3e+07	Hessian modified twice
9	51	1.20835e+08	0	1	-1.48e+06	1.48e+06	Hessian modified twice
10	58	1.20727e+08	0	0.0625	-1.48e+06	2.73e+06	
11	73	1.2072e+08	0	0.000244	-1.41e+06	2.03e+06	Hessian modified twice
12	77	1.20715e+08	0	0.5	-1.48e+06	1.85e+06	
13	86	1.20709e+08	0	0.0156	-1.48e+06	1.48e+06	
14	104	1.20709e+08	0	3.05e-05	-1.48e+06	4.53e+06	Hessian modified twice
15	110	1.20708e+08	0	0.125	-1.48e+06	1.48e+06	Hessian modified twice
16	120	1.20708e+08	0	0.00781	-1.48e+06	1.78e+06	
17	127	1.207e+08	0	0.0625	-1.48e+06	8.24e+06	Hessian modified twice
18	141	1.20699e+08	0	0.000488	-1.48e+06	9.57e+07	Hessian modified twice

Local minimum possible. Constraints satisfied.

fmincon stopped because the size of the current search direction is less than twice the selected value of the step size tolerance and constraints are satisfied to within the default value of the constraint tolerance.

<stopping criteria details>

Figure 76: fmincon run-2 iterations

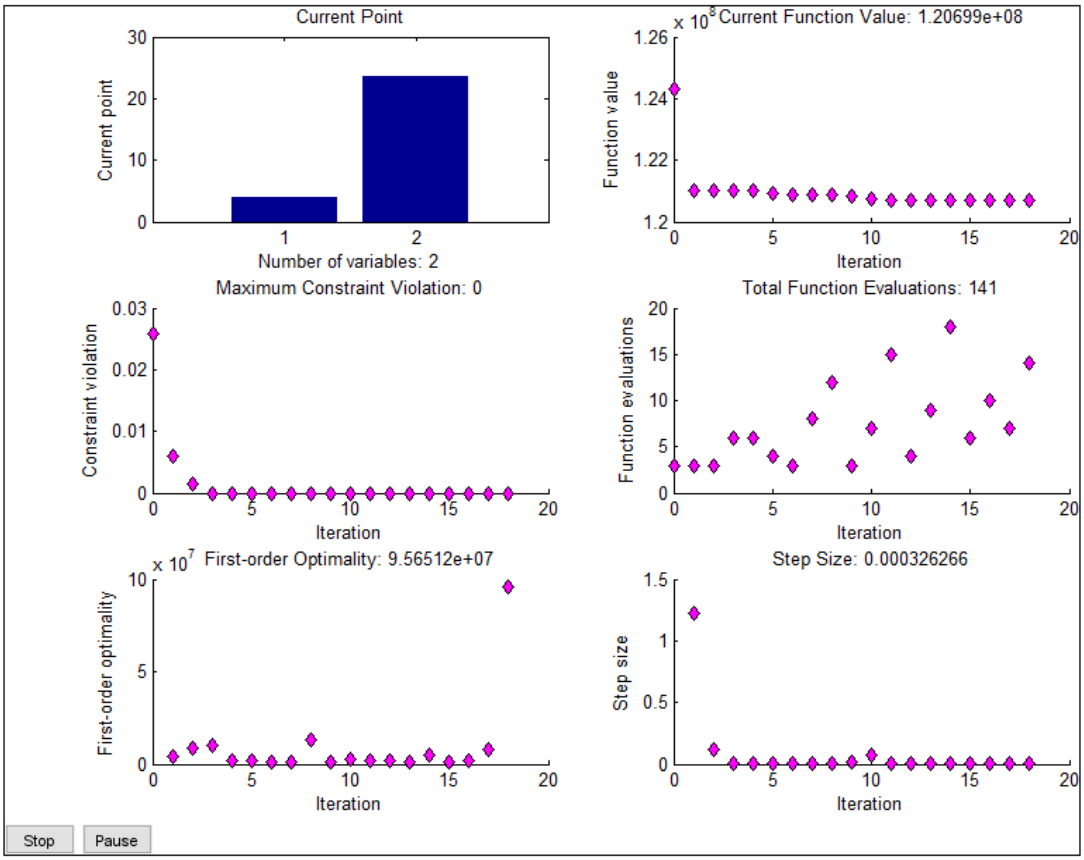

Figure 77: Plot Functions for fmincon run-2

Fmincon run-3

Initial Design Points: X0= [5 23] where,

X0(1) =shell thickness
X0(2) =flange thickness

Lower and Upper Bounds on Design parameters: XL=[4 16] XU=[10 30]

Optimization Settings: optimoptions(@fmincon, 'Algorithm', 'active-set', DiffMinChange', 0.1, 'MaxIter', 10000, 'MaxFunEvals', 10000, 'TolX' ,1e-4, 'PlotFcns', {@optimplotx,@optimplotfval,@optimplotconstrviolation,@optimplotfunccount,@optimplotfirstorderopt,@optimplotstepsize}, 'display', 'iter')

Optimized Design Parameters: XOPT= [4.1338 22.8975]

Optimized Objective Function (Minimized Volume): FOPT=121669870

$$\text{Total Volume Reduction} = \frac{198559610 - 121669870}{198559610} \times 100 = 38.72\%$$

Iter	F-count	f(x)	Max constraint	Line search steplength	Directional derivative	First-order optimality	Procedure
0	3	1.34561e+08	0				
1	7	1.27761e+08	0	0.5	-1.09e+07	6.07e+06	
2	11	1.24817e+08	0	0.5	-7.56e+06	1.23e+07	
3	16	1.23446e+08	0	0.25	-1.09e+07	3.25e+06	Hessian modified twice
4	21	1.22589e+08	0	0.25	-1.1e+07	3.46e+06	
5	29	1.22567e+08	0	0.0313	-8.7e+06	5.87e+06	
6	35	1.22275e+08	0	0.125	-7.06e+06	4.48e+06	Hessian modified twice
7	44	1.22237e+08	0	0.0156	-1.48e+07	2.57e+06	
8	50	1.22228e+08	0	0.125	-1.29e+07	8.56e+06	
9	54	1.22193e+08	0	0.5	-9.62e+06	1.26e+07	
10	64	1.22128e+08	0	0.00781	-2.07e+06	5.92e+06	Hessian modified twice
11	67	1.22004e+08	0	1	-8.34e+06	3.3e+06	
12	74	1.2197e+08	0	0.0625	-1.41e+07	1.21e+07	
13	85	1.21961e+08	0	0.00391	-1.43e+07	2.09e+06	Hessian modified
14	98	1.21959e+08	0	0.000977	-1.4e+07	1.82e+07	
15	103	1.21958e+08	0	0.25	-9.12e+06	1.47e+07	dependent
16	110	1.21956e+08	0	0.0625	-1.23e+07	1.47e+07	dependent
17	113	1.2192e+08	0	1	-1.47e+07	1.47e+07	dependent
18	120	1.21914e+08	0	0.0625	-1.46e+07	1.8e+07	Hessian modified twice
19	133	1.2191e+08	0	0.000977	-3.83e+06	2.12e+06	Hessian modified twice
20	139	1.21866e+08	0	0.125	-1.45e+07	9.22e+06	
21	148	1.21751e+08	0	0.0156	-2.04e+06	5.63e+06	Hessian modified twice
22	157	1.21731e+08	0	0.0156	-6.96e+06	8.14e+06	
23	167	1.2167e+08	0	0.00781	-1.97e+06	5.96e+06	Hessian modified twice
24	182	1.2167e+08	0	0.000244	-4.86e+06	4.81e+06	
25	199	1.2167e+08	0	-6.1e-05	-4.17e+06	1.9e+06	Hessian modified twice
26	216	1.2167e+08	0	-6.1e-05	-4.17e+06	1.9e+06	Hessian modified twice
27	232	1.2167e+08	0	0.000122	-4.17e+06	1.9e+06	Hessian modified twice
28	238	1.21292e+08	0.005992	0.125	-4.17e+06	1.95e+06	Hessian modified twice
29	241	1.17976e+08	0.06925	1	-3.05e+06	1.8e+06	Hessian modified twice
30	245	1.18186e+08	0.04673	0.5	1.48e+06	3.62e+06	Hessian modified twice
31	248	1.17991e+08	0.04006	1	-1.47e+06	1.46e+06	
32	251	1.1703e+08	0.1055	1	-2.33e+06	1.47e+07	infeasible
33	254	1.19024e+08	0.06859	1	6.27e+06	2.12e+06	
34	257	1.23705e+08	0	1	1.23e+07	2.42e+07	
35	260	1.20673e+08	0.03699	1	-1.25e+07	3.01e+06	
36	263	1.23918e+08	0	1	1.03e+07	4.11e+06	Hessian modified
37	266	1.22751e+08	0	1	-6.25e+06	1.07e+06	
38	269	1.2174e+08	0.008303	1	-1.47e+07	1.85e+06	
39	272	1.22422e+08	0.004306	1	1.47e+07	1.23e+07	
40	275	1.22699e+08	0	1	1.47e+07	8.31e+06	Hessian modified
41	281	1.22563e+08	0	0.125	-1.33e+07	7.02e+06	
42	284	1.22413e+08	0	1	-1.27e+07	7.73e+06	
43	287	1.22049e+08	0	1	-1.46e+07	8.96e+06	
44	296	1.22029e+08	0	0.0156	-1.48e+07	1.17e+07	Hessian modified twice
45	301	1.20677e+08	0.005287	0.25	-2.06e+06	1.3e+07	
46	304	1.14479e+08	0.155	1	-2.66e+06	2.04e+07	Hessian modified twice
47	307	1.16729e+08	0.1109	1	1.3e+07	4.09e+06	
48	310	1.22752e+08	0.02502	1	1.45e+07	1.1e+07	
49	317	1.22753e+08	0.02438	0.0625	5.87e+04	3.21e+06	
50	320	1.25341e+08	0.009452	1	1.3e+07	1.07e+07	
51	323	1.2545e+08	0.0007375	1	1.33e+06	1.22e+07	
52	326	1.15817e+08	0.1131	1	-9.53e+06	2.45e+06	Hessian modified twice
53	331	1.15303e+08	0.1146	0.25	-1.47e+06	1.05e+07	
54	336	1.79537e+08	0	0.25	1.03e+07	1.48e+07	infeasible
55	339	1.3292e+08	0	1	-7.38e+06	1.53e+07	
56	342	1.28546e+08	0	1	-3.73e+06	2.51e+06	Hessian modified twice
57	345	1.26476e+08	0	1	-1.5e+06	9.4e+06	Hessian modified
58	348	1.26321e+08	0	1	-1.47e+07	8.82e+06	Hessian modified twice
59	351	1.26295e+08	0	1	-1.49e+06	1.49e+06	
60	354	1.26002e+08	0	1	-1.49e+06	2.39e+06	
61	357	1.22324e+08	0.05591	1	-1.49e+06	7.5e+06	Hessian modified twice
62	360	1.25854e+08	0	1	4.83e+06	1.25e+11	Hessian modified twice
63	366	1.25695e+08	0	0.125	-2.07e+06	5.22e+07	
64	375	1.25587e+08	0	0.0156	-2.27e+06	4.91e+06	Hessian modified twice
65	379	1.25517e+08	0	0.5	-1.24e+07	1.43e+07	
66	387	1.25493e+08	0	0.0313	-1.37e+07	1.38e+07	Hessian modified

Local minimum possible. Constraints satisfied.

fmincon stopped because the size of the current search direction is less than twice the selected value of the step size tolerance and constraints are satisfied to within the default value of the constraint tolerance.

Figure 78: fmincon run-3 iterations

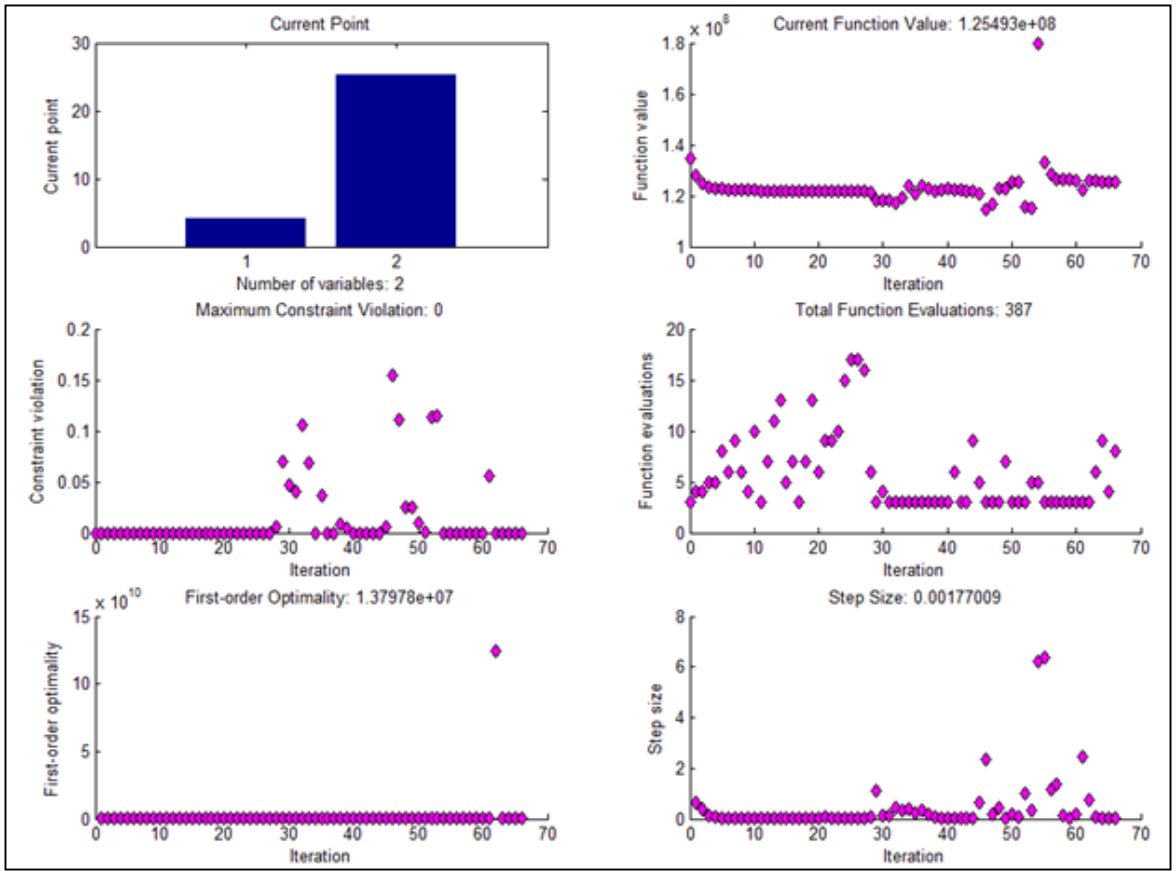

Figure 79: Plot Functions for fmincon run-3

Fmincon run-4 (sqp-algorithm)

Initial Design Points: X0= [4.1 23] where,

X0(1) =shell thickness
X0(2) =flange thickness

Lower and Upper Bounds on Design parameters: XL=[4 16] XU=[10 30]

Optimization Settings: optimoptions(@fmincon, 'Algorithm', 'sqp', DiffMinChange', 0.01, 'MaxIter', 10000, 'MaxFunEvals', 10000, 'TolX' ,1e-2, 'PlotFcns', {@optimplotx,@optimplotfval,@optimplotconstrviolation,@optimplotfunccount,@optimplotfirstorderopt,@optimplotstepsize}, 'display', 'iter')

Optimized Design Parameters: XOPT= [4.2339 22.8461]

Optimized Objective Function (Minimized Volume): FOPT= 122918140

$$\text{Total Volume Reduction} = \frac{198559610 - 123065150}{198559610} \times 100 = 38.02\%$$

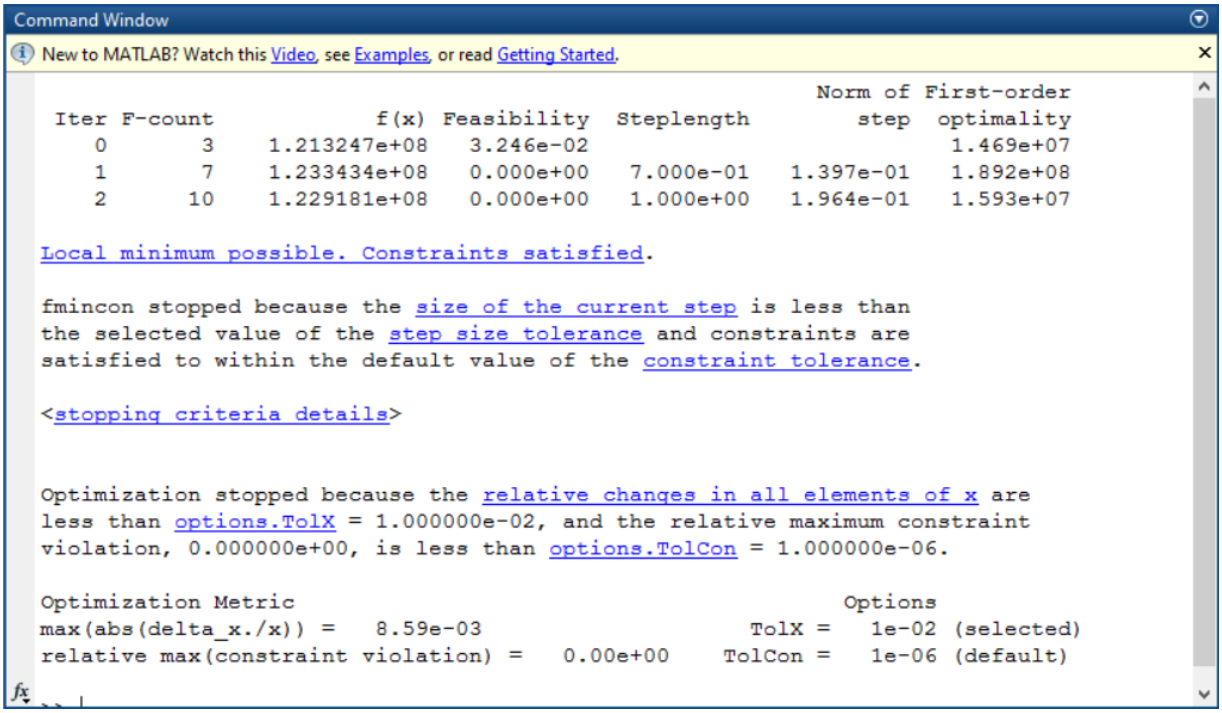

Figure 80: fmincon run-4 iterations

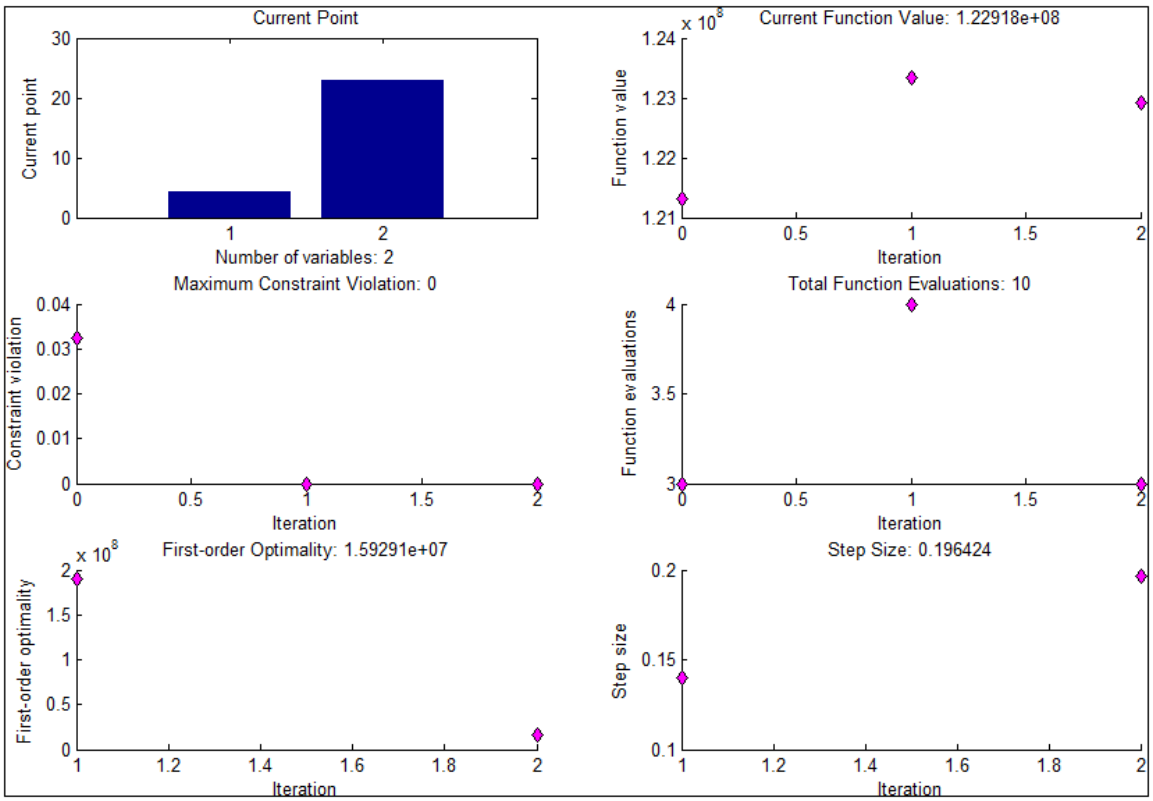

Figure 81: Plot functions for fmincon run-4

Fmincon run-5 (sqp-algorithm)

Initial Design Points: X0= [4.8 29] where,

X0(1) =shell thickness
X0(2) =flange thickness

Lower and Upper Bounds on Design parameters: XL=[4 16] XU=[10 30]

Optimization Settings: optimoptions(@fmincon, 'Algorithm', 'sqp', DiffMinChange', 0.01, 'MaxIter', 10000, 'MaxFunEvals', 10000, 'TolX' ,1e-2, 'PlotFcns', {@optimplotx,@optimplotfval,@optimplotconstrviolation,@optimplotfunccount,@optimplotfirstorderopt,@optimplotstepsize}, 'display', 'iter')

Optimized Design Parameters: XOPT= [4.0000 28.9607]

Optimized Objective Function (Minimized Volume): FOPT= 128726400

$$\text{Total Volume Reduction} = \frac{198559610 - 128726400}{198559610} \times 100 = 35.17\%$$

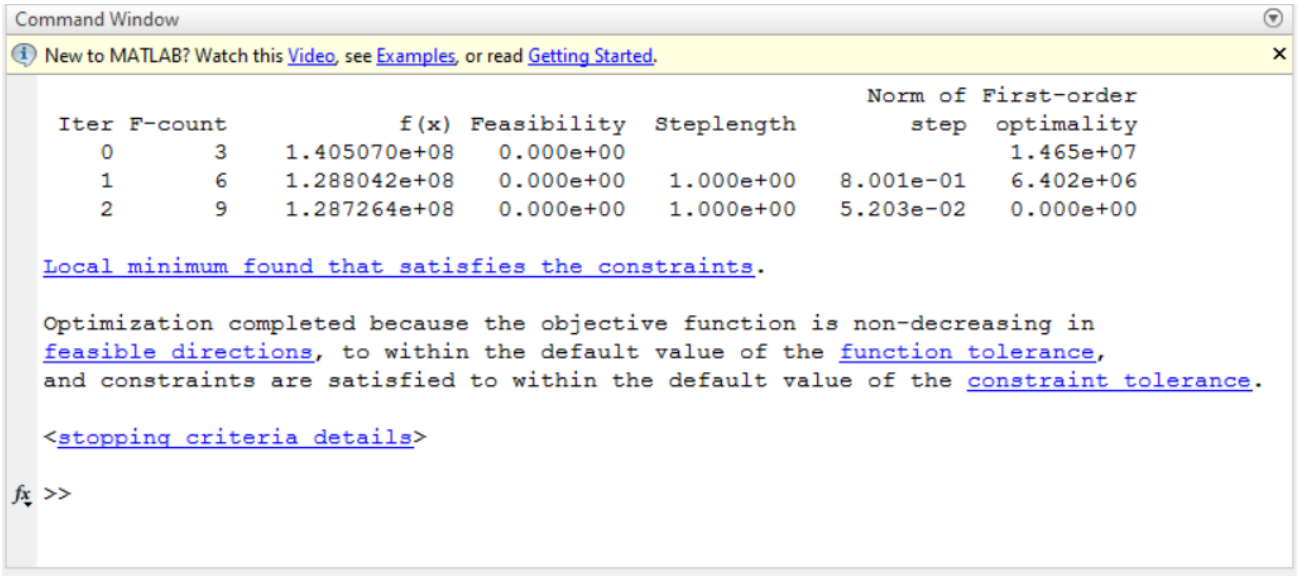

Figure 82: fmincon run-5 iterations

Fmincon run-6 (sqp-algorithm)

Initial Design Points: X0= [4.8 29] where,

X0(1) =shell thickness
X0(2) =flange thickness

Lower and Upper Bounds on Design parameters: XL=[4 16] XU=[10 30]

Optimization Settings: optimoptions(@fmincon, 'Algorithm', 'sqp', DiffMinChange', 0.01, 'MaxIter', 10000, 'MaxFunEvals', 10000, 'TolX' ,1e-3, 'PlotFcns',

{@optimplotx,@optimplotfval,@optimplotconstrviolation,@optimplotfunccount,@optimplotfirstorderopt,@optimplotstepsize}, 'display', 'iter')

Optimized Design Parameters: XOPT= [4.0000 26.7502]

Optimized Objective Function (Minimized Volume): FOPT= 125423580

$$\text{Total Volume Reduction} = \frac{198559610 - 125423580}{198559610} \times 100 = 36.83\%$$

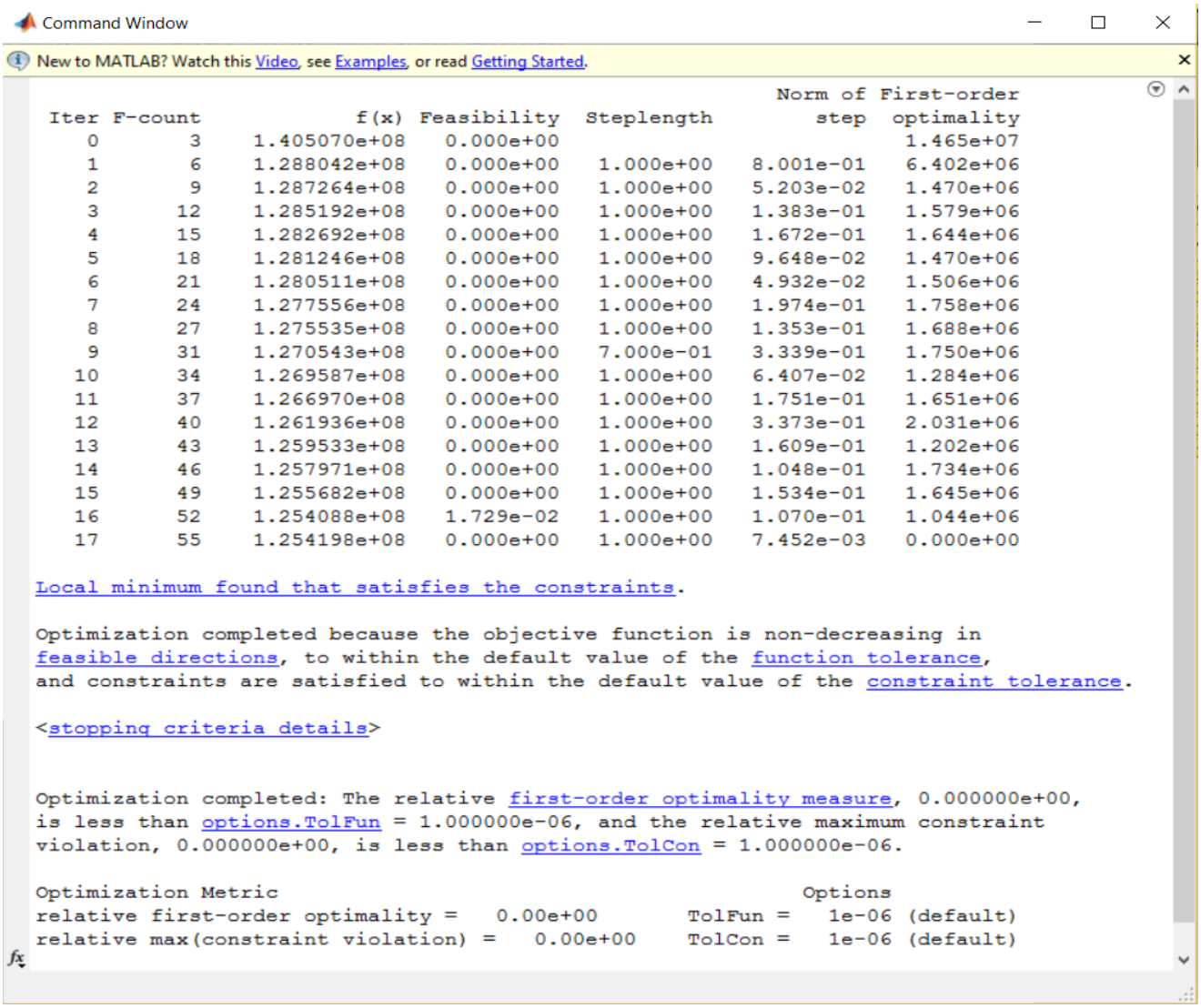

Figure 83: fmincon run-6 iterations

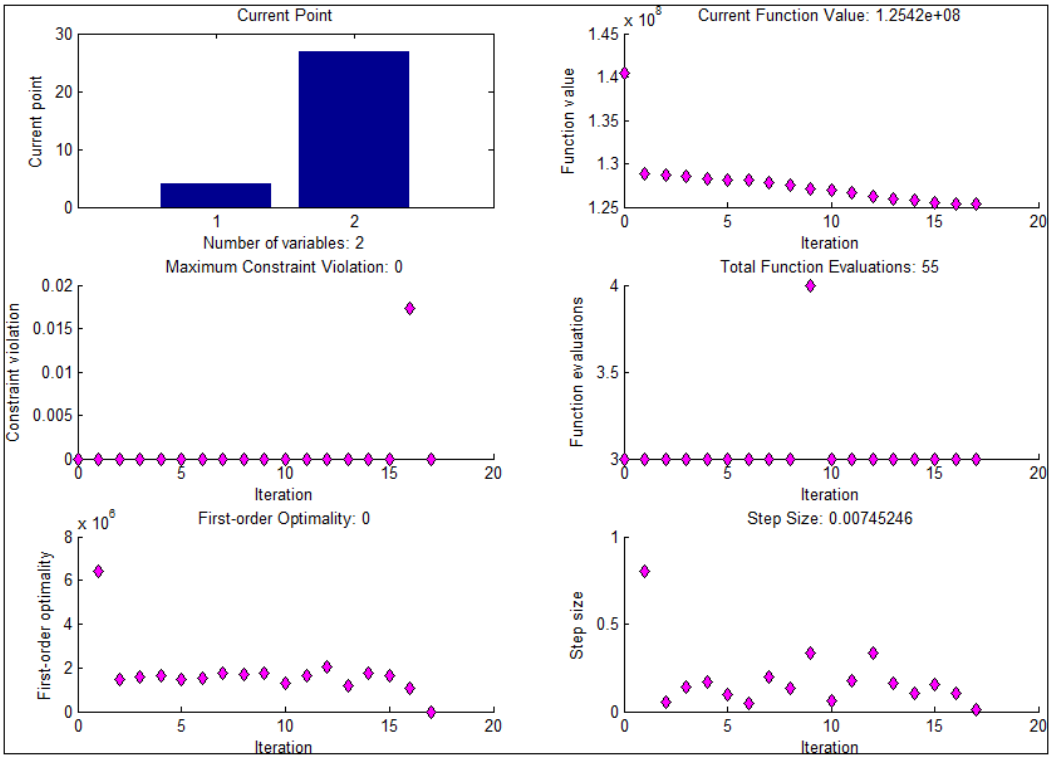

Figure 84: Plot functions for fmincon run-6

Fmincon run-7 (sqp-algorithm)

Initial Design Points: X0= [4.8 29] where,

X0(1) =shell thickness
X0(2) =flange thickness

Lower and Upper Bounds on Design parameters: XL=[4 16] XU=[10 30]

Optimization Settings: optimoptions(@fmincon, 'Algorithm', 'sqp', DiffMinChange', 0.01, 'MaxIter', 10000, 'MaxFunEvals', 10000, 'TolX' ,1e-4, 'PlotFcns', {@optimplotx,@optimplotfval,@optimplotconstrviolation,@optimplotfunccount,@optimplotfirstorderopt,@optimplotstepsize}, 'display', 'iter')

Optimized Design Parameters: XOPT= [4.0000 26.7051]

Optimized Objective Function (Minimized Volume): FOPT= 125356370

$$\text{Total Volume Reduction} = \frac{198559610 - 125356370}{198559610} \times 100 = 36.86\%$$

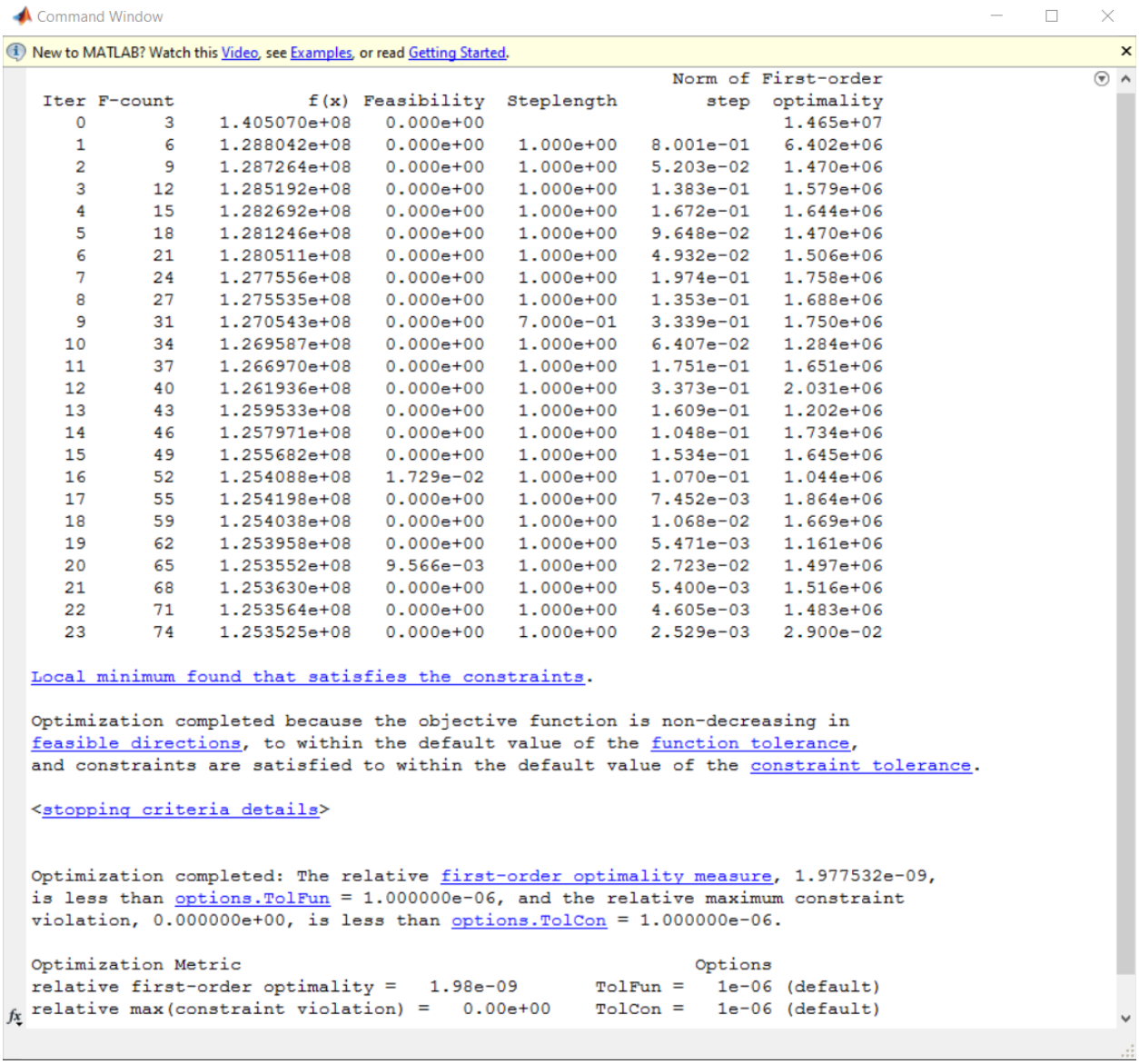

Figure 85: fmincon run-7 iterations

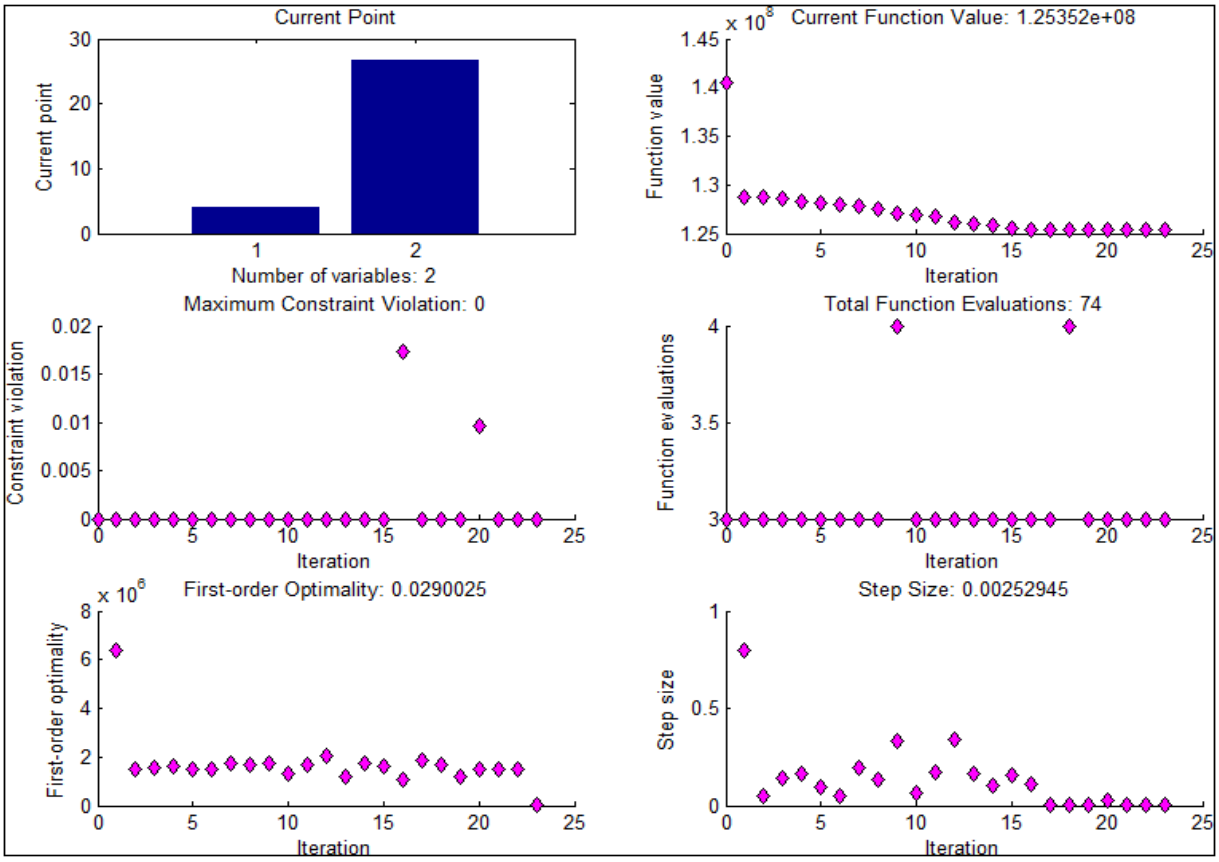

Figure 86: Plot Functions for fmincon run-7

Fmincon run-8

Initial Design Points: X0= [5 23] where,

X0(1) =shell thickness
X0(2) =flange thickness

Lower and Upper Bounds on Design parameters: XL=[4 16] XU=[10 30]

Optimization Settings: optimoptions(@fmincon, 'Algorithm', 'active-set', DiffMinChange', 0.1, 'MaxIter', 10000, 'MaxFunEvals', 10000, 'TolX' ,1e-3, 'PlotFcns', {@optimplotx,@optimplotfval,@optimplotconstrviolation,@optimplotfunccount,@optimplotfirstorderopt,@optimplotstepsize}, 'display', 'iter')

Optimized Design Parameters: XOPT= [4.1442 22.9901]

Optimized Objective Function (Minimized Volume): FOPT= 121959420

$$\text{Total Volume Reduction} = \frac{198559610 - 121959420}{198559610} \times 100 = 38.58\%$$

Command Window

New to MATLAB? Watch this Video, see Examples, or read Getting Started.

```
     1      7   1.27761e+08                0                0.5     -1.09e+07      6.07e+06
     2     11   1.24817e+08                0                0.5     -7.56e+06      1.23e+07
     3     16   1.23446e+08                0               0.25     -1.09e+07      3.25e+06  Hessian
     4     21   1.22589e+08                0               0.25      -1.1e+07      3.46e+06
     5     29   1.22567e+08                0             0.0313      -8.7e+06      5.87e+06
     6     35   1.22275e+08                0              0.125     -7.06e+06      4.48e+06  Hessian
     7     44   1.22237e+08                0             0.0156     -1.48e+07      2.57e+06
     8     50   1.22228e+08                0              0.125     -1.29e+07      8.56e+06
     9     54   1.22193e+08                0                0.5     -9.62e+06      1.26e+07
    10     64   1.22128e+08                0            0.00781     -2.07e+06      5.92e+06  Hessian
    11     67   1.22004e+08                0                  1     -8.34e+06       3.3e+06
    12     74    1.2197e+08                0             0.0625     -1.41e+07      1.21e+07
    13     85   1.21961e+08                0            0.00391     -1.43e+07      2.09e+06  Hessian
    14     98   1.21959e+08                0           0.000977      -1.4e+07      1.82e+07

Local minimum possible. Constraints satisfied.

fmincon stopped because the size of the current search direction is less than
twice the selected value of the step size tolerance and constraints are
satisfied to within the default value of the constraint tolerance.

<stopping criteria details>

No active inequalities.
>>
```

Figure 87: fmincon run-8 iterations

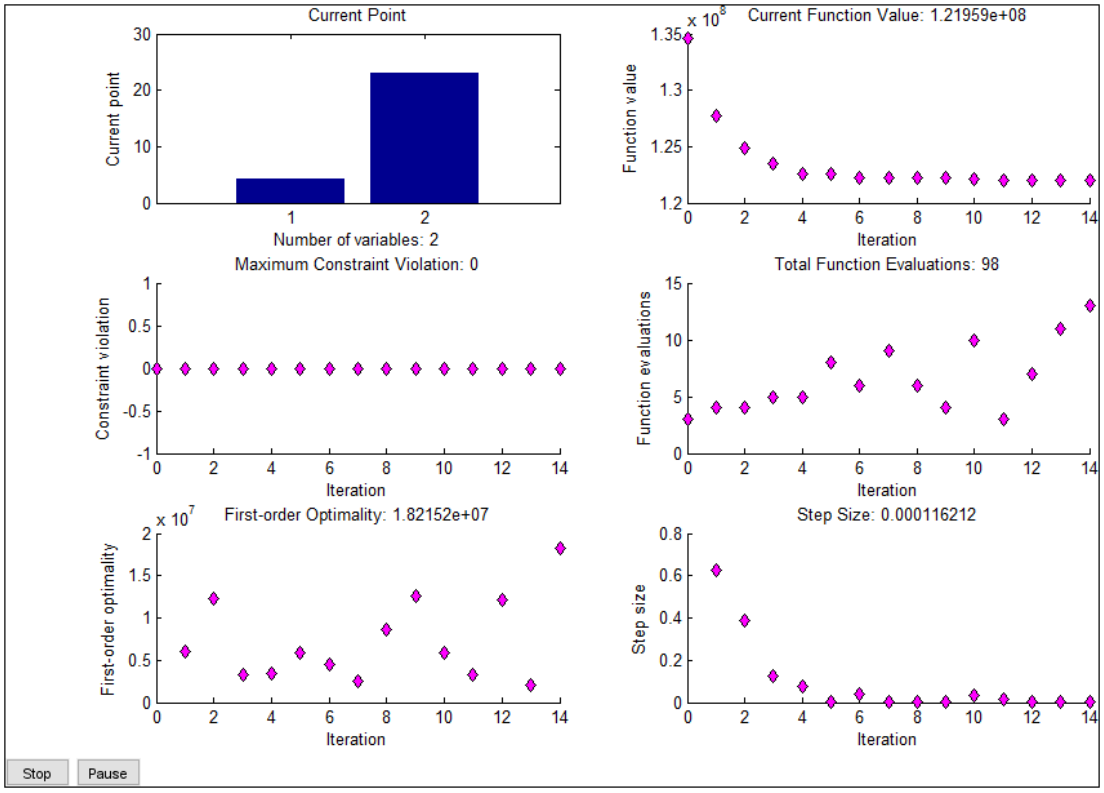

Figure 88: Plot Functions for fmincon run-8

Table 44: fmincon Optimization Convergence for different step tolerance limits

fmincon Algorithm	Active-set			SQP		
	Run-1	Run-8	Run-3	Run-5	Run-6	Run-7
Step tolerance 'tolx'	1e-2	1e-3	1e-4	1e-2	1e-3	1e-4
Initial Design Variable X0	[5 23]	[5 23]	[5 23]	[4.1 29]	[4.1 29]	[4.1 29]
Optimized Design Variable Xopt	[4.1609 23.0116]	[4.1442 22.9901]	[4.1338 22.8975]	[4.0000 28.9607]	[4.0000 26.7502]	[4.0000 26.7051]
Weight Reduction %	38.43	38.58	38.72	35.17	36.83	36.86
Number of iterations taken	7	14	66	2	17	23

Table 45: Optimization Results Summary

fmincon		Optimized Design Variables		Optimal Objective: Total Volume (mm3)	Weight Reduction %	Design Constraints	
		x1: shell thickness (mm)	x2: flange thickness (mm)			Maximum Membrane stress (MPa)	Maximum Membrane Plus Bending stress (MPa)
Initial Design		10	16	198559610	NA	159.4	249.1
Active-set	Run-1	4.1609	23.0116	122236730	38.43	205.30	340.67
	Run-2	4.0000	23.5703	120699140	39.21	204.70	337.73
	Run-3	4.1338	22.8975	121669870	38.72	205.46	338.07
	Run-8	4.1442	22.9901	121959420	38.58	205.35	350.07
sqp	Run-4	4.2339	22.8461	122918140	38.02	205.05	353.59
	Run-5	4.0000	28.9607	128726400	35.17	191.19	296.37
	Run-6	4.0000	26.7502	125423580	36.83	204.29	313.46
	Run-7	4.0000	26.7051	125356370	36.86	204.02	304.88
Best Solution	Run-2	4.0000	23.5703	120699140	39.21	204.70	337.73

7.2 Conclusions

The total weight of the pressure vessel was reduced by 39%. The optimal design parameters for the pressure vessel are obtained and the objective minimization of cost by reducing weight of the Pressure vessel is achieved. Design parameters, shell thickness and flange thickness, are optimized while limiting the maximum linearized membrane and membrane plus bending stresses

below the allowable limits. Based on the comparison of different fmincon runs, weight reduction obtained by using active-set algorithm was in the range of 38% - 39% whereas the reduction obtained by using sqp algorithm was in the range of 35% - 37%. As predicted from the design space analysis, the optimal point in fact does lies in the estimated optimal solution region. Hence, it can be concluded that this kind of interfacing approach where powerful FEA softwares such as ANSYS are integrated with robust optimization tools like MATLAB, can be used to solve different types of complex design optimization problems. It was also found that the optimization in design of pressure vessel using FEA is a safe and promising method as it has successfully satisfied the goal of weight reduction. The methodology implemented in this study is very effective and can be a successful tool for advance analysis in the structural design field. The integrated approach used in this thesis work is desired for solving optimization problems because the process is completely automated and does not require any kind of user intervention until an optimum solution is found.

Optimization solution for finite element model of this pressure vessel is mesh dependent, but since we have a discontinuity in the model, the mesh density was kept fixed throughout the optimization process. In particular, the optimization problem was solved by using MATLAB inbuilt optimization solver called 'fmincon'. As FMINCON gives the local minimum within the limits specified for the design variables, the minimum weight value obtained in this study is a local minimum.

7.3 Future Work

- This pressure vessel structure was also modeled in ANSYS workbench with the purpose of performing the optimization using workbench's goal-driven optimization tool. But due to time constraint, this study could not be conducted.

- The analysis can be reexamined by modeling the thin cylindrical shell body of the pressure vessel using shell elements. Optimized results obtained from this shell model investigation can be compared and verified with the results obtained from the current work.

- Integrating Altair Hypermesh, ANSYS and MATLAB. Optimization of design by pre-processing including meshing the finite element model in Hypermesh, solving the model in ANSYS, followed by the optimization in MATLAB. Altair Hypermesh provides superior meshing options with good element level control compared to all FEA softwares

available in the market. This will definitely give a much accurate solution since user can exploit the desired unique features limited to each software.

- Further analysis can be conducted on this pressure vessel by considering a few more design parameter such as radius of the cylindrical shell body, length of the cylindrical shell body, head thickness, head height, height of the nozzle openings etc.

- Metaheuristic based global optimization algorithms like genetic algorithm, Ant colony optimization algorithm, Differential Evolution and Simulated Annealing can be used to find the global optimum for the pressure vessel model used in this work.

- Shape or Topology Optimization can be implemented to remove the redundant material from specific components of the pressure vessel.

REFERENCES

1. A. Gauchía, B.L. Boada, M.J.L. Boada and V. Díaz (2014). Integration of MATLAB and ANSYS for Advanced Analysis of Vehicle Structures, MATLAB Applications for the Practical Engineer, Mr. Kelly Bennett (Ed.), InTech, DOI: 10.5772/57390. Available from:http://www.intechopen.com/books/matlab-applications-for-the-practical-engineer/integration-of-matlab-and-ansys-for-advanced-analysis-of-vehicle-structures

2. Levi B. de Albuquerque and Miguel Mattar Neto. STRESS CATEGORIZATION IN NOZZLE TO PRESSURE VESSEL CONNECTION FINITE ELEMENT MODELS, published in Pressure Vessel and Piping Codes and Standards - 2000 PVPVol . 407, ed. A. F. Deardorff, p. 271-275, ISBN No. 0-7918-1888-8.

3. Carlos A. de J. Miranda, Altair A. Faloppa, Miguel Mattar Neto and Gerson Fainer, “ASME STRESS LINEARIZATION AND CLASSIFICATION – A DISCUSSION BASED ON A CASE STUDY”, 2011 International Nuclear Atlantic Conference - INAC 2011Belo Horizonte, MG, Brazil, October 24-28, 2011 ISBN: 978-85-99141-04-5.

4. R. Carbonari, P. Munoz-Rojas, E. Andrade, G. Paulino, K. Nishimoto, E. Silva, “Design of pressure vessels using shape optimization: An integrated approach”, International Journal of Pressure Vessels and Piping, Volume 88, May 2011.

5. Prof. Vishal V. Saidpatil and Prof. Arun S. Thakare, "Design & Weight Optimization of Pressure Vessel Due to Thickness Using Finite Element Analysis”, International Journal of Emerging Engineering Research and Technology Volume 2, Issue 3, June 2014, PP 1-8 ISSN 2349-4395 (Print) & ISSN 2349-4409 (Online).

6. Sulaiman Hassan, Kavi Kumar, Ch Deva Raj and Kota Sridhar, "Design and Optimisation of Pressure Vessel Using Metaheuristic Approach", Applied Mechanics and Materials Vols. 465-466 (2014) pp401-406, Trans Tech Publications, Switzerland.

7. K. Sahitya Raju and Dr. S. Srinivas Rao, "DESIGN OPTIMISATION OF A COMPOSITE CYLINDRICAL PRESSURE VESSEL USING FEA", International Journal of Scientific and Research Publications, Volume 5, Issue 12, December 2015, ISSN 2250-3153.

8. The American Society of Mechanical Engineers, "Rules for construction of Power Boilers", ASME Boiler and Pressure Vessel Comitte July-1 2010 New York.

9. Arturs Kalnins, "Stress Classification in Pressure Vessels and piping", Pressure Vessel and Piping Systems.

10. "The Nuts and Bolts of Stress Linearization", Pressure Vessel Engineering Ltd.

11. Achille Messac, "Optimization in Practice with MATLAB for Engineering Students and Professionals", published by CAMBRIDGE University press NY-2015.

12. Alan R. Parkinson, Richard J. Balling and John D. Hedengren, "Optimization Methods for Engineering Design", 2013 Brigham Young University.

13. Ajaykumar Menon, "STRUCTURAL OPTIMIZATION USING ANSYS AND REGULATED MULTIQUADRIC RESPONSE SURFACE MODEL", Thesis Report, The University of Texas at Arlington, December 2005.

14. Miguel Mattar Neto, Carlos Alexandre de Jesus Miranda, Altair Antonio Faloppa and Gerson Fainer, "ASME Stress Linearization and Classification of a WYE piping juction", 2011 ANSYS Conference & ESSS Users Meeting.

15. ITER STRUCTURAL DESIGN CRITERIA FOR IN-VESSEL COMPONENTS, APPENDIX B - GUIDELINES FOR ANALYSIS, IN-VESSEL COMPONENTS

16. MATLAB fmincon, https://www.mathworks.com/help/optim/ug/fmincon.html

17. Constrained Nonlinear Optimization Algorithms, https://www.mathworks.com/help/optim/ug/constrained-nonlinear-optimization-algorithms.html

18. ANSYS Solid95 Elements: http://www.ansys.stuba.sk/html/elem_55/chapter4/ES4-95.htm

19. Stress Categories for Design by Analysis of Pressure Vessels, Talk for ANSYS USERS GROUP - June 1999

20. PV Eng - Linearization, http://pveng.com/home/fea-stress-analysis/linearization/

21. ANSYS Linearized Stress document, https://www.sharcnet.ca/Software/Ansys/17.0/enus/help/wb_sim/ds_linearized_stresses.html

22. ASME SGDA-99-2, PROPOSED NON-MANDATORY APPENDIX for Subcommittees III & VIII, Interpretation of Finite Element Analysis Stress Results, Rev 4, 2000

APPENDIX

HOPPER DIAGRAGM

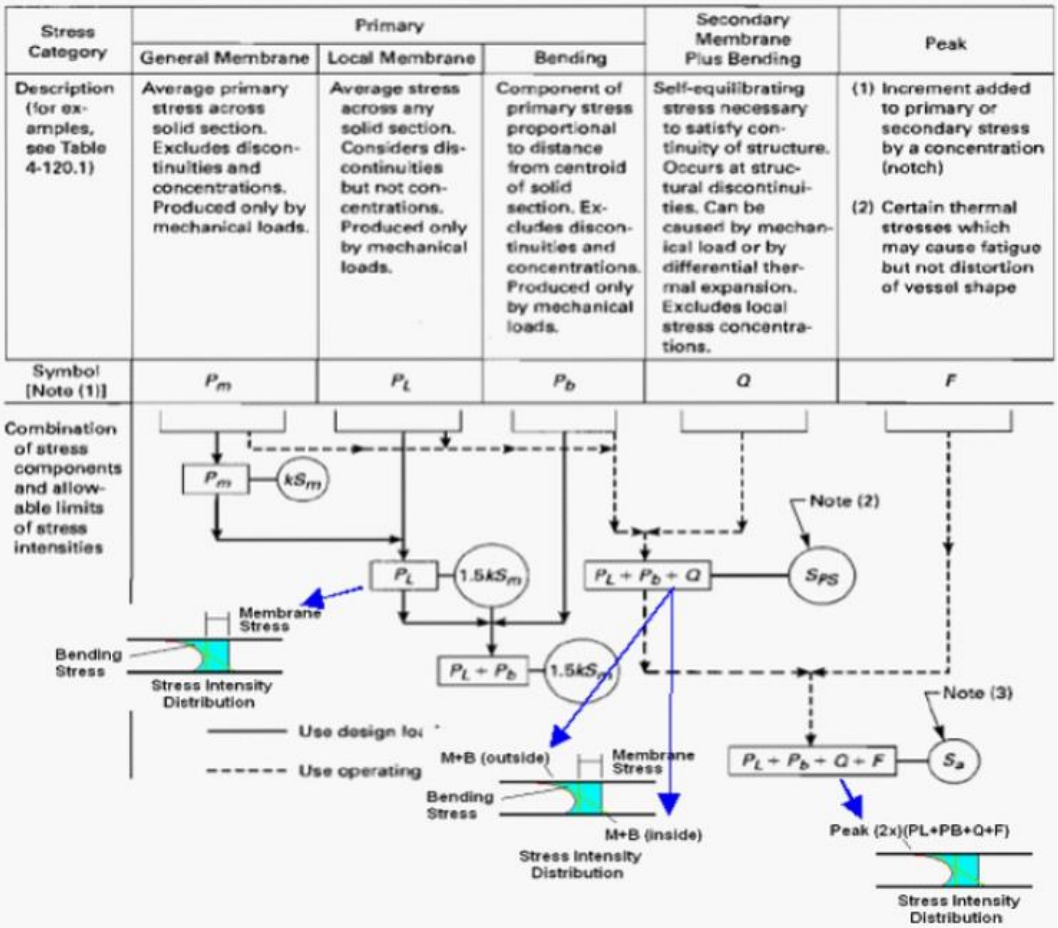

Figure 12 – ASME Figure 4-130.1 Amplified

BIBLIOGRAPHY

Artik Patel enrolled in PES Institute of Technology, Bangalore, India in 2008 and earned his B.E. (Bachelor of Engineering) in Mechanical Engineering in June 2012. After his graduation, he worked as a Project Engineer at Wipro technologies, Bangalore, India from August 2012 to April 2014. He had started his M.S. (Master of Science) degree in Mechanical Engineering at The University of Texas at Arlington, Arlington, Texas in August 2014 and earned M.S. Degree in Mechanical Engineering in December 2016 with a 4.0 G.P.A. During his tenure as a master's student, he served as the Graduate Teaching Assistant of Dr. Raul Fernandez, Dr. Adrian Rodriguez and Dr. Kent Lawrence. His thesis was based on the design optimization of pressure vessel structure subjected to design constraints specified by the ASME Boiler and Pressure Vessel code. His current research interests are finite elements, structural optimization and computer aided design. His long-term goal is to work as a structural analyst in the engineering industry.